Die approbierte Originalversion dieser Dissertation ist in der Hauptbibliothek der Technischen Universität Wien aufgestellt und zugänglich.
http://www.ub.tuwien.ac.at

The approved original version of this thesis is available at the main library of the Vienna University of Technology.
http://www.ub.tuwien.ac.at/eng

TECHNISCHE UNIVERSITÄT WIEN
Vienna University of Technology

Dissertation

Quantification strategies for elemental imaging of biological samples using Laser Ablation-Inductively Coupled Plasma-Mass Spectrometry (LA-ICP-MS)

ausgeführt zum Zwecke der Erlangung des akademischen Grades eines Doktors der technischen Wissenschaften unter der Leitung von

Associate Prof. Dipl.-Ing. Dr. Andreas Limbeck
Institut für Chemische Technologien und Analytik (E164)
TU Wien

eingereicht an der TU Wien,
Fakultät für Technische Chemie
von

Maximilian Bonta

Mat.-Nr.: 0825213
Höfergasse 1a/1/6, 1090 Wien, Österreich

Wien, am 13.09.2016 _____

Acknowledgment

First of all, I would like to express my gratitude to the supervisor of my PhD thesis, Dr. Andreas Limbeck, head of the Division Instrumental Analytical Chemistry of the Institute of Chemical Technologies and Analytics at TU Wien. He had always an open door whenever I needed his support. I want to say thanks for the countless fruitful, encouraging, and interesting discussions we had. It was an honor to learn from his wide knowledge and I could not imagine having a better PhD supervisor.

I am proud that I have been part of the MEIBio PhD program of the TU Wien, in which framework I conducted my PhD thesis. Thus, I would like to thank Dr. Martina Marchetti-Deschmann for supervision of this PhD program, as well as all faculty members and fellow PhD students. Apart from some excellent scientific cooperation, the program also brought us together at a human level. From those colleagues, I especially want to thank Anna Balbekova and Florian Brenner for the work we performed together.

During my PhD thesis I had the great honor to work at the Lawrence Berkeley National Laboratory in California as a guest researcher under the supervision of Prof. Rick E. Russo. His immense knowledge and experience helped me a lot to improve my scientific skills. I would also like to thank Dr. Jhanis J. Gonzalez for many hours of interesting and entertaining discussions while driving me to work. Furthermore, I am also grateful to Dayana Oropeza, Dr. Derrick Quarles, and all other colleagues from California for creating a pleasant working atmosphere and becoming friends to me.

I also want to thank my fellow PhD colleagues from the group of Dr. Andreas Limbeck – Gerald Bauer, Felix Horak, Sara Hosseinzadegan, and Winfried Nischkauer – for their help and support whenever necessary; our working environment was always inspiring and welcoming and we indeed had a great time together. Apart from the mentioned PhD

students, I also want to thank all undergraduate students who were doing the work for their Bachelor's and Master's theses under my supervision; they all did a great job.

I want to say thanks to my colleagues from my undergraduate as well as postgraduate studies for having such great times together. Most of them started spreading around the world after their graduation, some are still at our university; I will always keep these times in good memory. I do not want to mention anybody in person, everybody will know that he or she is addressed by this.

There are of course also friends outside from university life I want acknowledge. We were (and still are) doing lots of things together. Travelling, going out, or doing sports. Those people have always provided me with the necessary amount of distraction from my studies. Thanks, Florian Karall, Albrecht Reimer, Nicole Rostok, and Katja Staudigl.

I also want to express my gratitude to my parents who always supported me during my time at university. Even at my time before I came to university, they always encouraged me to do what I find the most interesting; probably that's even why I became a researcher. But not only the moral support, but also the financial care for a student who is usually not earning a lot of money has to be addressed.

Last but not least, I want to thank my partner, Victoria Mohr, for supporting me and for understanding that I had to write one or the other article from home.

Abstract – Dissertation Maximilian Bonta

Metals are an important part of every functioning biological system. Variations in their concentration can indicate altered physiological conditions in an organism. Besides endogenous abundance, trace elements can also be introduced into organisms from external sources such as the environment or intentionally during medical treatments. Either way, accurate assessment of metal concentrations including their spatial distribution in biological samples (*e.g.*, tissues) is an important aspect of modern medical research.

This PhD thesis aims at the development of improved analytical procedures for elemental imaging of biological samples using Laser Ablation-Inductively Coupled Plasma-Mass Spectrometry (LA-ICP-MS). Especially the extremely low limits of detection for most elements and the wide accessible range of elements make LA-ICP-MS perfectly suitable for elemental mapping analysis of biological samples. Main target of the research was the development and optimization of quantification strategies for multi-element imaging in biological samples. During an LA-ICP-MS measurement, the bulk composition of the analyzed sample ('matrix') usually influences the detected analyte signals. Laser-material interaction, transport of the generated aerosol towards the ICP-MS device, as well as atomization and ionization of the analytes in the ICP strongly depend on the bulk composition of the investigated sample. Thus, suitable external standards are necessary if quantification of the detected signals is desired. Methods for simple but still accurate quantification should be developed within this PhD thesis, including the evaluation of internal standards to compensate aforementioned matrix effects to a certain extent.

Besides analytical method development, also method application for medical questions was an important aspect. One special target of analysis was platinum, commonly used

during anti-cancer treatments. LA-ICP-MS was aspired to visualize the actual drug distribution in tumor samples, complementing histological investigations.

One major achievement of this PhD thesis is the successful development of simple and accurate quantification strategies of trace elements in tissue samples. Using an approach employing patterns printed on paper using a conventional office inkjet printer to be used as external standard, single-element quantification could successfully applied for the determination of platinum contents in tissue samples. In further work, multi-element quantification was accomplished using dried droplets on filter paper. Multi-elemental analysis showed to provide deep insight into physiological processes when fused with conventional histological techniques. Both quantification approaches were successfully combined with thin gold layers as pseudo-internal standard. They offer accuracies and limits of detection comparable with classical calibration approaches (*i.e.*, matrix-matched tissue standards) while reducing the workload required for standard preparation and characterization to a minimum. To extend the multi-elemental capabilities of LA-ICP-MS, the technique has been applied simultaneously with Laser Induced Breakdown Spectroscopy (LIBS) in a Tandem LA/LIBS system, to access biological bulk elements such as hydrogen, carbon, and oxygen alongside with trace metals.

In addition to methodological improvements, also the topic image accuracy could be addressed by defining a metric for the determination of image quality and accuracy compared to a reference image. Further work included interdisciplinary research where LA-ICP-MS was used in multimodal imaging combined with Time-of-Flight Secondary Ion Mass Spectrometry (ToF-SIMS), Matrix-assisted Laser Desorption/Ionization-Mass Spectrometry (MALDI-MS), and infrared (IR) microscopy. In these multimodal approaches, the fusion of elemental and molecular information gained insightful results for medical interpretation.

Kurzfassung – Dissertation Maximilian Bonta

Metalle sind ein wichtiger Bestandteil von jedem intakten biologischen System. Abweichungen von ihrer typischen Konzentration können auf veränderte physiologische Bedingungen in einem Organismus hinweisen. Neben natürlich im einem biologischen System vorkommenden (essentiellen) Metallen, die für biologische Funktionen notwendig sind, können Spurenmetalle auch durch externe Quellen in einen Organismus eingebracht werden. Dies kann beispielsweise umweltbedingte Ursachen haben, oder auch während einer medizinischen Behandlung passieren, wenn das Medikament Metalle enthält. Unabhängig von der Art der Aufnahme ist eine genaue Bestimmung von Metallkonzentrationen in Geweben inklusive ihrer örtlichen Verteilung ein wichtiger Aspekt moderner medizinischer Forschung.

Ziel dieser Doktorarbeit war die Enwicklung von verbesserten Analysenstrategien für die Bestimmung von Elementverteilungen in biologischen Proben mittels Laser Ablation-Inductively Coupled Plasma-Mass Spectrometry (LA-ICP-MS). Speziell sie niedrigen erreichbaren Nachweisgrenzen sowie der weite Bereich an zugänglichen Elementen machen die Methode perfekt für diese Art von Analyse geeignet. Ein Kernaspekt der Forschung war die Entwicklung und Optimierung von Strategien zur Multielement-Quantifizierung in biologischen Proben. Während einer LA-ICP-MS Messung beeinflussen die Hauptbestandteile der Probe (sog. Matrix) typischerweise die registrierten Analytsignale. Interaktion der Probe mit dem Laser, Transport des generierten Aerosols, sowie Atomisierung und Ionisierung der Analyten im ICP hängen stark von der Probenmatrix ab. Deshalb sind externe Kalibrationsstandards notwendig, um eine akkurate Quantifizierung der detektierten Analytsignale zu gewährleisten. In der vorliegenden Doktorarbeit sollten einfache und dennoch genaue Quantifizierungsmethoden entwickelt werden. Weiters sollten geeignete interne

Standards evaluiert werden, um zuvor erwähnte Matrixeffekte in einem gewissen Ausmaß kompensieren zu können.

Neben analytischer Methodenentwicklung war auch die Anwendung im medizinischen Bereich ein wichtiger Aspekt. Ein Element, dem spezielles Interesse gewidmet wurde war Platin, welches in Form von Komplexverbindungen in der Krebstherapie eingesetzt wird. LA-ICP-MS sollte dabei mit der Information über tatsächliche Verteilungen des Medikaments im Gewebe eine wichtige Zusatzinformation zu histologischen Untersuchungen liefern.

Eine wichtige Leistung im Rahmen dieser Doktorarbeit ist die erfolgreiche Eintwicklung von einfachen und genauen Quantifizierungsstrategien für Spurenelemente in Gewebeproben. Im ersten Ansatz werden definierte Muster mit einem handelsüblichen Tintenstrahldrucker auf Papier gedruckt; dabei ist die Tinte mit dem interessierenden Element versetzt. Diese Druckmuster können in weiterer Folge als externe Kalibrationsstandards verwendet werden. Einzelelement-Quantifizierung konnte so erfolgreich für Platin in Tumorproben erreicht werden. In einer weiteren Arbeit konnte Multielement-Quantifizierung mittels getrockneten Standards auf Filterpapier erreicht werden. Diese Multielementanalyse erlaubte in Kombination mit klassischen histologischen Techniken einen tiefen Einblick in pysiologische Prozesse. Beide Quantifizierungsmethoden konnten erfolgreich mit der Verwendung von dünnen Goldfilmen as pseudo-internem Standard kombiniert werden. Die Methoden erlauben Bestimmungsgrenzen und –genauigkeiten, welche mit typischerweise verwendeten Quantifizierungsmethoden (z.B. homogenisierte Gewebe) vergleichbar sind, während der Arbeitsaufwand für die Herstellung und Charakterisierung der Standards auf ein Minimum reduziert wird. Um die Multielement-Möglichkeiten von LA-ICP-MS zu erweitern, wurde die Technik simultan mit Laser Induced Breakdown Spectroscopy (LIBS)

in einem sogenannten Tandem LA/LIBS System verwendet. Dadurch waren neben Metallen auch in biologischen Proben als Hauptkomponenten vorkommende Elemente wie etwa Wasserstoff, Sauerstoff oder Kohlenstoff für die Analyse zugänglich.

Zusätzlich zu methodischen Entwicklungen wurde auch das Thema Qualität von Element-Verteilungsbildern behandelt. Es konnte eine Maßzahl für die quantitative Bestimmung der Übereinstimmung eines gemessenen Verteilungsbildes mit einem Referenzbild definiert werden. Weitere Arbeiten beinhalten interdisziplinäre Forschung wo LA-ICP-MS in der multimodalen Verteilungsanalytik in Kombination mit Time-of-Flight Secondary Ion Mass Spectrometry (ToF-SIMS), Matrix-assisted Laser Desorption/Ionization-Mass Spectrometry (MALDI-MS) und Infrarot (IR) Mikroskopie eingesetzt wurde. In diesen multimodalen Ansätzen konnte die Kombination aus Element- und Molekülinformation wichtige Ergebnisse für medizinische Fragestellungen liefern.

Contents

Acknowledgment I

Abstract – Dissertation Maximilian Bonta III

Kurzfassung – Dissertation Maximilian Bonta V

1 Outline 3

2 Introduction 5

3 Metals in biological tissues 8

3.1 Endogenous (trace) metals 8

3.2 Exogenous trace metals 10

4 Scientific questions 12

4.1 Proposed analytical techniques 12

4.2 Analytical improvements 14

4.3 Medical questions 16

5 Scientific publications 18

5.1 Research performed for the PhD thesis 18

5.2 Life sciences applications 23

5.3 Applications for material analysis 26

5.4 Selected publications 27

Quantitative LA-ICP-MS imaging of platinum in chemotherapy treated human malignant pleural mesothelioma samples using printed patterns as standard ..... **Error! Bookmark not defined.**

Application of dried-droplets deposited on pre-cut filter paper disks for quantitative LA-ICP-MS imaging of biologically relevant minor and trace elements in tissue samples ..... **Error! Bookmark not defined.**

Elemental mapping of biological samples by the combined use of LIBS and LA-ICP-MS ..... **Error! Bookmark not defined.**

A metric for evaluation of the image quality of chemical maps derived from LA-ICP-MS experiments..... **Error! Bookmark not defined.**

Recent advances in quantitative LA-ICP-MS analysis: challenges and solutions in the life sciences and environmental chemistry ..... **Error! Bookmark not defined.**

Elemental and Molecular Imaging of tumour tissues with ToF-SIMS in combination with LA-ICP-MS..... **Error! Bookmark not defined.**

Multimodal (FTIR and LA-ICP-MS) imaging of a tumor treated with Sunitinib and Cisplatin ..... **Error! Bookmark not defined.**

6 List of abbreviations 96

7 References 97

8 Curriculum Vitae – Maximilian Bonta 101

1 Outline

This PhD thesis was performed at the Institute of Chemical Technologies and Analytics of the TU Wien between November 2013 and October 2016. It was conducted within the framework of an interdisciplinary PhD program of the TU Wien entitled 'Molecular and Elemental Imaging in Biosciences' (MEIBio). The author spent four months as a guest researcher at the Lawrence Berkeley National Laboratory in California during his PhD thesis. Work performed within the complete thesis resulted in the publication of ten articles (thereof six as first author) in internationally renowned and peer-reviewed journals. Additionally, the work was presented in twelve oral presentations and nine poster presentations at international conferences and meetings during the time of the PhD thesis. Two posters were awarded with a poster prize.

The main objectives addressed within this thesis were:

- Establishment of strategies for the accurate determination of bulk, major, and trace element distributions in different types of tissue samples with a background of medical interest.
- Development of quantification strategies for trace elements in tissue samples. Besides qualitative distribution images, a quantification of the analyte content detected at each single pixel of the image allows inter-sample comparisons in a larger sample pool. Suitable internal standardization approaches as well as external quantification strategies should be developed and validated.
- Tailoring the desired image quality of elemental distribution images with the possibility of having a flexible lateral resolution which can be selected with regards to the demand of the given experiment (*i.e.*, high-resolution imaging in the low

µm-range for detailed sample areas *vs.* overview scans over larger samples with lower lateral resolution).

- Strategies for the determination of image quality with a special focus on optimizing the time-requirement for imaging experiments while not compromising accuracy of the distribution image.
- Expansion of the multi-element imaging approach for metals using LA-ICP-MS to the analysis of non-metallic sample constituents (*e.g.*, C, H, N, O) by LIBS and simultaneous use of the two methods in a Tandem LA/LIBS setup.
- Use of the developed methods for applications of medical interest, for example in cancer research: Quantitative elemental distribution imaging is expected to answer existing questions in current medical research, *e.g.*, in drug uptake studies.

The present work consists of five chapters: After a short general introduction, an overview of the importance of trace elements in biological tissues will be given. Besides the function of naturally occurring metals, the use of platinum containing drugs for anti-cancer treatment – an important application part addressed within this PhD thesis – will be described. This section will be followed by a discussion of the scientific considerations which this thesis was based on. Herein, the characteristics of the used analytical techniques – Laser Ablation-Inductively Coupled Plasma-Mass Spectrometry (LA-ICP-MS) and Laser Induced Breakdown Spectroscopy (LIBS) – will be described briefly; challenges and limitations of the analytical methods will be highlighted. The introductory section will be followed by a discussion of the scientific work performed during the PhD thesis, including a discussion of the core aspects of published scientific journal articles. In the last chapter, a selection of journal papers published in the course of this thesis will be presented.

2 Introduction

Nowadays, trace metals are recognized to play an essential role in biological processes. Either occurring as free ions (*e.g.*, to maintain a constant osmotic pressure), or bound to proteins or other macromolecules, metals have shown to influence the function of all living organisms. In the early 2000s, the analysis of metals in biological systems has been introduced into the field of the omics-sciences under the term *metallomics*, which has been mainly shaped by Haraguchi [1]. From this time on, the number of applications and targeted questions grew constantly. Besides the analysis of overall trace element concentrations in tissues and chromatography-based investigations on liquid samples (*e.g.*, lysates, extracts), laterally resolved element distributions quickly came into the focus of the researchers. Interaction of metals with specific tissue structures could not be investigated just by average trace element information. Laterally resolved analysis gave the opportunity to compare the obtained elemental distributions with morphological features and results from histological or immunohistochemical analysis, providing deep insight into physiological properties, as well as allowing conclusions on metal-protein interaction.

For most investigations, Laser Ablation-Inductively Coupled Plasma-Mass Spectrometry (LA-ICP-MS) provides an excellent toolset [2]. The attractiveness of the technique has been mainly driven by the figures of merit such as the extremely low limits of detection (far below µg g^{-1} for most elements), the wide dynamic range, and the possibility of quantification (which is still a challenging aspect) [3]. Further important aspects are the possibility to perform multi-element analysis, the acquisition speed of the method, the achievable lateral resolution, as well as the variable sample size from single cells up to large tissue slices. Additionally, no vacuum is required which allows also the analysis of samples that would be unstable under reduced pressure. First applications focused on the

distributions of naturally occurring (endogenous) trace elements such as Cu, Zn, or Fe [4, 5]. Such multi-element analyses are still of great interest. However, inter-relations between different elements are very complex, which makes interpretation of the obtained data often difficult. Nevertheless, it showed that trace element distributions can be altered in pathogenic conditions of tissues, for example during tumor genesis [6] or neural diseases such as Parkinsonism [4]. Such 'elemental histology' can surely be an important aspect in modern medical research, perfectly complementing other chemical imaging techniques accessing molecular information such as matrix-assisted laser desorption/ionization-mass spectrometry (MALDI-MS) [7], or infrared (IR) microscopy [8]. Besides the analysis of endogenous trace elements, also the investigation on artificially introduced trace metals has become an important aspect. Such metals can be either brought into organisms coincidentally (*e.g.*, in the course of intoxications), or on purpose during medical treatments or diagnostic procedures. Prominent examples for the latter type of metal uptake are gadolinium from Gd-containing contrast agents used during clinical diagnosis [9], or platinum from Pt-containing anti-tumor drugs such as cisplatin [10].

In the last years, the field of LA-ICP-MS has experienced major improvements regarding available instrumentation and used analytical methods. For example has accurate quantification been a very often targeted aspect. Starting from qualitative elemental distribution images, quantification has been optimized by time. The preparation of matrix-matched tissue standards prepared from homogenized tissue material spiked with different levels of the elements of interest has emerged to the most commonly calibration strategy [11]. However, the routine applicability of this approach is hampered by the larger workload required for preparation and characterization of the standards. Thus, the main focus in more recent work, including this PhD thesis, was set on increasing the ease

of use as well as the accuracy of the existing matrix-matched tissue approach [12]. Other current improvements are also thriving towards improved lateral resolutions. Some special cases may require sub-µm resolutions (*e.g.*, single cell imaging), achieved by the latest types of LA-washout cells [13, 14]. Based on these improvements, today's applications of LA-ICP-MS in the life sciences are very wide. High sample throughput gives the opportunity to analyze large samples in a reasonable amount of time; even investigations on multiple consecutive tissue thin-cuts to compute 3-dimensional distribution images became possible [15, 16]. On the other hand, even small samples (*e.g.*, single cells) can nowadays be analyzed exploiting the latest instrumentation [17, 18]. Not only the range of reported sample types has been wide, also the amount of analytes of interest. Due to the flexibility of ICP-MS detection, the analysis protocol can be optimized for single-element to multi-element analysis. If the multi-element capabilities of commonly used quadrupole mass analyzers are not sufficient, recently available Time-of-Flight-ICP-MS instrumentation has shown to provide excellent features with the complete analysis of a mass spectrum [18]. All these applications have led to a wide acceptance of LA-ICP-MS in the life sciences, thriving the importance of elemental analysis for biomedical studies.

3 Metals in biological tissues

3.1 Endogenous (trace) metals

Besides carbon, hydrogen, oxygen, phosphorus, and sulfur – the five major building blocks of living tissues – also components occurring in lower concentrations play important roles in a functioning organism. These are in most cases metals which can be sub-divided into two groups: Minor elements such as Na, K, Ca, and Mg which are typically present in the concentration rage of some 1,000 to some 100 µg g^{-1}, and trace elements like Cu, Ni, or Zn with average concentrations in most tissues lower than 100 µg g^{-1}. Some examples will be given below with a short explanation of their main function in organisms (in alphabetical order).

- **Cu:** With concentrations in the low µg g^{-1} range [19], copper is already a very lowly concentrated metal in biological systems. Nevertheless, it has a variety of functions as cofactor of diverse enzymes: It is located in the active center of superoxide dismutases, which are involved in the degradation of oxygen radicals and peroxides [20]. Some ATPases also employ Cu as cofactor and it is also a part of enzymes initiating the crosslinking of elastin and collagen.
- **Fe:** As one of the higher concentrated trace elements (around 100 µg g^{-1} [19]), iron is mainly involved in oxygen transport in organisms. Bound to the heme cofactor, it allows the function of the major oxygen transporter in blood – hemoglobin. It is also found in myoglobin, which is used for oxygen transport in muscle tissue. Furthermore, iron is also a cofactor for enzymes involved in the biosynthesis of steroids and vitamins. In most cases, iron may be substituted by manganese [21].

- **Mg:** Concentrations are typically in the some 100s µg g^{-1} region [19]. Mg is an element acting as cofactor in many enzymes, for example used during replication of deoxyribonucleic acid (DNA), or for the transfer of phosphate by phosphatases.
- **Mn:** Even if the concentrations in most tissues are below the µg g^{-1} range [19], manganese is an essential trace element in all higher species. Occurring as catalytic core mainly for hydrolytic reactions, it is involved in a number of key processes [22]. Exchange of iron with manganese is also possible in a number of proteins [23].
- **Na and K:** Both elements usually have the highest concentration of metals in tissues with often above 1000 µg g^{-1} [24]. The concentrations are tightly bound to each other; their function is closely related. Regulation of the Na/K balance is mainly performed by the membrane-bound Na^+/K^+ ATPase acting as an ion pump [25]. Na and K are mainly used to keep up the intercellular membrane pressure; a concentration gradient can also serve to build up a potential used for signal transduction.
- **Ni:** Even though nickel is not found in many enzymes, is function in biological systems is diverse. The trace element is found in hydrogenases, reductases, and superoxide dismutase [26]. In plants, nickel is an important part of the carbon cycle [27].
- **Zn:** After iron, zinc is the second most found trace metal in eukaryotic organisms. More than 300 proteins utilizing zinc as functional core are known today [28]. Besides catalytic functions, it also plays an important role in DNA folding during binding of transcription factors, via the well-known zinc finger domain.

These examples already demonstrate the vast variety of functions of metals in biological systems. Slight deviations in absolute and/or relative concentrations can already

significantly alter the function of the organism, which makes the analysis of trace elements in tissues a valuable aspect for modern medical research.

3.2 Exogenous trace metals

A couple of metals are very prominent for exogenous uptake into organisms. Firstly, the group of toxic trace metals including for example Pb, Hg, or Cd has to be named. Organisms can uptake these metals from the environment, leading to diverse detrimental health effects. No detailed discussion will be given on this group, as neither of these elements has been targeted during the present PhD thesis. The second group are metals introduced into organisms during the process of a medical treatment. The two most prominent elements are gadolinium and platinum. The earlier one is used as contrast agent in magnetic resonance imaging (MRI) investigations. Administered in the form of larger organic complexes (*e.g.*, Gadovist®, Bayer Schering Pharma, Leverkusen, Germany), it has already shown to accumulate in some tissue structures leading to certain pathological conditions, even a couple of years after administration [29].

The second well known example are Pt-containing cytostatic agents (*e.g.*, Platinol®, cisplatin for injection, Corden Pharma Latina, Sermoneta-Latina, Italy). Despite the fact that they have been successfully used for the treatment of many tumor types since more than four decades [30], their mechanism of action is still not fully understood; side effects are also a major concern. General function is the binding of the platinum core of an organic complex to structures of the DNA. Inter- and intra-strand cross-linking of helices will inhibit DNA transcription [31]. Furthermore, formational changes in the helical structure will trigger DNA repair mechanisms within the cell [32]. However, due to strong cross-linking these processes will be unsuccessful, leading to induction of an apoptotic cell state, resulting in cell death. Common side effects are neuro- and hepatotoxicity [33],

which can partly be modulated by alterations of the chemical structure of the drug. Thus, alternative drugs to the common cisplatin have been developed, differing in efficacy as well as the harshness of side effects.

In addition to side effects, resistance mechanisms are nowadays of great concern and thus popular target of medical research. Some tumor types only respond weakly or not at all to cytostatic treatment with cisplatin or its derivatives. To date, these mechanisms are not completely understood. Some hypotheses include the dependence of resistance to the expression of certain transcription factors, or a modulation of the apoptotic cell state [34]. Knowledge about the actuals drug distribution combined with histological and immunohistochemical investigations can help to reveal answers to such questions.

4 Scientific questions

Due to the apparently extremely high importance of trace metals for biological processes it is desirable to develop adequate analytical methods for their analysis. The field of metallomics represents a rapidly growing discipline within the life sciences. Thus, the progress made in the last years by the scientific community has been tremendous. Several aspects were also desired to be addressed within this PhD thesis; on the one hand these were analytical improvements, and on the other hand application-related questions driven by medically relevant questions.

4.1 Proposed analytical techniques

Due to the very low concentrations of most elements in biological tissues, very sensitive analytical techniques are required for their analysis. Standard techniques with such capabilities that have been optimized for investigations on biological specimen throughout the years are either x-ray based (*e.g.*, micro x-ray fluorescence (µXRF) [35, 36], particle induced x-ray emission (PIXE) [37, 38]) or mass spectrometry based (LA-ICP-MS, Time-of-Flight-Secondary Ion Mass Spectrometry (ToF-SIMS) [39]). Being very sensitive and offering the possibility of accurate quantification, µXRF is an excellent method for trace element imaging in tissues. However, for fast measurements with high lateral resolutions, the use of a synchrotron light source is necessary. This fact hampers the accessibility of the measurements especially for routine use. Also the wider application of two other methods is limited by practical considerations: PIXE and ToF-SIMS instruments can be directly situated in a laboratory, but the acquisition cost of such instrumentation is very high. One great advantage of all three methods is the high achievable lateral resolution, which enables trace element imaging at the single cell level

[40]. Furthermore, simultaneous measurement of the analytes is possible, not necessitating analyte selection prior to analysis.

Even though the usual lateral resolution of the method is lower and in usually employed quadrupole mass analyzers analysis is performed sequentially, LA-ICP-MS has emerged to the prime method used for metal imaging in biological tissues in the last years [41]. With sensitivities for most elements below µg g^{-1} scale, variable lateral resolutions between some µm and more than 100 µm, and a wide dynamic range over up to 9 orders of magnitude, this technique is perfectly fitted for a tailored type of analysis [42]. Compared to earlier mentioned methods, LA-ICP-MS is less expensive and the instrumentation can be easily implemented into an existing laboratory environment. No or only little sample preparation is required for the analysis of the investigated sample types, so that the contamination risk as well as the possibility of distorting the actual analyte concentration and distribution is kept at a minimum. The fact that no vacuum is required for sample analysis is also advantageous for the samples. Preparation of biological samples is performed in analogy to histological investigations, not interfering with the typical workflow of sample preparation. However, LA-ICP-MS is still a rather young technique; especially in the field of life sciences, vast methodological improvements are required to exploit the possibilities of this method; this mostly concerns optimization of measurement time and data acquisition, quantification strategies, and the availability for routine use.

In addition to LA-ICP-MS, another laser-based technique for chemical analysis – Laser Induced Breakdown Spectroscopy (LIBS) – was desired to be implemented for analysis of biological samples. While this technique usually has weaker detection power for metallic analytes compared to LA-ICP-MS in commercial setups, it is capable of analyzing non-metals such as H, N, and O, which are not accessible for an ICP-MS

measurement. Additionally, simultaneous analyte detection is possible, which enables extremely fast sample analysis. LIBS as a stand-alone technique has already been presented to be used for trace element imaging in tissues [43]. If higher sensitivities are required, both methods can be combined in a so-called Tandem LA/LIBS system, giving access to the full elemental range of a typical biological sample [44]. Knowledge of the bulk element distributions alongside with trace analytes is expected to further increase the value of such elemental mapping analyses.

4.2 Analytical improvements

A major part of this PhD thesis has been devoted method-related topics facing fundamental analytical questions. One of the most important challenges to be addressed was the question how to overcome matrix-effects. During LA-ICP-MS analysis, the sample composition (*i.e.*, matrix) can influence the results of the analysis in several ways. Different matrix composition may alter the laser-material interaction, ablation behavior, transport properties of the generated aerosol, as well as ionization of the analytes in the ICP. Especially in biological samples with inhomogeneous matrix composition even within one sample, these matrix-effects can be quite extensive and need to be compensated using an internal standard. The normalization of the signals to no or an unsuitable internal standard can lead to a bias of the resulting distribution images and distortion of the results. Homogeneous and/or well-known distribution of this internal standard on the complete sample is an important prerequisite for proper analysis. Furthermore, the first ionization potential of the internal standard should be comparable with the analytes of interest [45]. For tissue analysis, carbon is often used as sample inherent internal standard. However, its high first ionization potential and the fact that it is often not homogeneously distributed makes it a problematic choice. Additionally,

carbon is often transported in the form of gaseous carbon dioxide rather than as condensed particles [46]. Thus, other strategies for internal standardization need to be developed to provide more accurate elemental distribution images. Given that a suitable internal standard is available, quantification of trace elements in tissues can be targeted. Such quantitative results are necessary for determination of element uptake, as well as for inter-sample comparisons.

The first part of this PhD thesis has been dedicated to investigations on possible internal standardization strategies. The necessity of an internal standard has already been demonstrated during the author's Master's thesis [47]. Within the PhD thesis, the options for internal standardization have been further optimized. Universal internal standardization strategies were evaluated, which could not only be applied to tissue thin-cuts but also to other sample types.

Besides internal standardization, improvements on lateral resolution and strategies to determine image accuracy were another goal of this PhD thesis. In LA-ICP-MS, washout effects of the aerosol from the sample chamber can lead to image blurring and loss of image quality. This fact will create a deviation in the laser beam diameter used for analysis and the actual lateral resolution of the resulting elemental distribution image. Depending on the used sample chamber, the settings have to be adjusted to obtain an accurate image in a reasonable amount of measurement time. To allow comparison of different instrumental settings and even various systems, a quantitative metric for determination of the image quality should be established. This metric should be applicable to all types of laterally resolved analysis using LA-ICP-MS.

After developing suitable internal standardization approaches, application of the strategy for the measurement of tissue samples could be targeted. The central question was how to achieve reliable quantification of trace elements in the samples. Different approaches

were evaluated, starting from single element quantification, until multi-element analysis. Compared to existing strategies (usually matrix-matched tissue standards), the developed approaches mainly aimed at increasing the ease of use and the quantification accuracy [48]. The main issue with matrix-matched tissue standards, as they are usually applied for signal quantification by external calibration, is that their production and characterization involves large workload and the resulting quantification might not be perfectly suitable for the analyzed sample. Thus, simple, reliable, and accurate quantification approaches are considered to be very important, if the wider application of this method in the life sciences should be promoted.

Besides multi-element quantification of trace elements, also the measurement of bulk tissue components should be enabled. This was found to be best achieved by LIBS, which is capable of analyzing all biological bulk components such as carbon, hydrogen, oxygen, and nitrogen. A strategy for elemental imaging of tissue samples in a Tandem LA/LIBS system providing simultaneous analysis of trace, minor and bulk elements in one tissue sample should be developed for this purpose. Information about the distribution of non-metals was expected to add valuable information for medical purposes.

4.3 Medical questions

The first question to be answered by the developed analytical methods was centered on the distribution of platinum containing drugs in different types of tissue samples. In the past, only the effects of drug treatment have been investigated by histological and immunohistochemical investigations. However, the actual amount of drug in the tissue as well its distribution has never been known. In this work, LA-ICP-MS should be used to detect platinum in the tissues, to quantify it, and to correlate the obtained platinum distributions with histological interpretations. The method should be applied to samples

from medical experiments (*i.e.*, animal models), as well as to real clinical samples from human patients. A study on mesothelioma patients should reveal if there is an actual correlation between platinum concentration and distribution in the tumor and survival rate. In further experiments, the single-element analysis of Pt was aimed to be expanded to multi-elemental approaches, to be able to also correlate the distribution of other trace elements with histological features. Analysis of bulk elements such as phosphorus, sulphur, and nitrogen using LIBS was also expected to reveal insight into biological processes and metal-tissue interaction. Apart from trace and bulk elements, also co-localization of trace elements and proteins with complementary analysis techniques was aspired. Such multimodal imaging approaches should allow to obtain information about binding properties of trace metals *in vivo*.

5 Scientific publications

Scientific publications produced during the course of this PhD thesis can be divided into two groups. Those which are focused on analytical method development, where LA-ICP-MS was the main focus of the work, and others, which were conducted in cooperation with other researchers from different fields. Probably the most important source of cooperation were fellow PhD students in the MEIBio PhD program. The fact that nine other PhD students were also working on topics related to bioimaging opened up excellent possibilities for interdisciplinary research. Cooperation with fellow researchers also provided the opportunity for the application of LA-ICP-MS for non-biologically related questions, such as in material science. All scientific publications derived from work performed within this PhD thesis are compiled in Table 1.

Table 1: Summary of the publication output of the author during his PhD thesis (status 13/09/2016)

Peer-reviewed journal publications (first author)	10 (6)
Submitted journal publications	2
Conference proceedings	2
Oral presentations at conferences (presenting author)	12 (10)
Poster presentations at conferences (presenting author)	9 (6)
Poster prizes	2

5.1 Research performed for the PhD thesis

Before method application in any aspect could be performed, large effort had to put into analytical method development. A very important cornerstone has been already set during the Master's thesis of the author of this PhD thesis with a first key publication entitled '*Application of gold thin-films for internal standardization in LA-ICP-MS*

imaging experiments' by Maximilian Bonta, Hans Lohninger, Martina Marchetti-Deschmann and Andreas Limbeck [47]. This work has to be shortly mentioned in this aspect, as it is an important basis of the papers published during this PhD thesis. This publication shows the possibility to use thin gold layers to be used as pseudo-internal standard in LA-ICP-MS imaging experiments. It could be shown that instrumental drifts and matrix-effects occur during imaging experiments. A thin gold layer deposited on the sample surface by sputtering techniques showed to correct instrumental drifts during measurement time, matrix-related ablation differences, as well as day-to-day variations in detection sensitivity. Compared to commonly used sample inherent internal standards such as carbon or sulphur [46], this method is not influenced by the high first ionization potential of non-metallic analytes and the different transport behavior compared to metals. Herein, it could be shown that gold as pseudo-internal standard can help to increase the accuracy of acquired elemental distribution images.

In the first publication of this PhD thesis, ***'Quantitative LA-ICP-MS imaging of platinum in chemotherapy treated human malignant pleural mesothelioma samples using printed patterns as standard'***, the concept of using gold as pseudo-internal standard has been extended for quantitative elemental analysis. In addition, a novel and simple strategy for the production of standards for signal quantification has been developed: Printed patterns on paper. Usually, homogenized tissues spiked with the elements of interest are used for signal quantification [11]. However, this process of standard preparation is laborious and extensive handling of biological material is required, which might not be desired in many trace element analysis laboratories. Thus, the concept of printed patterns on paper has been introduced here. Commercially available printer ink is spiked with the element of interest and printed onto a plain paper surface in regular patterns. The absolute amount of analyte deposited on the paper can be defined

by a variation of the density of ink application; the absolute amount of platinum deposited on the paper is exactly determined by acid digestion and liquid ICP-MS measurement of some of the printed patterns. Together with gold as pseudo-internal standard, this elegant and simple quantification approach showed to deliver correct quantification results for samples with known analyte content. In this work, the printed pattern approach has been used for quantification of platinum in a human tumor sample (malignant pleural mesothelioma, MPM). Already in this first application example it could be shown that the measured platinum distribution correlated well with histological features such as areas of viable tumor tissue and blood vessel density. To the best of the authors' knowledge, this has been the first published work where the platinum distribution has been measured in a human tumor sample after cisplatin treatment.

To further improve the quantification approach, it should be extended to a multi-elemental method. Experiments to adapt the printed pattern approach for multi-element printing failed due to the insufficient susceptibility of the printer ink for too high salt concentrations. Due to high abundance of for example alkaline metals in tissues, those should also appear at an elevated concentration in the ink, leading to destabilization of the ink formulation: Another quantification approach had to be found. Already earlier, Nischkauer et al. [49] reported dried droplets on circular filter pieces to be used for the analysis of liquid samples with high matrix load. It was tested if an adaptation of such filter pieces were a suitable standard material for the quantification of trace elements in tissue samples. The final analysis method was published in the article ***'Application of dried-droplets deposited on pre-cut filter paper disks for quantitative LA-ICP-MS imaging of biologically relevant minor and trace elements in tissue samples'***. Circular filter pieces were cut out and a defined volume of an aqueous standard solution was pipetted onto the filters. Compared to the printed pattern approach, there

was no restriction with regards to the salt concentration in the standard; even concentrations of 1.0 g L^{-1} did not pose any problem. After drying, the filters were ablated with radial line scans across the full diameter of the filter piece. Averaged signal intensities yielded excellent correlations with the applied analyte amounts; quantification of homogenized tissues with known analyte concentrations was in good accordance with the actual trace element fractions. Again, the quantification was assisted by thin gold layers as pseudo-internal standard. Compared to the printed pattern approach, this method provides some advantages: The analyte concentration and the number of analytes is virtually unlimited, and no acid digestion of the standards is necessary, as the absolute amount of deposited analyte is known. This very straightforward quantification approach gave the possibility to analyze the complete range of minor and trace elements in tissue samples. This was demonstrated using a human malignant pleural mesothelioma (MPM) sample before cisplatin treatment. Seven different physiologically relevant trace elements (Na, K, Cu, Mn, Fe, Zn, Ni) were quantified in the tumor sample. Similarities and differences between the distributions allowed conclusions on their use in different enzymes. Additionally, good correlation with the histological stainings was found, demonstrating the applicability of 'elemental histology' for medical investigations.

The extensive methodological work has led to elaborate quantification methods for the analysis of virtually all possibly occurring minor and trace metals in biological tissues. To obtain a global image of the elemental constituents of biological tissues, also the analysis of bulk components like carbon, hydrogen, nitrogen, or oxygen was desired. While LA-ICP-MS as a standalone technique is not capable of analyzing hydrogen, nitrogen, and oxygen, also the analysis of carbon is connected with a couple of pitfalls. Thus, LIBS was employed for detection of the bulk sample components. Thorough optimization of the measurement conditions was required in order to perfectly harmonize

both domains of the system. Laser conditions, gas flows, and other instrumental parameters were important settings to be optimized in this frame. Simultaneous use of LIBS with LA-ICP-MS in a Tandem LA/LIBS setup reported in ***'Elemental mapping of biological samples by the combined use of LIBS and LA-ICP-MS'*** allowed parallel detection of bulk, minor, and trace elements in a single tissue sample. In a first application example, the applicability of a Tandem LA/LIBS system for the elemental mapping of biological samples has been demonstrated using a human MPM sample. Good correlation of the oxygen and phosphorus distribution indicated higher abundance of phosphate in viable tumor tissue. To the best of the authors' knowledge, it is the first publication of this type.

Besides the importance of accurate quantification and multi-element measurements, image accuracy and lateral resolution is considered a critical issue in LA-ICP-MS. Due to the nature of the technique, where a generated sample aerosol is washed out from the sample chamber using a gas stream, the measurement is affected by the aerosol washout time. Scanning the sample with elevated speed may result in signal carry-over between neighboring pixels. Scanning the sample in a slower manner will increase the total measurement time in an unnecessary and un-economic way. Thus, a metric for determination of the image quality of LA-ICP-MS images has been developed. The method has been described in ***'A metric for evaluation of the image quality of chemical maps derived from LA-ICP-MS experiments'***. Again, printed patterns were employed for this task. Copper-containing ink was printed onto paper which was free of copper. Thus, a microscopic image would not only represent the distribution of ink but also the distribution of copper on the paper. After scanning of the sample using LA-ICP-MS, the copper distribution image could be mathematically compared with the microscopic image. Higher error indicated lower image quality and *vice versa*. The metric

named area mismatch percentage (AMP) was successfully used for optimization of LA parameters with regards to scan duration and image quality. Work for this publication was completely performed during the abroad stay at Lawrence Berkeley National Laboratory.

In addition to the research articles, the author of the PhD thesis also contributed to one review article entitled ***'Recent advances in quantitative LA-ICP-MS analysis: challenges and solutions in the life sciences and environmental chemistry'***. Due to the fact that LA-ICP-MS is a rapidly emerging analysis technique, the developments in the last years have been diverse. Especially in the life sciences and the environmental sciences, accurate quantification is still a major problem. Main issue is the high variability of possible matrices which requires the use of a multitude of quantification strategies. This review discusses currently existing quantification strategies for various sample types, as well as future trends in this topic. The author of this PhD thesis contributed to this article with the chapter about quantification of trace elements in tissue samples, as well as quantification in combination with laterally resolved analysis.

5.2 Life sciences applications

The MEIBio PhD program provided an excellent source for cooperation within the field of bioimaging. Especially work performed together with Florian Brenner (research group Physical Analysis, Prof. Herbert Hutter) and with Anna Balbekova (research group Process Analytics, Prof. Bernhard Lendl) from the Institute of Chemical Technologies and Analytics of the TU Wien is worth to be mentioned.

During his PhD thesis, Florian Brenner worked on the application of Time-of-Flight-Secondary Ion Mass Spectrometry (ToF-SIMS) for use in bioimaging. An outstanding feature of ToF-SIMS is the high lateral resolution down to the 100 nm scale [39]. Even if

not necessary in most questions within the life sciences, it can be useful in special applications, like single cell analysis. However, two problems aggravate the analysis of biological samples using ToF-SIMS: Due to the high lateral resolution the measurement area is limited, which often makes it impossible to cover complete tissue sections. Secondly, quantification is severely influenced by matrix-effects (usually much stronger than LA-ICP-MS), which makes accurate quantification in inhomogeneous tissue samples almost impossible. Thus, tissue samples were investigated using LA-ICP-MS subsequently to ToF-SIMS analysis. This gave the opportunity to 'magnify' certain areas of interest, before obtaining an overall image with lower lateral resolution of the complete tissue sample. Quantification of trace elements was also performed using LA-ICP-MS, which circumvents the necessity to quantify the results from ToF-SIMS analysis. In addition to elemental analytes, ToF-SIMS also showed to be suitable for detection of small molecules, such as fragments from phospholipids. Data from this cooperation has been presented at the 16th European Conference on Applications of Surface and Interface Analysis, Granada, Spain.

Anna Balbekova performed her PhD thesis with a focus on infrared (IR) microscopy. The technique allows laterally resolved analysis of molecular features in solid samples. For example is it possible to determine the DNA content in samples, or to analyze different structural properties of proteins. The combination of IR microscopy and LA-ICP-MS analysis offered the possibility to obtain molecular as well as elemental information from a single tissue sample. Fusion of these two techniques of chemical analysis with histological investigations showed to provide an excellent data set for comprehensive investigations on biological samples. For example was it possible to correlate the platinum distribution (measured by LA-ICP-MS) in mouse tissue with apoptotic sample areas and regions with higher DNA content (both measured by IR). The non-destructive nature of

IR microscopy gave the opportunity to analyze one tissue slice with both techniques. Results from this cooperative project have been presented as a poster with the title 'Multimodal (FTIR and LA-ICP-MS) imaging of a tumor treated with Sunitinib and Cisplatin' at SPEC 2016 in Montreal, Canada. The poster has been awarded with a poster prize. A journal publication is currently in preparation.

Another cooperation has been performed with Matthias Holzlechner, also a PhD student from the Institute of Chemical Technologies and Analytics at TU Wien (Omics Technologies, Prof. Martina Marchetti-Deschmann). In this work, matrix-assisted laser desorption/ionization-mass spectrometry (MALDI-MS) is used in a multi-modal imaging approach together with LA-ICP-MS. The fusion of lipid and protein distributions with trace element information already showed to deliver valuable results. Knowledge about co-localization of platinum and proteins in tumor samples is expected to give deeper insight into the *in vivo* function of platinum containing drugs. Currently, the final measurements for a research paper are performed.

A collaboration with Prof. Per Andren from Uppsala University, Sweden was also focused on multi-modal imaging. In the publication ***'Direct imaging of elemental distributions in tissue sections by laser ablation mass spectrometry'*** in the journal Methods, Laser Ablation-MS and LA-ICP-MS have been compared regarding their suitability for elemental imaging; future possibilities and perspectives have been highlighted [50].

In a cooperation with Elisabeth Gludovacz from the Department of Biotechnology from the University of Natural Resources and Life Sciences, knowledge on liquid ICP-MS could be applied to a practical example. The author of the thesis performed measurements for the determination of trace elements in protein extracts. Together with a protein quantification, this information could be used for the determination of the occupation of

copper binding sites in biotechnologically produced proteins. The work was published in the article ***'Characterization of recombinant human diamine oxidase (rhDAO) produced in Chinese Hamster Ovary (CHO) cells'*** in the journal Biotechnology [51].

5.3 Applications for material analysis

Apart from the biosciences and geology [52], LA-ICP-MS has also a wide potential application range in material science. Steel research and industry, the semiconductor sector, the field of ceramics and many other industrial applications can benefit from the exceptional figures of merit of LA-ICP-MS. The purpose of the review article entitled ***'Improvements in the direct analysis of advanced materials using ICP-based measurement techniques'*** by Andreas Limbeck, Maximilian Bonta, and Winfried Nischkauer submitted to the Journal of Analytical Atomic Spectrometry tries to highlight the state-of-the-art as well as the future possibilities of LA-ICP-MS in this field of research. The author of this PhD thesis contributed with the chapter about depth profiling and laterally resolved analysis to this article.

An interesting imaging application in the field of materials testing is ***'Quantification of chloride in concrete samples using LA-ICP-MS'*** by Maximilian Bonta, Armin Eitzenberger, Stefan Burtscher and Andreas Limbeck published in Cement and Concrete Research [53]. Knowledge about imaging using LA-ICP-MS could be transferred to completely different sample types than the usual ones. The technique of LA-ICP-MS has been successfully applied for the measurement of bulk components of concrete.

'Development of a multi-variate calibration approach for quantitative analysis of oxidation resistant Mo-Si-B coatings using laser ablation inductively coupled plasma mass spectrometry' by Anja Cakara, Maximilian Bonta, Helmut

Riedl, Paul H. Mayrhofer, and Andreas Limbeck represents an example from the field of material sciences [54]. This paper deals with the handling of matrix-effects using multivariate calibration approaches. The author of this PhD thesis contributed with his knowledge about statistical data evaluation techniques to this publication.

Experience with dried droplet analysis using LA-ICP-MS could be applied to a question from the field of synthetic chemistry. Ionic liquids are widely used in scientific, as well as industrial applications. Chemical analysis of impurities is an important aspect, as they can essentially influence the physical and chemical properties of the product. Due to the high viscosity and non-volatility, analysis using traditional methods. In the submitted manuscript ***'Determination of the residual chloride content in ionic liquids using LA-ICP-MS'*** by Maximilian Bonta, Thomas Anderl, Alice Cognigni, Mahtab Hejazifar, Katharina Bica, and Andreas Limbeck, an analysis procedure for the quantification of remaining chloride in ionic liquids has been presented. The approach is based on easy and fast preparation of dried droplets and subsequent LA-ICP-MS measurement.

5.4 Selected publications

In the following section, four research articles, one review article, and two abstracts for posters are shown. These publications summarize the main work performed in the frame of this PhD thesis.

Quantitative LA-ICP-MS imaging of platinum in chemotherapy treated human malignant pleural mesothelioma samples using printed patterns as standard

Maximilian Bonta, Hans Lohninger, Viktoria Laszlo, Balazs Hegedus and Andreas Limbeck, *Journal of Analytical Atomic Spectroscopy*, 2014

JAAS

PAPER

View Article Online
View Journal

CrossMark click for updates

Cite this: DOI: 10.1039/c4ja00245h

Quantitative LA-ICP-MS imaging of platinum in chemotherapy treated human malignant pleural mesothelioma samples using printed patterns as standard

Maximilian Bonta,[a] Hans Lohninger,[a] Viktoria Laszlo,[b] Balazs Hegedus[bc] and Andreas Limbeck*[a]

Received 24th July 2014
Accepted 27th August 2014

DOI: 10.1039/c4ja00245h

www.rsc.org/jaas

LA-ICP-MS has often been applied for the analysis of trace elemental distributions in biological tissues. However, the strong matrix dependence of LA-ICP-MS analyses and highly variable matrix conditions aggravate reliable qualitative distribution analyses and thus for obtaining quantitative information elaborate quantification strategies have to be applied. In this work printed patterns on paper with thin gold layers as pseudo-internal standard have been proposed as an alternative approach to the commonly used matrix-matched tissue standards. Besides a major reduction of the workload for standard preparation the presented method allows for compensation of instrumental drifts during measurement as well as a reduction of matrix related effects. The developed method has been verified using matrix-matched tissue standards (deviations from the actual metal content less than 5% with relative standard deviations of less than 7%) and applied to platinum imaging on human malignant pleural mesothelioma samples after administration of individuals with platinum containing cytostatic drugs.

Published on 29 August 2014. Downloaded by Universitätsbibliothek Bern on 01/10/2014 14:04:44.

Introduction

In clinical applications platinum containing drugs (*e.g.* cisplatin, carboplatin and oxaliplatin) are used to treat a large variety of cancer types. Being known since the early 1970s as cytostatic drugs[1–3] the mechanism of interaction during cell proliferation has been described in detail.[4] However, the uptake and distribution of platinum drugs within the tumor tissue is still not fully understood. Due to major side effects of platinum containing drugs the dose should be kept as low as possible[5] and therefore investigations on platinum uptake are of great medical value. Revealing platinum distributions in tumorous tissue of individuals treated with the aforementioned drugs can contribute to a better understanding of the processes of the therapeutic effect of these drugs. The ultra-trace capability of ICP-MS combined with laterally resolved analysis using laser ablation gives the possibility of depicting the distribution of major constituents as well as trace elements in biological tissues (bioimaging), but only a limited number of studies describe platinum distributions in tissues using LA-ICP-MS imaging after the uptake of platinum containing drugs.[6–9]

Due to the fact that LA-ICP-MS measurements are linked to a variety of problems concerning sample and measurement conditions even reliable qualitative analyses may need a correction of the monitored raw signals. The major concerns are compensation of instrumental drifts or matrix-related ablation differences within one sample mostly accomplished by internal standards. Often the use of sample inherent matrix elements such as carbon as internal standard has been reported in the literature.[10,11] However, due to the strongly varying constitution of biological tissues even within single tissue sections the use of carbon as internal standard does not represent a suitable strategy for complete compensation of all possible changes in absolute signal intensity as changing structures within the tissue may exhibit changed carbon content. Additionally, due to the weak ionization behavior of carbon its use as internal standard does not seem to be an optimal choice. Furthermore, carbon may be transported both as particulate matter as well as in a gaseous state. This may lead to altered transport behavior compared to the analytes of interest which are predominantly transported in the form of aerosol particles.[12] Due to the possible inhomogeneity of matrix elements leading to distortion of the resulting normalized image the use of layers applied on or beneath the sample for signal normalization has been proposed as a possible improvement for LA-ICP-MS measurements. Other approaches that have been recently proposed are

[a]*Institute of Chemical Technologies and Analytics, Vienna University of Technology, Getreidemarkt 9/164-IAC, 1060 Vienna, Austria. E-mail: andreas.limbeck@tuwien.ac.at*

[b]*Department of Thoracic Surgery, Comprehensive Cancer Center, Medical University of Vienna, Austria*

[c]*MTA-SE Molecular Oncology Research Group, Hungarian Academy of Sciences, Budapest, Hungary*

Published on 29 August 2014. Downloaded by Universitätsbibliothek Bern on 01/10/2014 14:04:44.

additionally applied thin polymeric layers doped with metals[13] or metallic layers on the sample surface.[14] The mentioned pseudo-internal standards have shown to compensate for matrix- or instrumentation-related variations in absolute signal intensity and can therefore be considered a major improvement in LA-ICP-MS imaging experiments.

Obtaining reliable quantitative information using LA-ICP-MS is a more challenging task and therefore in the past only a limited number of strategies for quantification have been described. The major problems for accurate quantification are matrix related ablation differences by the laser, varying transport efficiency of the transported material and changing plasma conditions due to the uptake of varying sample materials. Signal quantification often relies on the use of matrix-matched tissue standards. Tissues are homogenized, spiked with the elements of interest and frozen, respectively. The frozen tissue standards are cryo-cut to a few μm thick sections and the actual amount of analyte in the tissue is determined after digestion using ICP-MS.[15–17] A crucial aspect in the preparation of matrix-matched standards is the homogeneity of the investigated analytes. However, the often highly variable sample conditions within single sections of the analyzed tissue are still a problem since homogenized standards cannot represent the varying tissue properties. Therefore alternative methods have been developed to overcome the limitations of matrix-matched standards and furthermore to ease the process of standard manufacturing. For example gelatin standards have been used as a replacement for matrix-matched standards,[6] sol–gel standards have been produced[11] or tissues have been embedded in resins to obtain a match of the standard material and sample.[18]

In this work we present a novel approach for quantification of platinum in human malignant pleural mesothelioma (MPM) samples based on the use of gold layers as pseudo-internal standard in combination with printed patterns as an alternative to matrix-matched standards for accurate and easy signal quantification in imaging experiments.[19] Systematic optimization of the parameters has been carried out to yield best results in terms of achievable spatial resolution and measurement certainty. Using conventionally prepared matrix-matched tissue standards the validity of the proposed quantification approach was confirmed followed by the application to samples of unknown platinum content. The investigated samples are of high medical interest as MPM is a devastating malignancy with dismal prognosis and platinum based chemotherapy is the most widely used therapeutic modality.[20] Unfortunately, MPM often shows therapy resistance and thus the analysis of intratumoral drug distribution is of outmost importance in this disease. However, there is no clinical data available which describe tissue platinum concentrations in MPM.

Experimental

Chemicals

For all experiments ultra pure water (resistivity 18.2 MΩ cm) dispensed from a Barnstead EASYPURE II water system (ThermoFisher Scientific, Marietta, OH) was employed. Conc. HNO_3 (p.a.), conc. HCl (p.a.) and 30% (v/v) H_2O_2 (p.a.) were supplied by Merck, Darmstadt, Germany. The liquid standards for ICP-MS measurements (platinum standard for ICP, 1 g L^{-1} in 5% (v/v) HCl and indium standard for ICP, 1 g L^{-1} in 5% (v/v) HNO_3) were purchased from Sigma-Aldrich, Buchs, Switzerland. For tuning of the instrument in liquid mode 'Tune B' solution supplied by Thermo Fisher Scientific, Bremen, Germany was employed. Printer ink for refill purposes was purchased from refill24, Vienna, Austria.

Instrumental

For the presented measurements quadrupole ICP-MS instrumentation (Thermo iCAP Qc, ThermoFisher Scientific, Bremen, Germany) was used. Qtegra software provided by the manufacturer was used for data acquisition. A commercially available laser ablation system (New Wave 213, ESI, Fremont, CA) with a frequency quintupled 213 nm Nd:YAG laser was employed for solid sampling experiments. The used washout cell is always held above the actual ablation site allowing for fast washout times below one second and avoiding the risk of signal distortions resulting from the slowly washed out sample material. Helium was used as carrier gas for cell washout and was subsequently mixed with Argon make-up gas upon introduction into the plasma. The tune settings of the MS instrumentation were optimized using a sputtered gold layer for a maximum ^{197}Au signal prior to each experiment; typical parameters used for the measurements of solid samples are shown in Table 1.

The imaging experiments were carried out with laser beam diameters varying from 10 to 100 μm. For all experiments the used laser energy and firing rate were adjusted to the analyzed materials to yield complete but yet controlled ablation behaviour. The sample material was ablated using line scan patterns with adjoining lines while each line was ablated in the same direction. Before firing the laser onto the sample surface it was allowed to warm up for 20 s. After placing the sample in the laser ablation device the sample chamber was purged with helium at a flow of 1 L min^{-1} for 20 min before measurement.

Table 1 Typical parameters of the solid sampling experiments

Laser ablation system	New Wave 213
Average fluence	4.9 J cm^{-2}
Laser diameter	10–100 μm
Scan speed	25–100 μm s^{-1}
Repetition rate	10 Hz
Carrier gas flow (He)	1 L min^{-1}
Make-up gas flow (Ar)	0.8 L min^{-1}
ICP-MS instrumentation	**Thermo iCAP Q**
Aux. gas flow	0.8 L min^{-1}
Cool gas flow	14 L min^{-1}
Dwell time per isotope	10 ms
RF power	1550 W
Cones	Ni
Mass resolution	$m/\Delta m = 300$
Measured isotopes	^{13}C, ^{31}P, ^{34}S, ^{194}Pt, ^{195}Pt, ^{196}Pt,^{197}Au

This journal is © The Royal Society of Chemistry 2014

Published on 29 August 2014. Downloaded by Universitätsbibliothek Bern on 01/10/2014 14:04:44.

Besides three platinum isotopes (^{195}Pt was used for data evaluation, the signals for the other isotopes were used for data verification and always showed comparable patterns) and ^{197}Au as the pseudo-internal standard the intensities of the isotopes ^{13}C, ^{31}P and ^{34}S were recorded to correlate the obtained distribution information with medical knowledge and morphological structures (data not shown).

Sample introduction for ICP-MS measurements was performed employing a Peltier cooled spray chamber equipped with a concentric quartz glass nebulizer; an ESI SC-2DX autosampler (Elemental Scientific, Inc., Omaha, NE) was used for automated sample introduction. The instrumental parameters were optimized for a maximum ^{115}In signal and a ^{140}Ce^{16}O/^{140}Ce ratio below 1.9% on a daily basis using a standard tuning solution. The amount of doubly charged ions was measured by the ^{137}Ba^{++}/^{137}Ba^{+} ratio which was below 3% for all performed experiments. Measurements were carried out employing the standard measurement parameters recommended by the manufacturer.

Preparation of printed standards

For the preparation of printed patterns conventional black printer ink used for refill purposes was spiked with platinum to a final concentration of 25 mg L^{-1}. The required amount of platinum standard solution was filled into a PE falcon tube and the solvent was allowed to evaporate using careful heating to 80 °C for one hour. After complete evaporation of the solvent and cooling of the tube a defined amount of black ink was added and mixed thoroughly. Using a syringe the original inkjet cartridge was filled with the prepared platinum containing ink. Several cycles of filling and depleting the cartridge were performed to obtain uniform distribution of platinum containing ink within the cartridge.

Squares of 1 × 1 cm in black colour and print density settings ranging from 20 to 100% were designed in Microsoft PowerPoint 2007 (Microsoft Corp, Redmond, WA). The patterns were printed on high gloss photo paper (280 g m^{-2}; Office Depot Europe B.V., Venlo, The Netherlands) using an HP deskjet 4200D office inkjet printer (Hewlett-Packard, Palo Alto, CA) equipped with the modified black cartridge at five different concentration levels. Print resolution was set to 600 × 600 dpi to obtain the highest possible lateral resolution of the printed patterns. All other printing parameters were optimized to yield optimal reproducibility of the prints. The used patterns were all printed subsequently and with a new inkjet cartridge to avoid problems concerning reproducibility due to clogging of the print head or other technical issues.

Preparation of matrix matched standards

Matrix matched tissue standards were prepared as described by Hare *et al.*[13] The procedure was slightly altered to obtain maximum compatibility of the method with the used tissue types. Porcine liver, kidney and brain (*Sus scofra domestica*) were obtained at a local market. After homogenization of the organs using a hand-held blender (AEG, Frankfurt am Main, Germany) 10, 20 and 40 μL of platinum standard solution for ICP (1 g L^{-1} Pt in 5% (v/v) HCl was purchased from Sigma-Aldrich, Buchs, Switzerland) were added to three portions of 5 g of each tissue to reach nominal platinum amounts of 5, 10 and 20 μg g^{-1} in the homogenized tissue; the mixtures were thoroughly homogenized for optimal distribution of the standard within the tissue. One additional portion of each tissue was not spiked allowing for blank correction. The homogenized matrix-matched tissue standards each were shock-frozen by dropping amounts of approx. 100 mg into liquid nitrogen. Until further analysis the standards were stored at −70 °C to prevent material degradation.

Preparation of samples for LA-ICP-MS measurements

The frozen pellets were attached to a sample holder using Shandon Cryomatrix (Thermo Scientific, Cat. no. 6769006) and 10 μm sections were cut using a cryotome (Leica CM3050 S) at −20 °C. The sections were collected on Superfrost ULTRA Plus glass slides (Thermo Scientific, Cat. no. 1014356145) and dried at room temperature. After attaching the tissue sections on glass slides the samples were sputtered with a thin gold layer used as pseudo-internal standard for LA-ICP-MS analysis. The coating process was performed using an Agar B7340 sputter coater (Agar Scientific Limited, Essex, UK) equipped with a gold sputtering target. Distance from the sample to the gold target was adjusted to 4 cm before every sputtering process. The time required for metallization was optimized in prior experiments and kept constant for every experiment to obtain comparability of different analyses. The sputtering current was set to 10 mA and before sputtering the sample cell was evacuated to a pressure of exactly 0.1 mbar. A sputtering time of 10 s (timer controlled) was used for the prepared samples. Reproducibility of the prepared gold layers has been demonstrated recently.[19]

Pieces of the printed patterns approximately 5 × 2 mm in size were cut out using ceramic scissors to prevent metallic contaminations and attached to microscopic glass slides using double sided tape for LA-ICP-MS measurements. Metallization with thin gold layers was performed in the same manner as described above for the tissue samples.

Sample pretreatment for ICP-MS measurements

To accurately determine the concentrations of platinum in tissue standards and in printed pattern samples digestion and ICP-MS measurement of the samples was performed.

Frozen pellets of the matrix-matched tissue standards (approx. 100 mg each) were allowed to thaw, weighed and completely digested in PE sample tubes with 1 mL of conc. HNO_3 and 30% H_2O_2 mixed in a ratio of 4 : 1 (v/v) in the presence of 100 μL conc. HCl to aid complexation of platinum. After a reaction time of 2 h at 40 °C in an ultrasonic bath the mixture was diluted to an overall volume of 9 mL with ultra pure water resulting in clear solutions. Aliquots of 250 μL of each sample were mixed with 250 μL of conc. HCl and diluted to 9 mL using 1% HNO_3 to be measured using ICP-MS.

The platinum amounts on the printed patterns were determined by digesting printed squares of 1 × 1 cm in 2 mL of conc. HNO_3 and 30% H_2O_2 mixed at a ratio of 4 : 1 (v/v) and 200 μL of

Published on 29 August 2014. Downloaded by Universitätsbibliothek Bern on 01/10/2014 14:04:44.

conc. HCl. Sonication at room temperature of the samples was used to aid the digestion process. After the reaction time of 2 h 500 μL of conc. HCl were added to the mixture and it was diluted to an overall volume of 9 mL using ultra pure water. Aliquots of 1 mL were diluted with 1% HNO_3 to 9 mL for ICP-MS measurements. The concentration determination was carried out in five replicates of sample preparation for every concentration level on the one hand to minimize errors made by sample preparation and on the other hand to demonstrate the reproducibility of the printing process. Indium standard solution was added to all measured samples for use as internal standard to a final concentration of 1 ppb. Aqueous platinum calibration standards in the range of 0.1 to 2 ppb were used for signal quantification.

Immunohistochemistry

The tissue sections were prepared from a snap frozen surgical tumor specimen. The 61 year old male MPM patient received three cycles of cisplatin–pemetrexed chemotherapy prior to the operation. The surgery was performed 26 days after the last cisplatin treatment. Informed consent was obtained from the patient and all procedures were approved by the Institutional Ethics Committee (EK #904/2009).

Air-dried section was washed in phosphate buffered saline (PBS), blocked with Ultra V Block solution for 10 minutes, then incubated with monoclonal mouse anti-CD34 antibody (IMGENEX; clone: ICO-115) for 1 hour at room temperature. After washing with PBS, specific antibody binding was visualized with the Ultravision LP Detection System (Thermo Scientific, Cat. no. TL-125-HL) and Liquid DAB + Substrate Chromogen System (Dako, Cat. no. K3468), according to the manufacturer's instructions. The section was counterstained with Gill's hematoxylin (Merck, Cat. no. 1051740500), dehydrated and embedded in Entellan (Merck, Cat no. 107960). Finally the slide was scanned with a Tissue FAXSi plus system (Tissue Gnostics).

All optical images were made using a Leica DM2500M microscope (Leica Microsystems, Wetzlar, Germany) in reflective-light mode.

Results and discussion

Optimization of measurement conditions

To obtain high quality images using LA-ICP-MS a careful optimization of the measurement parameters is required. As described by Lear *et al.*[21] two crucial parameters are quadrupole dwell time and laser scan speed.

For an optimal compromise between image quality and acquisition time the scan speed employed at a certain laser beam diameter is a critical parameter. The effect of laser scan speed on image quality has been studied using a line pattern printed with platinum containing ink. The pattern consisted of five lines with 500 μm width and 500 μm spaces between the lines. Laser scan speeds of 25, 50 and 100 μm s^{-1} have been investigated and evaluated in terms of cell washout and related image blurring effects. A constant laser beam diameter of 50 μm was employed. Representative signal/time plots of ^{195}Pt are summarized in Fig. 1. Interpreting the derived results it has to be considered that slight signal changes on the plateaus result from the printing process as indicated in the first row of the figure showing a microscopic image of the print pattern.

The vertical dashed lines at every line series indicate the nominal width of one printed line *i.e.* the distance of 500 μm covered by the laser beam in the corresponding time frame for each scan speed. The patterns at 25 and 50 μm s^{-1} exhibit nearly optimal correlation of the platinum peak widths with the nominal line widths whereas a scan speed of 100 μm leads to significant broadening of the printed line. Considering this line being a feature in a real sample it would appear larger than it actually is. Furthermore the platinum signal does not decrease to the background level between the printed lines as it does at 25 and 50 μm s^{-1}. This fact may lead to wrongly assumed concentrations and blurred images. Considering the blurring effect due to the cell washout time and the 'broadening' of actual features a scan speed of 50 μm s^{-1} seems to be the most appropriate corresponding to a 1 : 1 ratio of laser beam diameter and scan speed for other laser beam diameters. Lower scan speeds than 50 μm s^{-1} do not seem reasonable due to longer measurement time and no major improvement of the resulting data quality.

The second crucial parameter for image quality and reliability of the obtained data is the quadrupole dwell time. Shorter quadrupole dwell times will lead to an increased number of acquired data points per pixel in an image; on the other hand longer dwell times will cause better signal stability. Therefore the optimal dwell time needed to be evaluated for the performed experiments. For critical assessment of the quadrupole dwell time a printed area on paper with platinum containing ink was employed; for each evaluated dwell time five lines of 60 s in length were measured. A laser scan speed of 50 μm s^{-1} at 50 μm laser beam diameter was used for the experiments. For evaluation of the optimal quadrupole dwell time the relative standard deviation (RSD) of the absolute signal intensities during one second was calculated as the signal acquired during one second would be averaged for image construction. Minimizing the signal RSDs will result in an increased reliability of the resulting data and thus allow even to differentiate between regions with similar intensity; at higher RSDs the signal intensity of one measured point may not be significantly different from the one of another point even if the measured averages may suggest so. At dwell times from 1 to 50 ms the relative standard deviation (RSD) of the absolute signal for ^{195}Pt was calculated. The average signal RSDs varied between 31.1% for 1 ms dwell time and 16.6% for 10 ms dwell time with standard deviations of the mean values between 1.0 and 1.5% ($n = 60$). Dwell times below and higher than 10 ms exhibited higher signal RSDs than the minimum value at 10 ms. Lower dwell times offer more data points per second but higher RSDs due to increased fluctuations in signal acquisition and at higher dwell times the number of data points acquired during the evaluation time of one second is decreased again resulting in higher RSD

 This journal is © The Royal Society of Chemistry 2014

Published on 29 August 2014. Downloaded by Universitätsbibliothek Bern on 01/10/2014 14:04:44.

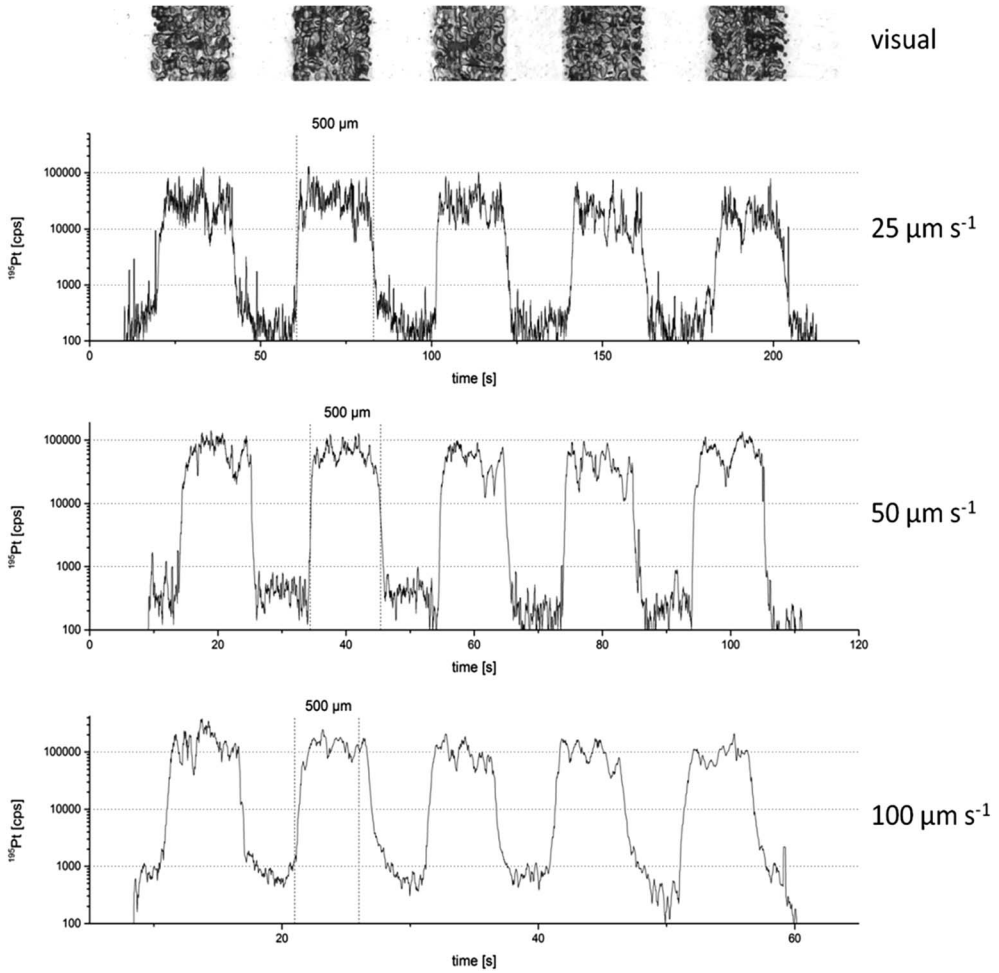

Fig. 1 Printed line pattern measured with different laser scan speeds at a constant laser beam diameter.

values. At 10 ms dwell time the number of data points acquired for each of the seven isotopes is 12 being a sufficient value for good statistical significance of the calculated averages as in the final image one second of acquired signal will be averaged for every pixel value.

Calibrations for signal quantification using the printed patterns on paper

Application of the printed pattern approach for signal quantification requires knowledge of the amount of deposited platinum on the printed patterns. As the actual amount of deposited ink on the printed patterns is unknown the platinum concentrations had to be determined *via* acid digestion of the patterns and ICP-MS measurement of the derived solutions. As platinum is only deposited on the surface of the print patterns the concentration of platinum cannot be determined as a mass per mass concentration (µg g^{-1}). The alternative notation of the platinum concentration being suitable for the printed patterns is mass per area (ng cm^{-2}).

The liquid determination of deposited platinum on the printed patterns showed low relative standard deviations of less than 5% for each concentration level. Considering that this value also reflects variations from sample preparation and ICP-MS measurement the low variance of the repetitive sample measurements indicates a good reproducibility of the printing process. Thus, also equality of the ink deposition on the different patterns can be declared and the concentration determined by ICP-MS measurements will be representative for the solid sampling measurements. The obtained signal intensities were between 100 000 and 1 000 000 cps for the lowest to the highest concentration level with a platinum signal of around 400 cps for blank samples resulting in a limit of detection (LOD) of 2 ng L^{-1} in the solutions and 0.01 ng cm^{-2} on the printed patterns, respectively. The derived concentrations for the printed standards were between 2 and 20 ng cm^{-2} platinum on the patterns.

The signals obtained from the LA-ICP-MS analysis of the same print patterns should correlate linearly with the concentrations of platinum determined using ICP-MS. For the measurements of the printed standards a laser energy setting of 50% at 50 µm laser beam diameter, 50 µm s^{-1} scan speed and a repetition rate of 10 Hz were applied to ensure controlled ablation behavior as well as complete ablation of

Published on 29 August 2014. Downloaded by Universitätsbibliothek Bern on 01/10/2014 14:04:44.

the applied ink. As platinum is only contained in the ink and not in the paper the whole sample material need not be ablated to reach quantitative results. To ensure that all the platinum containing material had been ablated in the first ablation cycle the pattern was ablated a second time on the same position resulting in platinum signals at the baseline level for all monitored platinum isotopes. To overcome instrumental drifts, matrix related ablation differences and day-to-day signal variation normalization of the analyte signals to the pseudo-internal standard gold were applied. The raw signal for ^{195}Pt was between 5000 and 50 000 cps for the standards printed on paper with 200 cps for the background signal resulting in a normalized signal of 0.001 and 0.01 units, respectively. The average normalized platinum concentrations showed a RSD below 5% ($n = 5$) for every concentration level resulting in statistically significant differences between the signals of the different concentrations. A linear regression with the ^{195}Pt signals normalized to the ^{197}Au signals obtained from five replicate measurements and the platinum amount per area of the printed patterns was obtained ($R^2 = 0.9996$). The calibration function has a negligible offset on the y-axis underlining the quality of the calibration.

Characterization of matrix-matched tissue standards

The applicability of the proposed quantification method using printed patterns was verified using in-house prepared matrix-matched standards of three different tissue types (porcine brain, liver and kidney) exhibiting distinct differences in their composition and tissue properties.

Prior to LA-ICP-MS measurements the exact concentration of platinum in the prepared liver, brain and kidney tissue samples was determined using ICP-MS. The measurements were carried out in five separately prepared replicates for every concentration level to minimize variations due to sample preparation and measurement uncertainty. The observed signals were in the order of 400 cps for non-spiked blank samples and between 200 000 and 2 000 000 for all tissue digests. Signal quantification was performed using external calibration with aqueous standards resulting in a LOD of 2.0 ng L^{-1} in the liquid samples and 1.6 ng g^{-1} in the matrix-matched tissues. The relatively small relative standard deviations of the replicates less than 4.1% for every sample state that not only the sample preparation was very reproducible but also that the homogeneity of the bulk concentrations is sufficient. The concentrations determined for the matrix-matched standards are in good agreement with the expected platinum concentrations in the real samples[6] ranging from 3.09 μg g^{-1} for the lowest to 27.14 μg g^{-1} for the highest platinum concentration.

Furthermore, homogenous distribution of the questioned analytes within the material is imperative to ensure that the results of laser ablation measurements are representative of the bulk concentration in the tissue samples. To prove the equal distribution of platinum on single slices of the matrix-matched tissue spot measurements were performed. A pattern consisting of nine neighboring spots with 50 μm laser beam diameter was measured on five positions distributed across the whole tissue slice. Dwell time per spot was 2 s to ensure complete ablation of the sample material. A firing rate of 10 Hz and a laser energy setting of 50% were chosen for the measurements. The patterns were placed nearby the left, right, upper and lower edges and in the middle of the tissue slice, respectively, to yield information about the distribution of platinum.

To test if the distribution of platinum was even on the whole tissue section the average signals of the nine spots on each of the five different locations across the tissue slice were compared using one-way ANOVA (analysis of variances). Statistical analyses were carried out using the software package DataLab (v.3.530, Epina GmbH, Pressbaum, Austria).[22] Slices of all different tissue types and at the three chosen concentration levels were tested; the ANOVA for each of the nine datasets (three tissue types with three concentration levels each) do not indicate a significant difference between the compared means at a 95% level of significance. Prior to ANOVA Levene's test ($p < 0.2$) was used to check for homogeneity and equality of variances of each processed dataset as a prerequisite for ANOVA. Results of the statistical analyses indicate that the platinum distribution within one slice is homogenous. Furthermore gold normalization did not affect the results of the statistical analyses proving that also the gold deposition within one sample is homogenous.

In addition to the measurements on one tissue slice the equality of the platinum signals on consecutive tissue slices was tested. Not only the homogeneity of the platinum distribution within the tissue but also the possibly differing sample thicknesses can be investigated using this experiment. Patterns of nine single spots with the same laser settings as described before were drawn on four different tissue slices of the same tissue and the same bulk concentration in each. ^{195}Pt as well as the gold normalized platinum signal was considered for data analysis. The mean values for every tissue slice were also compared using one-way ANOVA as described above. The statistical analysis does not indicate a difference in the four means in each of the three concentration levels and three tissue types at a 95% level of significance for both normalized and non-normalized data. The results of the statistical analysis point out that the platinum distribution on different tissue sections does not differ with any statistical significance.

Measuring tissue slices using LA-ICP-MS the results are in a mass per area unit when using the printed pattern calibration approach for signal quantification. To compare the concentrations determined by LA-ICP-MS with the bulk concentrations of platinum in the tissues the units need to be converted. Using the density of the investigated tissues the mass per area concentration of platinum on the printed pattern standards can be changed into a mass per mass concentration for the tissue slices at a known tissue thickness. The density of the matrix matched tissue standards was determined based on the protocol by DiResta *et al.*[23] using a pycnometric method. The determined densities are 1.0505 ±

 This journal is © The Royal Society of Chemistry 2014

Published on 29 August 2014. Downloaded by Universitätsbibliothek Bern on 01/10/2014 14:04:44.

0.0036 g cm^{-3} for kidney, 1.0220 ± 0.0109 g cm^{-3} for liver and 0.9508 ± 0.0152 g cm^{-3} for brain.

Variation of the laser beam diameter for the investigation of the effect of altered plasma load to the platinum signal

Varying material intake and changing particle size distributions in the plasma may change the ionization efficiency of the analytes.[24] Higher matrix load of the plasma can potentially lead to delayed ionization resulting in effectively decreased analyte detection. To investigate the applicability of this effect on the investigated tissue samples matrix-matched liver tissue has been analyzed applying different laser beam diameters. Six different laser beam diameters ranging from 10 to 100 μm have been used and the platinum signal as well as the gold signal has been recorded for data evaluation. The expected outcome is that with an increased laser beam diameter the detected signal should constantly increase due to a higher amount of analyte transported into the plasma. Normalizing the raw platinum signal to the ablated area should result in equal analyte signals when no effects of the altered plasma load to the ionization behavior would appear. Fig. 2 shows the platinum raw signals normalized to the ablated area. Due to matrix effects linked with the aforementioned delayed ionization of the analytes the area normalized platinum signal decreases. The same effect of decreasing signal is reflected in the area normalized signal of the sputtered gold layer. As a consequence, when normalizing the platinum to the gold signal the differences between the laser beam diameters are reduced as the ionization of platinum and gold as pseudo-internal standard has shown to be affected in the same manner by the described matrix effects.

The results underline the suitability of thin gold layers for signal normalization showing that gold normalization can compensate changed ionization behavior due to altered material intake into the plasma. Furthermore it could be shown that laser beam diameters can be easily varied in a certain range without needing new calibrations for more flexible analyses in terms of accessible lateral resolutions.

Applicability of printed patterns for signal quantification on matrix-matched tissue standards

To test the applicability of the printed pattern approach to tissue samples the set of matrix-matched standards characterized before was analyzed using LA-ICP-MS and quantified using the printed pattern calibration. The signals of three adjacent lines each 2 mm in length were averaged for signal quantification to reduce the effect of random signal fluctuations. For each concentration level and tissue type the described line patterns were measured on three different positions on the tissue to calculate a measurement uncertainty.

Calculating regressions from the platinum intensities before gold normalization showed that the slopes for the three tissue types varied significantly between 863.4 arbitrary units for brain over 706.3 arbitrary units for kidney to 494.1 arbitrary units for liver indicating large matrix differences between the tissue types. After gold normalization the slopes have comparable values not differing more than 5% from their mean value. Thus, the effectiveness of gold layers as pseudo-internal standard is proved. Gold has thereby shown to compensate not only matrix related ionization differences (see previous item) but also ablation and transport related alterations in absolute signal intensity derived from changed matrix conditions.

Using the regression function obtained from the measurement of the printed pattern calibration amount-per-area concentrations of platinum on the tissue slices were calculated. Derived findings were in the order of 3 to 30 ng cm^{-2}.

Using the determined material densities of the matrix-matched standards an amount-per-mass concentration was calculated using the known tissue thickness of 10 μm. The calculated concentrations in the non spiked tissue samples were always below the limit of detection of 0.1 μg g^{-1}. The determined bulk concentrations were found in the range between 2.9 and 27.5 μg g^{-1} with good relative standard deviations around 5% for three replicate measurements of every sample. A comparison of the bulk values determined by ICP-MS and the values determined by laser ablation measurements is presented in Fig. 3 demonstrating the applicability of

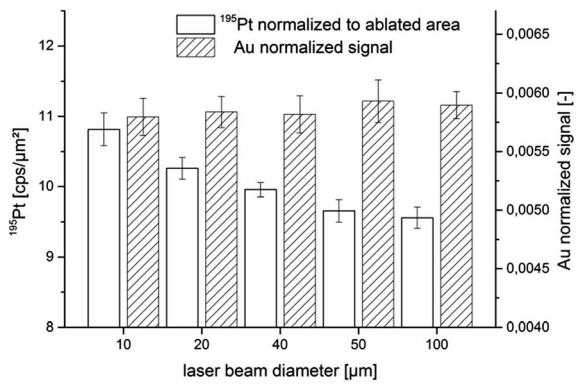

Fig. 2 Platinum raw signals normalized to the ablated area and gold normalized platinum signals on platinum spiked liver measured with different laser beam diameters.

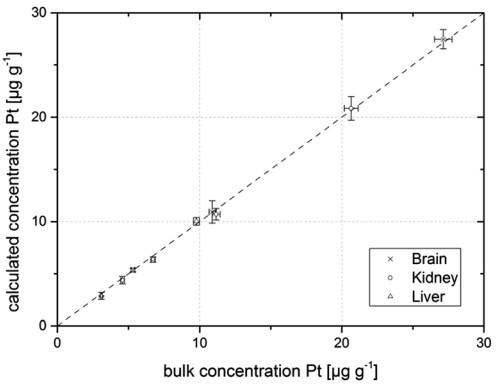

Fig. 3 Comparison of platinum bulk concentrations and results from LA measurements with quantification from the printed pattern approach. The dashed line represents the identity of the actual and the calculated concentration.

Published on 29 August 2014. Downloaded by Universitätsbibliothek Bern on 01/10/2014 14:04:44.

the proposed quantification method for tissue samples with unknown platinum concentration.

Measurement of human malignant pleural mesothelioma tissue sections

Imaging of human malignant pleural mesothelioma sections was performed using a laser beam diameter of 40 μm to increase the obtained lateral resolution of the resulting image. A scan speed of 40 μm s^{-1} was chosen to keep the scan speed at an equal value as the laser beam diameter; ImageLab[25] (v.0.40, Epina GmbH, Pressbaum, Austria) was used for image processing. Fig. 4 shows the analyzed tissue section with images of consecutively cut sections after immunohistochemical staining.

In the image differences of the platinum concentration of more than one order of magnitude can be identified. While some areas of the tissue section exhibit only platinum concentrations of below 1 μg g^{-1} on other areas more than 10 μg g^{-1} of platinum in the tissue can be found. The patterns of the platinum distribution correlate well with the results from the staining. In order to correlate the obtained platinum distribution with the intratumoral heterogeneity of blood vessel density and with the distribution of viable tumor cells a higher magnification area is presented in Fig. 5.

The high platinum concentration overlaps with the regions where there are no viable tumor cells left. In contrast viable tumor cell (blue nuclei) and blood vessel (brown stain) rich regions do not contain any platinum.

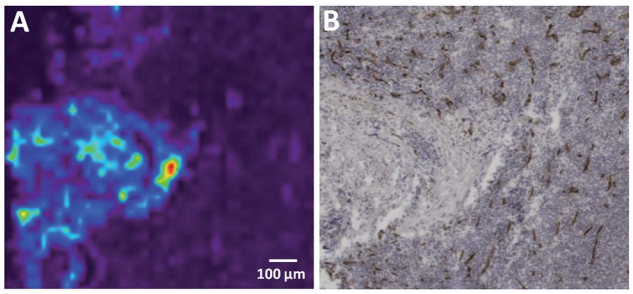

Fig. 5 Magnification of the marked area in Fig. 4 for intratumoral distribution analysis of platinum and tumor vasculature. (A) The high lateral resolution of platinum imaging provides the opportunity to characterize the platinum concentrations in small clusters of cells. (B) Note the same area in the CD31 labeled and hematoxylin counterstained high magnification microscopy field.

Our initial comparative analysis of platinum distribution and immunohistochemical markers in MPM tissue sections demonstrates that the proposed methodology is robust enough to investigate the high resolution intratumoral heterogeneities in biological parameters and platinum concentrations. This is a pivotal step in understanding the parameters that influence therapeutic sensitivity of MPM tumors in platinum based chemotherapy.

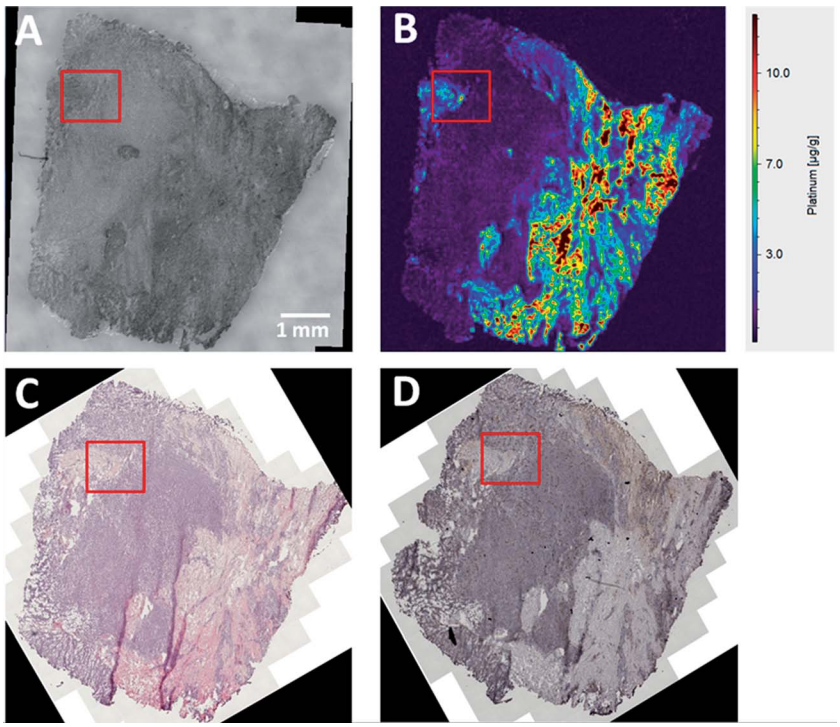

Fig. 4 The analyzed MPM tissue section. (A) Light microscopy image of the LA-ICP-MS analyzed section prior to the measurement. (B) The quantitative platinum distribution based on the printed pattern calibration. (C) A consecutive section stained with hematoxylin and eosin. (D) The next section was stained for blood vessels (anti-CD34 antibody) and counterstained with hematoxylin. Note the similar overall tissue structure in the consecutive sections that makes the accurate alignment of sections with different imaging information possible. The area magnified in Fig. 5 is marked in the images.

This journal is © The Royal Society of Chemistry 2014

Published on 29 August 2014. Downloaded by Universitätsbibliothek Bern on 01/10/2014 14:04:44.

Conclusions

In this work the use of printed patterns on paper with ink containing platinum as the analyte of interest in combination with thin gold layers as the pseudo-internal standard proved to be comparable with commonly used matrix-matched standards. Due to the major reduction of the workload for standard preparation not only the time required for the experiments can be drastically reduced but also the reliability of the obtained results may be improved due to the use of standards at an increased number of concentration levels. Furthermore printed patterns can be easily stored with no need for special sample treatment compared to tissue samples. While in the presented experiments the focus was set on the quantification of platinum it is possible to spike conventional printer ink with any analyte of interest; even multi-elemental inkjet standards can be manufactured to allow quantification for a large range of analytes in tissues with only one printed standard. Thus, the presented method can be a versatile and easy way for reliable quantification in LA-ICP-MS imaging experiments in different bioanalytical and medical questions.

Acknowledgements

All authors would like to thank Balazs Dome and Mir Alireza Hoda for support in sample collection, interpretation of the medical implications and manuscript proof-reading. Furthermore thanks needs to be addressed to Elisabeth Eitenberger for her assistance during gold sputtering. M.B. wants to thank the MEIBio PhD program of the Vienna University of Technology for providing a scholarship for the period 2013–2016.

References

1 G. R. Gale, M. G. Rosenblum, L. M. Atkins, E. M. Walker Jr, A. B. Smith and S. J. Meischen, *J. Natl. Cancer Inst.*, 1973, **51**, 1227–1234.
2 A. J. Lippman, C. Helson, L. Helson and I. H. Krakoff, *Cancer Chemother. Rep., Part 1*, 1973, **57**, 191–200.
3 J. S. Kovach, C. G. Moertel, A. J. Schutt, R. G. Reitemeier and R. G. Hahn, *Cancer Chemother. Rep., Part 1*, 1973, **57**, 357–359.
4 R. C. Todd and S. J. Lippard, *Metallomics: Integrated Biometal Science*, 2009, **1**, 280–291.
5 S. Murata, S. Onozawa, C. Kim, H. Tajima, R. Kimata, E. Uchida and S. I. Kumita, *Acta Radiol.*, 2013, **55**, 793–801.
6 D. Gholap, J. Verhulst, W. Ceelen and F. Vanhaecke, *Anal. Bioanal. Chem.*, 2012, **402**, 2121–2129.
7 E. Moreno-Gordaliza, C. Giesen, A. Lazaro, D. Esteban-Fernandez, B. Humanes, B. Canas, U. Panne, A. Tejedor, N. Jakubowski and M. M. Gomez-Gomez, *Anal. Chem.*, 2011, **83**, 7933–7940.
8 F. Vanhaecke, M. Resano, M. Pruneda-Lopez and L. Moens, *Anal. Chem.*, 2002, **74**, 6040–6048.
9 O. Reifschneider, C. A. Wehe, K. Diebold, C. Becker, M. Sperling and U. Karst, *J. Anal. At. Spectrom.*, 2013, **28**, 989–993.
10 I. B. Levitan, *Annu. Rev. Neurosci.*, 1988, **11**, 119–136.
11 J. C. Fontecilla-Camps, P. Amara, C. Cavazza, Y. Nicolet and A. Volbeda, *Nature*, 2009, **460**, 814–822.
12 D. A. Frick and D. Günther, *J. Anal. At. Spectrom.*, 2012, **27**, 1294–1303.
13 C. Austin, F. Fryer, J. Lear, D. Bishop, D. Hare, T. Rawling, L. Kirkup, A. McDonagh and P. Doble, *J. Anal. At. Spectrom.*, 2011, **26**, 1494–1501.
14 I. Konz, B. Fernandez, M. L. Fernandez, R. Pereiro, H. Gonzalez, L. Alvarez, M. Coca-Prados and A. Sanz-Medel, *Anal. Bioanal. Chem.*, 2013, **405**, 3091–3096.
15 D. Hare, B. Reedy, R. Grimm, S. Wilkins, I. Volitakis, J. L. George, R. A. Cherny, A. I. Bush, D. I. Finkelstein and P. Doble, *Metallomics: Integrated Biometal Science*, 2009, **1**, 53–58.
16 D. J. Hare, J. Lear, D. Bishop, A. Beavis and P. A. Doble, *Anal. Methods*, 2013, **5**, 1915–1921.
17 D. C. Mahan and R. G. Shields Jr, *J. Anim. Sci.*, 1998, **76**, 506–512.
18 O. Reifschneider, C. A. Wehe, I. Raj, J. Ehmcke, G. Ciarimboli, M. Sperling and U. Karst, *Metallomics: Integrated Biometal Science*, 2013, **5**, 1440–1447.
19 M. Bonta, H. Lohninger, M. Marchetti-Deschmann and A. Limbeck, *Analyst*, 2014, **139**, 1521–1531.
20 B. T. Mossman, A. Shukla, N. H. Heintz, C. F. Verschraegen, A. Thomas and R. Hassan, *Am. J. Pathol.*, 2013, **182**, 1065–1077.
21 J. Lear, D. Hare, P. Adlard, D. Finkelstein and P. Doble, *J. Anal. At. Spectrom.*, 2012, **27**, 159–164.
22 DataLab, http://www.lohninger.com/datalab/de_home.html, 05/08/2014.
23 G. R. DiResta, J. Lee, N. Lau, F. Ali, J. H. Galicich and E. Arbit, *Acta Neurochirurgica. Suppl.*, 1990, **51**, 34–36.
24 K. Niemax, *Spectrochim. Acta, Part B*, 2012, **76**, 65–69.
25 ImageLab, http://www.imagelab.at/, 05/08/2014.

Application of dried-droplets deposited on pre-cut filter paper disks for quantitative LA-ICP-MS imaging of biologically relevant minor and trace elements in tissue samples

Maximilian Bonta, Balazs Hegedus and Andreas Limbeck, *Analytica Chimica Acta*, 2016

Analytica Chimica Acta 908 (2016) 54–62

Contents lists available at ScienceDirect

Analytica Chimica Acta

journal homepage: www.elsevier.com/locate/aca

Application of dried-droplets deposited on pre-cut filter paper disks for quantitative LA-ICP-MS imaging of biologically relevant minor and trace elements in tissue samples

Maximilian Bonta [a], Balazs Hegedus [b, c], Andreas Limbeck [a, *]

[a] TU Wien, Institute of Chemical Technologies and Analytics, Vienna, Austria
[b] Department of Thoracic Surgery, Comprehensive Cancer Center, Medical University of Vienna, Austria
[c] MTA-SE Molecular Oncology Research Group, Hungarian Academy of Sciences, Budapest, Hungary

HIGHLIGHTS

- Simple preparation of standards for LA-ICP-MS imaging.
- No handling of biological materials is required.
- Multi-elemental quantification, almost unlimited analyte range and concentrations.
- Accuracy of the results is improved by using gold as pseudo-internal standard.

GRAPHICAL ABSTRACT

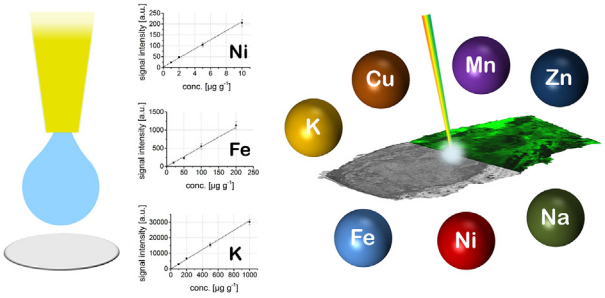

ARTICLE INFO

Article history:
Received 29 October 2015
Received in revised form
21 December 2015
Accepted 22 December 2015
Available online 11 January 2016

Keywords:
LA-ICP-MS
Biological specimen
Imaging
Quantification
Trace elements

ABSTRACT

In this work, a novel calibration approach for minor and trace element quantification in LA-ICP-MS imaging of biological tissues is presented. Droplets of aqueous standard solutions are deposited onto pre-cut pieces of filter paper, allowed to dry, and sputtered with a thin gold layer for use as pseudo-internal standard. Analysis of the standards using LA-ICP-MS is performed using radial line-scans across the filters. In contrast to conventionally used preparation of matrix-matched tissue standards, the dried-droplet approach offers a variety of advantages: The standards are easy to prepare, no characterization of the standards using acid digestion is required, no handling of biological materials is necessary, and the concentration range, as well the number of investigated analytes is almost unlimited. The proposed quantification method has been verified using homogenized tissue standards with known analyte concentrations before being applied to a human malignant mesothelioma biopsy from a patient who had not received any chemotherapeutic treatment. Elemental distribution images were acquired at a lateral resolution of 40 μm per pixel, limits of detection ranging from 0.1 μg g^{-1} (Mn, Ni, Cu, Zn) to 13.2 μg g^{-1} (K) were reached.

© 2016 Elsevier B.V. All rights reserved.

1. Introduction

Today LA-ICP-MS is used for the analysis of solid samples in a variety of applications. Thanks to its capability of performing laterally resolved analyses with resolutions down to the low μm

* Corresponding author. TU Wien, Institute of Chemical Technologies and Analytics, Getreidemarkt 9/164-IAC, 1060 Vienna, Austria.
E-mail address: andreas.limbeck@tuwien.ac.at (A. Limbeck).

http://dx.doi.org/10.1016/j.aca.2015.12.048
0003-2670/© 2016 Elsevier B.V. All rights reserved.

scale, LA-ICP-MS is also widely used for mapping of analytes on sample surfaces (imaging). Besides applications in geological and environmental sciences, LA-ICP-MS imaging is also spreading in the life sciences for use on biological samples [1–3]. As minor and trace elements play a vital role in biological processes, not only their bulk concentration but also their distribution in biological systems is an important factor; the knowledge thereof can lead to an improved understanding of biological mechanisms. However, analyses using LA-ICP-MS are linked to a variety of problems. Therefore, imaging experiments on biological samples have to be planned carefully and several aspects have to be considered. Experiments on biological tissues offering a reasonable resolution with an image size of several thousands of pixels may take many hours for measurement [4]. During measurement, a considerable instrumental drift might occur due to changes in laser focus and/or slight variations of the conditions in the ICP-MS device due to clogging of cones, changing vacuum conditions, or other issues. This drift has to be compensated using an internal standard. Thus, even simple qualitative distribution images of metals in biological tissues may lack in reliability when no suitable internal standard is used during the measurement. Optimally, this internal standard will also correct for matrix effects involving changing ionization efficiency, altered transport behavior, or changed plasma load when ablating different material structures and introducing them into the plasma [5,6]. Additionally to the aspects mentioned above for qualitative analyses, quantitative measurements require a suitable standard material which enables reliable and reproducible quantification.

Most commonly carbon is used as internal standard as it is abundant in almost every biological sample. It has been shown earlier that carbon is not the perfect choice for an internal standard due to unequal distribution within tissues, transport properties which are not comparable with other elements of interest (carbon is partly transported as gaseous carbon dioxide), and high first ionization potential [7]. Besides carbon, sulphur has also been used as sample inherent internal standard [8]. However, none of the sample inherent elements seems to be an optimal internal standard. As an alternative, elements that do not naturally occur in the sample can be added to be applied as internal standard. Amongst those, notable examples are intercalation of iridium [9], or metal-spiked polymer layers [6]. Also the online addition of aerosol form a nebulized liquid standard is feasible [10]. A more detailed summary of state-of-the-art internal standardization techniques used in LA-ICP-MS imaging of biological samples can be found elsewhere [11]. Previously it has been shown that sputtered gold layers can compensate the majority of ablation-, transport- and ionization-related changes in signal intensity [12,13], providing that the sample material is completely ablated within one analysis cycle. Those have proven to be a feasible pseudo-internal standard in LA-ICP-MS imaging experiments. By reducing matrix related ablation and ionization differences gold thin layers as pseudo-internal standard cannot only help to make qualitative analyses more reliable but they can also provide novel quantification strategies.

In a majority of the quantitative analyses presented in the past, matrix-matched tissue standards have been used for quantification [14]. The preparation of those standards involves major workload. Furthermore, for every analyzed tissue type, element of interest, and concentration level new standards have to be prepared. Some alternatives such as gel-based standards [15–17], embedding the analyzed tissues in epoxy resins [18], or adding thin layers of spiked polymers below or above the analyzed tissue slices [19] have been proposed as alternative to the use of matrix-matched standards. Improved methods for signal quantification are desired, due to problems regarding the required workload or the reliability of the quantification. Recently, printed patterns on paper have been used in combination with gold thin layers as pseudo internal standard for the quantification of platinum in human tumor samples of individuals treated with platinum containing drugs [20]. However, even if this method worked well for single-element quantification at trace levels, it was not applicable for a multi-elemental approach, as conventional printer ink is not susceptible for high salt concentrations. As some metals such as alkalines are highly abundant in biological tissues, also their concentration in the standard has to be high.

In this work, the use of dried droplets on precut filter punches in combination with gold thin layers as pseudo-internal standard is presented as a novel quantification strategy for LA-ICP-MS imaging experiments, giving the possibility of reliable and easy multi-elemental quantification. Dried standards on filter punches have been shown to be a useful method for quantitative LA-ICP-MS analysis of dried liquids [21]. Standards may be used in every concentration needed, and the number as well as the concentration of different analytes is almost unlimited. Here, we have adapted and optimized this approach for multi-element analysis in tissue samples. A large variety of different analyte concentrations had to be covered as biologically relevant metals range from high concentrations (e.g., Na and K, in most tissues in the 1000 $\mu g\ g^{-1}$ range), over smaller concentrations (e.g., Zn, Fe in the 100 $\mu g\ g^{-1}$ range), to trace elemental concentrations (e.g., Cu, Ni, Co, below 10 $\mu g\ g^{-1}$) [22]. The presented quantification approach attempts to combine the quantification of all these elements in a large concentration range over some orders of magnitude in one calibration step. The development of the method is described, the validity of the quantification approach is verified using matrix-matched tissue standards of known metal content, and the method is applied in an imaging experiment of a sample with unknown elemental concentrations.

2. Experimental

2.1. Chemicals

Metal-free water (resistivity 18.2 $M\Omega\ cm^{-1}$) dispensed from a Barnstead EASYPURE II water system (ThermoFisher Scientific, Marietta, OH) was used for all experiments. Conc. HNO_3 (p.a.) and 30% (v/v) H_2O_2 (p.a.) were supplied by Merck, Darmstadt, Germany. Liquid standards for ICP-MS measurements (ICP-multi elemental solution VIII, 24 elements at 100 mg L^{-1} in diluted HNO_3 and indium standard for ICP, 1 g L^{-1} in 5% HNO_3) were purchased from Sigma–Aldrich, Buchs, Switzerland. Sodium nitrate, potassium nitrate, magnesium nitrate, calcium nitrate, iron–(III)–nitrate, manganese nitrate, nickel nitrate, copper–(II)–nitrate and zinc nitrate were all of analytical grade and purchased from Merck, Darmstadt, Germany. 'Tune B' solution for tuning of the ICP-MS instrumentation was supplied by ThermoFisher Scientific, Bremen, Germany.

2.2. Instrumental

All experiments were performed using quadrupole ICP-MS instrumentation (iCAP Qc, ThermoFisher Scientific, Bremen, Germany) in standard measurement mode. Qtegra software provided by the manufacturer was used for data acquisition. A commercially available laser ablation system (New Wave 213, ESI, Fremont, CA) was used for analysis of the solid samples. A fast washout ablation cell provided by the manufacturer of the laser was employed. Helium was used as ablation gas and mixed with argon as make-up gas before introduction of the aerosol into the plasma. Prior to every experiment, the instrumental performance was tuned for a maximum intensity of the ^{115}In signal by ablating NIST 612 trace elements in glass standard (National Institute of Standards and

Technology, Gaithersburg, MD). Typical measurement parameters are listed in Table 1. For solid sampling experiments, the laser output was adjusted to yield optimal ablation behavior, meaning complete ablation of the material within the diameter of the laser beam while maintaining sample integrity on adjacent sample areas. The sudden removal of large sample pieces visible in the microscope of the laser ablation instrument was avoided. Before firing on the sample the laser was allowed to warm up for 10 s to reach stable output energy.

Sample introduction for conventional ICP-MS measurements of liquid sample digests was performed using an ESI SC-2DX automated sample changer. For sample introduction into the plasma, a concentric PFA nebulizer and a Peltier cooled quartz spray chamber were employed. The instrumental parameters were optimized daily using Tune B solution (ThermoFisher Scientifc, Bremen, Germany) to yield maximum intensity for the ^{115}In signal while keeping the oxide ratio ($^{140}Ce^{16}O/^{140}Ce$) below 1.9%. Furthermore, the amount of doubly charged ions ($^{138}Ba^{++}/^{138}Ba^{+}$) was kept below 3% for all experiments. Standard parameters recommended by the manufacturer were used for the measurements.

2.3. Preparation and LA-ICP-MS analysis of dried droplet standards

A stock standard solution of common minor and trace elements in biological tissues (Na, K, Mg, Ca, Fe, Mn, Ni, Cu and Zn) was prepared by dissolving the respective nitrate salts in 1% HNO_3. Concentrations were chosen that a calibration with this stock solution would be in the range of the concentrations of the chosen metals in typical biological tissues. The applied element concentrations are based on the acid digestion and ICP-MS measurement of the elemental concentrations in the matrix-matched tissues as well as on values found in literature [22]. 1% HNO_3 was used to prepare the stock solution from nitrate salts of the respective analytes. The final concentration of the metals was 10.0 mg L^{-1} for Na, K and Mg, 4.0 mg L^{-1} for Ca and Fe, 2.0 mg L^{-1} for Zn, 1.0 mg L^{-1} for Mn and 0.40 mg L^{-1} for Ni and Cu, respectively.

For preparation of the dried droplet standards, a similar procedure as reported by Nischkauer et al. [21] was employed. In preliminary experiments, different filter materials and double sided tapes have been tested with regards to their background signal for the relevant elements. Filter discs from mixed cellulose ester filters (GI-4 0.8 μm, Pall Corp., Ann Harbor, MI) 5 mm in diameter were cut using a steel punching tool. The discs were attached to glass slides which were equipped with double sided tape (tesa Powerbond INDOOR, tesa GmbH, Vienna, Austria). Six replicates per concentration level were prepared. The above described stock solution was applied to the filters in undiluted state and diluted by the factors 20, 5.0, 2.5 and 1.0. Additionally, a blank value was prepared using 1% HNO_3. Indium from a liquid standard was added to the solutions before application to the filter discs to correct for volume variations of the applied droplets. The concentration of indium in every dilution of the standard was 1 mg L^{-1} 5–20 μL of standard were applied to each filter disc. After application of the liquids to the filters the standards were allowed to dry at room temperature overnight in a VFT 1525 ultraclean laminar flow hood (WEISS Technik, Austria) before being processed as described below.

The prepared standards were coated with thin gold layers for use as pseudo-internal standard in the LA-ICP-MS measurements. Gold coating was performed using an Agar B7340 sputter coater (Agar Scientific Limited, Essex, UK) equipped with a gold sputter target. Sputtering was performed 10 s (timer controlled) at a pressure of 0.1 mbar with a constant distance of 3.0 cm between sputter target and sample. Reproducibility and homogeneity of the sputtered gold layers have been reported previously [13]. For the measurement of the dried droplet standards, laser power and scan speed were chosen to fully ablate the material of the filter in one single run. This was performed to accomplish quantitative detection of the standard material. One single line was ablated along the diameter of the filter. This procedure has been reported recently to yield representative results for the overall amount of analyte on the filter [21]. The measured average signal across the filter was taken into consideration for calculating a calibration function.

2.4. Sample preparation and LA-ICP-MS measurement of tissue samples

Tissue samples were obtained from a 66 year old male malignant pleural mesothelioma (MPM) patient. Informed consent was obtained from the patient and all procedures were approved by the Institutional Ethics Committee (EK #904/2009). The snap frozen tumor samples (human MPM) were attached to a sample holder using Shandon Cryomatrix (Thermo Scientific, Cat. No: 6769006) and 10 μm sections were cut using a cryotome (Leica CM3050 S) at −20 °C. The sections were collected on 1 × 1 cm large pieces of a high purity silicon wafer (Infineon, Villach, Austria) and dried at room temperature.

Prior to LA-ICP-MS analysis, tissue specimens were coated with a thin gold layer as described for dried droplet standards. Measurement of the tissue samples was performed in line scan mode at a laser beam diameter of 40 μm. All lines scanned across the sample were adjacent to each other (0 μm spacing between the lines) and ablated in the same direction. The laser scan speed was set to 120 μm s^{-1}) which had shown to deliver signals without major carry-over effects using the employed washout chamber and tubing system. The time resolved intensities for the monitored ions were processed to distribution images using ImageLab (Epina

Table 1
Typical parameters used for the LA-ICP-MS experiments.

laser ablation system	**New Wave 213**
average fluence	4.9 J cm^{-2}
laser diameter	40 μm
scan speed	120 μm s^{-1}
repetition rate	10 Hz
carrier gas flow (He)	1 L min^{-1}
make-up gas flow (Ar)	0.8 L min^{-1}
ICP-MS instrumentation	**Thermo iCAP Q**
aux. gas flow	0.8 L min^{-1}
cool gas flow	14 L min^{-1}
dwell time per isotope	10 ms
RF power	1550 W
cones	Ni
mass resolution	$m/\Delta m = 300$
measured isotopes	^{23}Na, ^{24}Mg, ^{25}Mg, ^{39}K, ^{42}Ca, ^{44}Ca, ^{55}Mn, ^{56}Fe, ^{57}Fe, ^{58}Ni, ^{60}Ni, ^{63}Cu, ^{64}Zn, ^{65}Cu, ^{66}Zn, ^{115}In, ^{197}Au

GmbH, Pressbaum, Austria) [23].

2.5. Preparation and ICP-MS measurement of matrix-matched tissue standards

Porcine liver and kidney (*Sus scofra domestica*) were purchased at a local market. After thorough homogenization of the tissues, pieces of the thereof, 0.2 mL in volume were shock frozen in liquid nitrogen and stored at −70 °C until further use. Cryo cuts of the homogenized tissues were prepared similarly to the cryo cuts of the tumor samples and analyzed as described before.

For determination of the bulk metal content, the prepared aliquots (0.1–0.2 g) of frozen tissue were allowed to thaw, weighed and thereafter acid digestion was conducted. The digestion was performed in open PE sample tubes in five replicates for every tissue type. 1 mL of conc. HNO_3 was added to each of the tissue aliquots and carefully mixed with the homogenized tissue. The mixture was heated in a water bath (Heidolph, Schwabach, Germany) to 80 °C for 2 h followed by addition of 250 μL 30% H_2O_2 to the reaction mixture and heating for another hour to 80 °C. After the reaction was complete (i.e., no more bubbles were forming in the mixture), the sample solution had become clear and no visible solid residues were left. The samples were allowed to cool to room temperature before diluting them with 8 mL of water. Indium was used as internal standard for the ICP-MS measurements and was added to all samples at a concentration of 1 μg L^{-1}. Prescreening of these samples gave a list of the elements to be investigated as well as the concentration range of the analytes to prepare suitable dilutions of the samples. Three different dilutions were found to be appropriate to cover the concentration range of all elements in the samples to be accessible for quantification. The final concentrations were chosen to be sufficient for proper detection (for all elements in the concentration range 5.0–100 μg L^{-1} in the analyzed samples). Signal quantification was performed using aqueous calibration with standards in the range between 1.0 and 200 μg L^{-1}. For method validation, a certified reference material (BCR-CRM278 mussel tissue powder) was digested and analyzed in analogy to the homogenized tissue samples.

3. Results and discussion

3.1. Optimization of the dried droplet approach

With regards to the drying behavior of the applied liquid standard, the amount of liquid on the pre-cut filter is an essential aspect. The optimal volume was evaluated using the standard with the highest concentration of analytes. A typical signal-time profile obtained from a scan across a filter after droplet application and drying is presented in Fig. 1a.

For all applied volumes, the highest signal intensities were obtained on the edges of the filter, decreasing towards the center. The signal distributions are symmetric with their center of symmetry in the middle of the filter, as demonstrated previously by Nischkauer et al. [21]. Even though these distribution patterns can be obtained very reproducibly, the signal difference between center and edge of the filter should be kept as low as possible to prevent any errors during quantification. So-called chromatographic effects during drying of the droplet lead to this phenomenon which is also known under the term 'coffee-stain effect' [24]. To investigate the excess of these chromatographic effects with regard to different droplet volumes, the signal intensities from the regions denoted by '1' and '3' were averaged and compared to the respective averaged signal intensities from region '2' (as illustrated in Fig. 1a). The ratio of these intensities was used as a measure describing the homogeneity of the analyte distribution across the filter diameter. Volumes of 5, 10 and 20 μL droplet volume were evaluated during this preliminary study. Volumes smaller than 5 μL would not evenly be soaked up by the filter piece and volumes larger than 20 μL would not remain on the filter in their whole volume. Therefore, only this range of volumes was investigated. The experiment has been carried out in six replicates of sample preparation for each amount of volume applied to achieve statistical significance of the data. The data are summarized in Fig. 1b. A droplet volume of 10 μL showed to offer the best drying properties with the lowest difference between the signal on the edges and the center of the filter. Results are presented for the internal standard indium; similar values were obtained for all other elements of interest contained in the standard.

3.2. Calibrations for signal quantification using the dried droplet approach

After the optimal amount of applied liquid had been evaluated, a calibration for signal quantification in the following imaging experiments was developed. Five dilution levels of the standard stock solution and a blank were considered for the calculation of regressions for each element of interest. Each concentration level was analyzed in six replicates for statistical relevance of the obtained data and the regression lines. For all measured elements except calcium, the signal for the lowest concentration level was significantly different from the blank value. The obtained averaged raw signals ranged between 300 cps (^{57}Fe) and 150,000 cps (^{39}K) for the lowest standard and 5000 cps (^{57}Fe) and 3,000,000 cps (^{39}K) for the highest standard. The signals were corrected to the internal standard indium present in each standard with a concentration of 1.0 mg L^{-1} to account for differences in liquid application. Furthermore, correction to the pseudo-internal standard gold was performed before calculating the regressions to enable application of the method to quantification in the following imaging experiments. All elements of interest except calcium delivered good calibration lines with a correlation coefficient above 0.99. Relative standard deviations for the replicate measurements were below 5% for every element and measured concentration level.

Wherever possible, two isotopes were chosen for the measurement (all measured elements except ^{23}Na, ^{39}K, and ^{55}Mn) to ensure that the calibrations were not affected by spectral interference of polyatomic ions. The slopes of the regression lines for two isotopes were compared to monitor possible deviations. In this course, the ratio of the slopes was found to be comparable to the natural abundances of the isotopes for all elements of which those ratios could be calculated, except for magnesium, most probably due to the presence of various C–C and C–N species being spectral interferences for all available isotopes. Considering the presence of spectral interference for calcium on two available isotopes (^{40}Ca – ^{40}Ar and ^{44}Ca – ^{4}He^{40}Ar) and ^{42}Ca being present only in low natural abundance (0.647%), no reliable regression function (R^2 below 0.900) for this element could be obtained in the range of the expected calcium concentrations in tissues. High background signal and signal instabilities were a major concern. Therefore, magnesium as well as calcium were excluded from the analysis to avoid unreliable results during analysis of the samples. For all other elements the slope ratios did not differ more than 5% from the natural abundance ratio. It has to be pointed out that the measurement conditions were not optimal for isotopic ratio measurements (q-ICP-MS instrumentation was used). Therefore, such high variations from the actual isotopic ratio were found to be acceptable. From all elements, iron shows the highest deviation from the natural ratio. This error can be contributed to the low abundance of ^{57}Fe. As a consequence, only low count rates were achieved for this isotope and larger deviations from the actual value are possible. Table 2

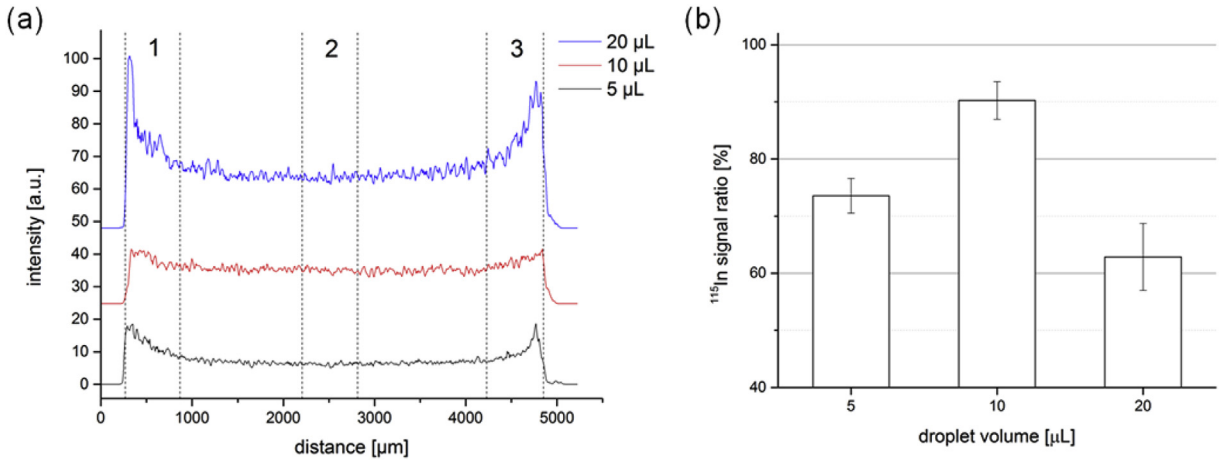

Fig. 1. Intensity profiles of ^{115}In during linescans across dried droplet standards with different application volumes (a). Comparison of the ^{115}In signal intensity ratio of edge and center (b).

Table 2
Summary of the slopes, slope ratios, natural isotopic ratios, possibly interfering polyatomic ions (without claiming to be exhaustive), and obtained limits of detection calculated for the 10 µm thick tissue specimen.

Isotope	Slope [a.u.]	Slope ratio	Natural isotopic ratio	Possible polyatomic interference	LOD [µg g^{-1}]
^{23}Na	8.67	n.a.			5.7
^{24}Mg	5.04	5.93	7.17	$^{12}C^{12}C$	2.3
^{26}Mg	0.75			$^{12}C^{14}N$, $^{13}C^{13}C$	10.6
^{39}K	6.10	n.a.		$^{38}Ar^{1}H$	13.2
^{55}Mn	6.50	n.a.		$^{40}Ar^{15}N$, $^{40}Ar^{14}N^{1}H$	0.1
^{56}Fe	3.80	37.95	41.69	$^{40}Ar^{16}O$	0.8
^{57}Fe	0.10			$^{40}Ar^{16}O^{1}H$	3.4
^{58}Ni	2.31	2.72	2.60	$^{40}Ar^{18}O$	0.1
^{60}Ni	0.85				0.4
^{63}Cu	2.29	2.15	2.24	$^{40}Ar^{23}Na$	0.1
^{65}Cu	1.07			$^{40}Ar^{25}Mg$	0.2
^{64}Zn	1.06	1.74	1.74	$^{40}Ar^{24}Mg$	0.1
^{66}Zn	0.61			$^{40}Ar^{26}Mg$	0.2

summarizes the slopes of the measured isotopes and their ratios compared with the natural abundances. In every case, the ratio of lighter and heavier isotope was calculated.

3.3. Characterization of matrix-matched tissue standards

Before application of the dried droplet quantification method on samples with uneven and unknown metal content, its validity had to be tested using samples with known element concentrations; homogenized porcine liver and kidney were used. The element concentrations in each of the two tissue types were determined by acid digestion and liquid ICP-MS measurement in five replicates of sample preparation as described in the experimental section. Raw signals were ranging from 30,000 to 20,000,000 cps for all investigated elements being significantly different from the reagent blank values (below 1000 cps for most elements). For signal quantification, aqueous calibrations were used, where the raw signals of the analytes were normalized to the signal intensities of the internal standard (indium). The actual element concentrations in the tissue were calculated with respect to the exact amount of used sample and the dilution factor; the results are presented in Table 3. Obtained low standard deviations of less than 5% for replicate measurements do not only demonstrate a reproducible sample preparation but also an even distribution of the elements of interest in all analyzed aliquots of the samples. Additionally, a certified reference material (BCR-CRM278 mussel tissue powder) was analyzed to verify the validity of the sample digestion procedure; sample preparation was performed in five replicates, none of the determined average concentrations differed significantly from the certified values.

Besides this macroscopic type of homogeneity, for LA-ICP-MS analysis also homogeneity in smaller scales (i.e., in the range of the laser beam diameter) is an important factor. Five single lines were measured across an area of 20 mm^2 of the cryo-cuts with a laser beam diameter of 40 µm and a scan speed of 120 µm s^{-1}. The resulting gold corrected intensity-time plots were divided into five sections of which an average was calculated. The resulting average was compared with each of the single region values. None of the regions yielded a signal which was significantly different from the average for all investigated elements on both analyzed tissues. Five of these lines were measured and the average signals of all lines were compared using one-way analysis of variances (ANOVA) using the statistical software package DataLab (Epina GmbH, Pressbaum, Austria) [26]. Statistical data analysis showed that none of the compared values differs from their common mean at a significance level of 95%. Levenes test ($p < 0.2$) was applied to all data sets prior to ANOVA to check for homogeneity and equality of variances. Based on the statistical analysis, it can be stated that all elements are homogenously distributed across the diameter of the cryo-cuts of both tissue types. Therefore, signals obtained from LA-ICP-MS analysis can be regarded as representative for the bulk concentration in the tissue.

A unit conversion had to be performed to use the dried-droplet calibration (amount of analyte per area) for the quantification of

Table 3
Element concentrations in homogenized porcine kidney and liver determined by ICP-MS; metal concentrations in mussel tissue reference material and certified values; errors are given as single standard deviation (n = 5).

	Kidney [μg g^{-1}]	Liver [μg g^{-1}]	BCR-CRM278 [μg g^{-1}]	Certified value [μg g^{-1}]
Na	1498 ± 32	713 ± 10	–	–
Mg	209 ± 2	226.1 ± 4.2	–	–
K	3292 ± 89	3847.1 ± 44.1	–	–
Ca	31.8 ± 1.8	22.1 ± 1.2	–	–
Mn	1.7 ± 0.02	3.2 ± 0.03	7.5 ± 0.3	7.69 ± 0.23
Fe	48.1 ± 1.3	178 ± 4	137.3 ± 3.3	133–137[a]
Ni	0.5 ± 0.02	1.2 ± 0.02	1.0 ± 0.03	1[a]
Zn	27.0 ± 0.1	133 ± 0.2	84.2 ± 2.0	84.1 ± 1.7
Cu	6.7 ± 0.3	27.5 ± 1.4	0.20 ± 0.006	0.196 ± 0.009

[a] GeoReM preferred value [25].

metals in tissues (amount of analyte per mass tissue). This conversion was achieved by determining the density of the tissue slices at a known thickness of the tissue slices (10 μm). Density determination was performed using a pycnometric method by DiResta et al. [27] and yielded densities of 1.0505 ± 0.0036 g cm^{-3} for kidney and 1.0220 ± 0.0109 g cm^{-3} for liver, respectively. This method of density determination has been reported previously to be used for the described conversion [20].

3.4. Signal quantification on matrix-matched tissues using calibrations from dried droplets on pre-cut filters

For quantification of the metals in the homogenized tissues, line scans across the diameter of the prepared cryo-cuts were measured. A preliminary evaluation of the background signals for the elements of interest showed that the derived backgrounds from the silicon wafers used for sample mounting were negligible for all investigated elements. Five lines were distributed over the sample surface and their gold normalized average signal was considered for signal quantification. A signal-time plot of the raw signals showed a constant signal course across the investigated samples for all elements of interest. Therefore, the recorded signals were considered to be representative for the bulk element concentrations. The derived signals ranged from 1000 cps for ^{58}Ni on kidney to 2,000,000 cps for ^{39}K on liver. The obtained raw signals were normalized to the ^{197}Au signal (pseudo-internal standard) and converted into mass concentrations employing the calibration function determined with the dried droplet standards. Whenever possible, two isotopes of every element were measured. The calculated concentrations did not differ significantly from each other for all investigated elements indicating the absence of major spectral interferences. Finally, the obtained results were compared with the results derived from sample digestion and conventional liquid analysis. Fig. 2 shows the correlation of the concentrations determined by ICP-MS measurement after liquid digestion and the concentrations calculated from the LA-ICP-MS measurements.

The results show an excellent correlation for both tissue types and all measured elements. Even the large concentration range of the investigated elements does not affect the quality of the results. Highly abundant (Na, K) as well as weakly abundant elements (Ni, Mn) were quantified with a satisfying accuracy. The dried droplet method in combination with gold sputtering as pseudo-internal standard delivers correct results for tissues of known analyte content. This allows the conclusion that reliable element concentrations can be obtained with this quantification approach also on samples with unknown analyte concentrations.

3.5. Application of the quantification approach to a tissue sample of unknown analyte content

For application of the developed quantification method on a tissue sample, a human MPM biopsy sample has been selected. The individual had not received any chemotherapeutics treatment before taking the biopsy. In this context, the distribution metal

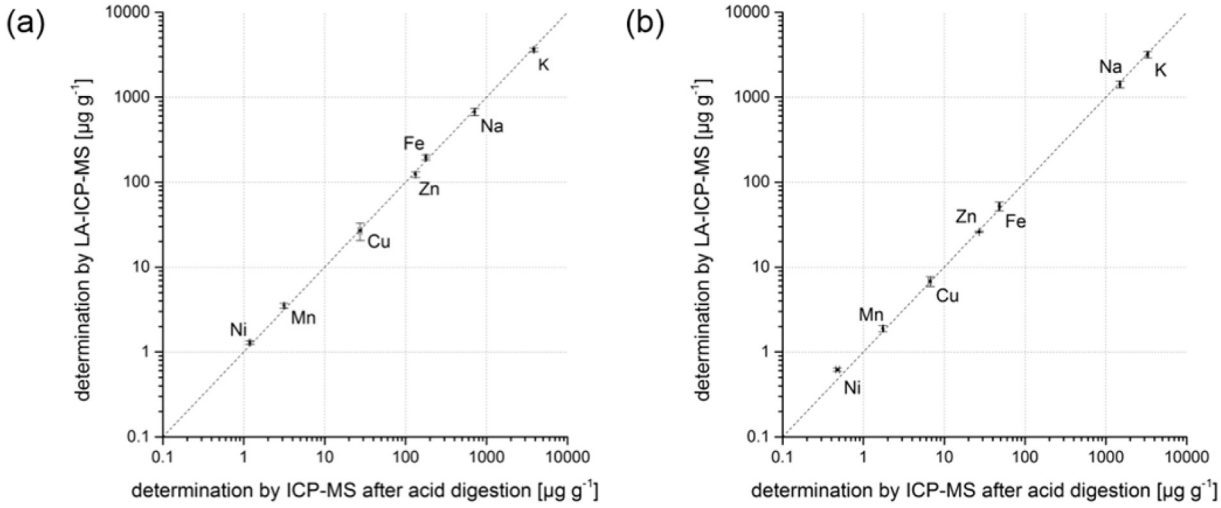

Fig. 2. Comparison of metal concentrations determined my conventional ICP-MS after acid digestion and concentrations determined by LA-ICP-MS in homogenized porcine liver (a) and kidney (b).

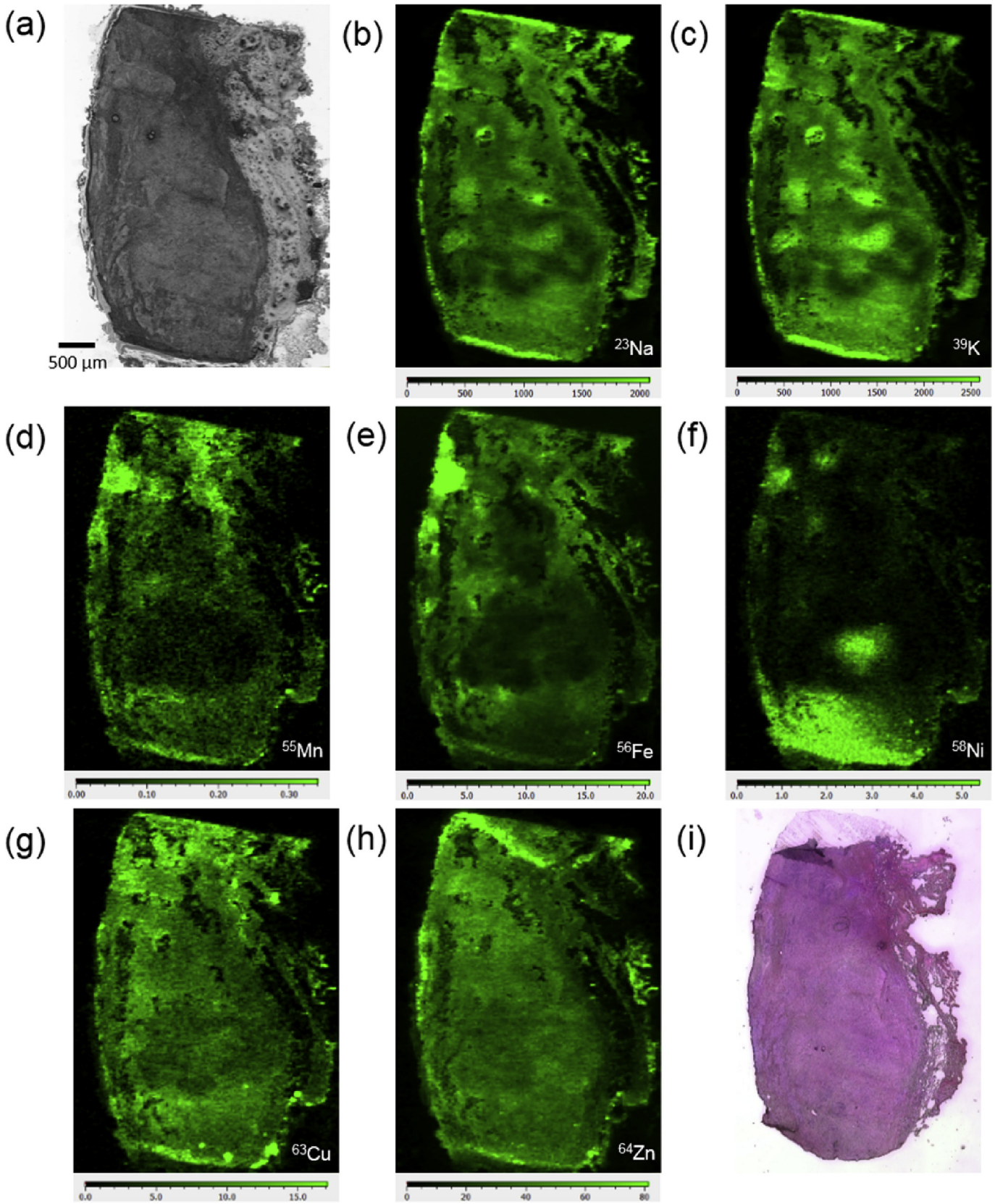

Fig. 3. Visual image of the analyzed cryo-cut of the tissue (a) and distribution of the elements Na (b), K (c), Mn (d), Fe (e), Ni (f), Cu (g), and Zn (h); all concentrations are given in µg g^{-1}, hematoxylin and eosin stain of a consecutive tissue section (i).

concentrations in different areas of the tissue would be interesting. A microscopic image of the analyzed tissue section is shown in

Fig. 3a. Hematoxylin and eosin staining (consecutive tissue thin-cut, Fig. 3i) was used to exhibit morphological structures of the investigated tissue specimen. While nuclei are stained blue/violet, the cytoplasm and extracellular structures are colored in various shades of red and pink. Besides the visual image, Fig. 3 shows the distribution of seven metals (Na, K, Mn, Fe, Ni, Cu, Zn) in the tissue. Quantification was achieved using the dried droplet quantification approach for the elements of interest during this study. For all elements, signals significantly higher than the background value were obtained. The acquired gold normalized signals were in the calibration range of the dried droplet standards for all investigated isotopes. Whenever possible, two isotopes were monitored to exclude that the distribution images are affected by any spectral interference. In no case, any indication for the presence of spectral interference was given. In Fig. 3 only the images resulting from the signals of the most abundant isotopes are shown.

Sodium (Fig. 3b) and potassium (Fig. 3c) show very similar distributions with concentrations of 1000 $\mu g\ g^{-1}$ and above. The high concentrations correlate well with literature values for bulk concentrations [22]. Intracellular levels of sodium and potassium are physiologically closely related and very tightly regulated. Thus, similar distribution patterns could be expected. Some structures of the visual and histological image showed distinct correlations with the elemental distributions, indicating a variable Na/K concentration in different morphological structures of the tissue. For instance, the right hand side of the tissue contains a fibrousos, non-tumorous region demonstrates lower Na/K concentrations.

Similarly, the distributions of manganese (Fig. 3d) and iron (Fig. 3e) show a good visual match. However, the measured concentrations vary significantly. While manganese could only be detected far below 1 $\mu g\ g^{-1}$, the found iron concentrations were up to 20 $\mu g\ g^{-1}$. The similar distribution can be explained by the comparable coordination preferences of those two elements in complexes. Almost all proteins utilizing iron as cofactor could substitute their metal core by manganese [28]. Prominent examples for iron-containing proteins are myoglobin and hemoglobin, both responsible for oxygen supply of the cell. Another notable class of proteins with iron and/or manganese metal cores are superoxide dismutases [29]. Their main function is protection of the cell from oxidative stress. Thus, all described proteins can be expected to be found in higher amounts in tissue with higher cellularity. The areas with high density of cells identified in the hematoxylin and eosin stain as darker or bluer areas (Fig. 3i) exhibit higher iron and manganese concentrations, which would support this hypothesis. Likewise, also copper (Fig. 3g) and zinc (Fig. 3h) exhibit comparable distributions. Those two elements have similar functions in biological systems and are often interchangeable. One major group of proteins utilizing Cu and Zn as cofactor are also superoxide dismutases [30]. The distribution of nickel (Fig. 3f) cannot be correlated with histological structures. However, also this trace element is very important in biological processes, for example acting as active center in some proteins of the carbon cycle [31,32].

Further interpretation and questions about medical relevance of the obtained results are subject to ongoing experiments to obtain representative results by investigation of a larger sample pool. During this work the objective was to demonstrate the applicability of the dried droplet quantification approach on a real sample.

4. Conclusion

The presented method is an easy-to-handle approach and represents a promising alternative to the commonly used matrix-matched tissue standards for signal quantification in imaging experiments on biological samples. The standard materials are easy to manufacture and standard preparation does only require minor workload. In contrast to matrix-matched tissue standards, no handling of biological material or time consuming acid digestions of the standards are needed. The proposed method is highly flexible in terms of analyzed elements and concentration range. Changes in those parameters may be easily performed by preparing new standards. The applicability of gold as pseudo-internal standard in imaging experiments has been already reported earlier [12,13,20] and is also demonstrated and applied in this work. This method is a valuable tool for the minimization of the effects of instrumental drifts, and material related ablation and transport differences. In contrast to the previously presented printed pattern method, the dried droplet approach offers multi-element capabilities with access to higher analyte concentration ranges for the calibration. The hereby described multi-element quantification approach can be further applied on other biological specimens including plant material.

The presented data indicate correlations of tissue morphology with element distributions. Detailed interpretation and the investigation of the medical relevance of tissue level element distribution requires further studies to provide a statistically representative cohort.

Acknowledgment

The authors would like to thank Elisabeth Eitenberger for assistance during gold sputtering and Hans Lohninger for the development of the ImageLab software. M.B. wants to thank the MEIBio PhD program of the TU Wien for providing a scholarship for the period 2013–2016.

References

[1] I. Konz, B. Fernandez, M.L. Fernandez, R. Pereiro, A. Sanz-Medel, Anal. Bioanal. Chem. 403 (2012) 2113.
[2] J. Koch, D. Günther, Appl. Spectrosc. 65 (2011) 155.
[3] J.S. Becker, M. Zoriy, A. Matusch, B. Wu, D. Salber, C. Palm, Mass Spectrom. Rev. 29 (2010) 156.
[4] D. Hare, B. Reedy, R. Grimm, S. Wilkins, I. Volitakis, J.L. George, R.A. Cherny, A.I. Bush, D.I. Finkelstein, P. Doble, Metallomics Integr. biometal Sci. 1 (2009) 53.
[5] F. Vanhaecke, H. Vanhoe, R. Dams, C. Vandecasteele, Talanta 39 (1992) 737.
[6] C. Austin, F. Fryer, J. Lear, D. Bishop, D. Hare, T. Rawling, L. Kirkup, A. McDonagh, P. Doble, J. Anal. Atomic Spectrom. 26 (2011) 1494.
[7] D.A. Frick, D. Günther, J. Anal. Atomic Spectrom. 27 (2012) 1294.
[8] M.-M. Pornwilard, R. Weiskirchen, N. Gassler, A.K. Bosserhoff, J.S. Becker, PloS one 8 (2013) e58702.
[9] D.A. Frick, C. Giesen, T. Hemmerle, B. Bodenmiller, D. Günther, J. Anal. Atomic Spectrom. 30 (2015) 254.
[10] C. O'Connor, B.L. Sharp, P. Evans, J. Anal. Atomic Spectrom. 21 (2006) 556.
[11] A. Limbeck, P. Galler, M. Bonta, G. Bauer, W. Nischkauer, F. Vanhaecke, Anal. Bioanal. Chem. 407 (2015) 6593.
[12] I. Konz, B. Fernandez, M.L. Fernandez, R. Pereiro, H. Gonzalez, L. Alvarez, M. Coca-Prados, A. Sanz-Medel, Anal. Bioanal. Chem. 405 (2013) 3091.
[13] M. Bonta, H. Lohninger, M. Marchetti-Deschmann, A. Limbeck, Analyst 139 (2014) 1521.
[14] D.J. Hare, J. Lear, D. Bishop, A. Beavis, P.A. Doble, Anal. Methods 5 (2013) 1915.
[15] D. Gholap, J. Verhulst, W. Ceelen, F. Vanhaecke, Anal. Bioanal. Chem. 402 (2012) 2121.
[16] H. Sela, Z. Karpas, H. Cohen, Y. Zakon, Y. Zeiri, Int. J. Mass Spectrom. 307 (2011) 142.
[17] H.J. Stärk, R. Wennrich, Anal. Bioanal. Chem. 399 (2011) 2211.
[18] O. Reifschneider, C.A. Wehe, I. Raj, J. Ehmcke, G. Ciarimboli, M. Sperling, U. Karst, Metallomics Integr. biometal Sci. 5 (2013) 1440.
[19] C. Austin, D. Hare, T. Rawling, A.M. McDonagh, P. Doble, J. Anal. Atomic Spectrom. 25 (2010) 722.
[20] M. Bonta, H. Lohninger, V. Laszlo, B. Hegedus, A. Limbeck, J. Anal. Atomic Spectrom. 29 (2014) 2159.
[21] W. Nischkauer, F. Vanhaecke, S. Bernacchi, C. Herwig, A. Limbeck, Spectrochim. Acta Part B At. Spectrosc. 101 (2014) 123.
[22] M.L. Carvalho, T. Magalhães, M. Becker, A. von Bohlen, Spectrochim. Acta Part B At. Spectrosc. 62 (2007) 1004.
[23] http://www.imagelab.at.
[24] G. Berteloot, A. Hoang, A. Daerr, H.P. Kavehpour, F. Lequeux, L. Limat, J. Colloid Interface Sci. 370 (2012) 155.

[25] K.P. Jochum, U. Nohl, K. Herwig, E. Lammel, B. Stoll, A.W. Hofmann, Geostand. Geoanalytical Res. 29 (2005) 333.
[26] http://www.lohninger.com/datalab/en_home.html.
[27] G.R. DiResta, J. Lee, N. Lau, F. Ali, J.H. Galicich, E. Arbit, Acta Neurochir. Suppl. 51 (1990) 34.
[28] J.A. Cotruvo Jr., J. Stubbe, Metallomics Integr. biometal Sci. 4 (2012) 1020.
[29] W.F. Beyer Jr., I. Fridovich, J. Biol. Chem. 266 (1991) 303.
[30] J.D. Crapo, T. Oury, C. Rabouille, J.W. Slot, L.Y. Chang, Proc. Natl. Acad. Sci. U. S. A. 89 (1992) 10405.
[31] J.L. Boer, S.B. Mulrooney, R.P. Hausinger, Archives Biochem. biophys. 544 (2014) 142.
[32] S.W. Ragsdale, J. Inorg. Biochem. 101 (2007) 1657.

Elemental mapping of biological samples by the combined use of LIBS and LA-ICP-MS

Maximilian Bonta, Jhanis J. Gonzalez, C. Derrick Quarles Jr, Richard E. Russo, Balazs Hegedus and Andreas Limbeck, *Journal of Analytical Atomic Spectroscopy*, 2016

JAAS

PAPER

View Article Online
View Journal | View Issue

CrossMark click for updates

Cite this: J. Anal. At. Spectrom., 2016, 31, 252

Elemental mapping of biological samples by the combined use of LIBS and LA-ICP-MS

Maximilian Bonta,[a] Jhanis J. Gonzalez,[bc] C. Derrick Quarles, Jr.,[b] Richard E. Russo,[bc] Balazs Hegedus[de] and Andreas Limbeck*[a]

Received 15th July 2015
Accepted 26th October 2015

DOI: 10.1039/c5ja00287g

www.rsc.org/jaas

In this study a combination of Laser Ablation Inductively Coupled Plasma Mass Spectrometry (LA-ICP-MS) and Laser Induced Breakdown Spectroscopy (LIBS) was used for laterally resolved elemental analysis of biological samples. In general LA-ICP-MS is an excellent technique for the analysis of many trace elements. However, bulk components such as H or O are not accessible using this technique. In addition to those elements, also some other elements that are difficult or impossible to investigate using LA-ICP-MS (*i.e.*, F, N, Cl, *etc.*), could be detected by LIBS. In this work, the simultaneous use of LIBS and LA-ICP-MS (tandem LA/LIBS) for the analysis of biological samples is presented, opening the door for the possibility of complete analysis of the elemental composition of a human tumor sample. Results show good correlation with the histological stainings. The obtained distribution images provide a valuable basis for further medical interpretation.

Published on 26 October 2015. Downloaded on 11/02/2016 08:21:58.

Introduction

In various fields of research, Laser Ablation-Inductively Coupled Plasma-Mass Spectrometry (LA-ICP-MS) is accepted as a powerful tool for laterally resolved analysis of trace elements.[1–3] Life sciences are one of the most prominent fields of LA-ICP-MS imaging, besides geology and geochemistry.[4,5] A great feature for this type of analysis is that thin-cut tissue samples can be analyzed just like they are commonly used in medical research (*e.g.*, histological studies). Comparison between trace element distributions with histological stainings of consecutive tissue slices can help to investigate biological processes in closer detail than it is possible to do with conventional methods used in clinical research. Over the last few years, numerous applications on various tissue types (*e.g.*, kidney,[6] brain,[7] tumor tissues[8,9]) have been presented. Even if LA-ICP-MS can complement the information obtained from histological investigations, one important aspect is not covered: more than 95% of the mass of a typical biological tissue are comprised of the elements C, H, N, O, P, and S, which are the main building blocks of organic matter. However, as LA-ICP-MS is not capable of analyzing H, N, and O, a full elemental analysis of a tissue specimen is not possible. Furthermore, the analysis of C using LA-ICP-MS is prone to a variety of problems, such as high background signal, unfavorable transport properties (*i.e.*, partial transport in the form of gaseous carbon compounds), as well as a high first ionization potential compared to other common analytes.[10]

Laser Induced Breakdown Spectroscopy (LIBS), is a powerful tool with access to every element in the periodic table with sensitivity in the medium μg g^{-1} range for most elements.[11,12] Applications for the analysis of minor and trace elements in biological tissues have already been presented in the past.[13,14] However, the concentration levels of the elements of interest in tissue samples are usually near or even below the detection limit of LIBS and thus, especially elemental mapping is often a difficult task.[15] Therefore, in order to obtain trace elemental composition from tissue samples at the same time as the major elements, LIBS data can be acquired simultaneously with LA-ICP-MS data. Thus, the analysis of one single sample, simultaneously using both techniques becomes feasible.[16–18] Therefore, LA-ICP-MS is used to analyze trace element components, whereas LIBS is used for the analysis of minor and major sample components including H and O. Besides expanding the elemental coverage range with the simultaneous use of LIBS and LA-ICP-MS, it also offers a few other advantages, such as simultaneous measurement of the complete spectral range and a very high sensitivity for alkaline and earth alkaline elements using LIBS. This can help to reduce the number of elements measured using LA-ICP-MS, which, in the case of typically used quadrupole or sector field mass analyzers, could lead to more precise results, especially important for isotope ratio investigations and quantitative analyses. Another beneficial aspect of

[a]TU Wien, Institute of Chemical Technologies and Analytics, Getreidemarkt 9/164-IAC, 1060 Vienna, Austria. E-mail: andreas.limbeck@tuwien.ac.at
[b]Applied Spectra, Inc., Fremont, CA, USA. E-mail: Jhanis@appliedspectra.com
[c]Lawrence Berkeley National Laboratory, Environmental Energy Technologies Division, Berkeley, CA, USA. E-mail: jjgonzalez@lbl.gov
[d]Department of Thoracic Surgery, Comprehensive Cancer Center, Medical University of Vienna, Austria
[e]MTA-SE Molecular Oncology Research Group, Hungarian Academy of Sciences, Budapest, Hungary

This journal is © The Royal Society of Chemistry 2016

Published on 26 October 2015. Downloaded on 11/02/2016 08:21:58.

this approach is that elements with m/z ratios being biased by spectral interferences (*e.g.*, Mg, polyatomic interference by C–C, or C–N species on all isotopes) can be detected using LIBS without those interferences.

In this work, an instrument capable of simultaneously performing LIBS and LA-ICP-MS measurements (tandem LA/LIBS) was used to develop a procedure for the analysis of biological samples with an expanded elemental coverage. Measurement parameters for both the LIBS and LA-ICP-MS were systematically optimized. Subsequently, this method was applied to a human tumor slice from an individual previously treated with cisplatin as anti-cancer drug. The simultaneous analysis of platinum (typically around 10 μg g^{-1} in the tissue), naturally occurring trace elements in the tissue (Fe, Ni, …), as well as major elements (C, H, O) has been performed, leading to an increased value for this type of elemental analysis. The use of tandem LA/LIBS for the elemental mapping of biological tissues will also give rise to improved quantification approaches and new ways for tissue analysis.

Experimental

Chemicals

Ultra-pure water (resistivity 18.2 MΩ cm) dispensed from a Barnstead EASYPURE II water system (ThermoFisher Scientific, Marietta, OH) was used for all experiments. (3-Aminopropyl)-triethoxysilane (APES), as well as acetone were of analytical grade and were purchased from Sigma-Aldrich, Buchs, Switzerland.

Instrumentation

All experiments were performed using a J200 Tandem LA/LIBS instrumentation (Applied Spectra Inc., Fremont, CA) equipped with a 266 nm frequency quadrupled Nd:YAG laser. For collection and spectroscopic analysis of the radiation emitted by the laser induced plasma, an optical fiber system connected to a Czerny–Turner spectrometer with a six-channel CCD detection was employed. For every laser shot, full spectra over the wavelength range from 190 to 1040 nm were recorded in Axiom data acquisition software provided by the manufacturer of the instrument. ICP-MS analysis of the generated aerosol was performed using a Thermo iCAP Qc quadrupole ICP-MS device (ThermoFisher Scientific, Bremen, Germany) and Qtegra data acquisition software (ThermoFisher Scientific, v.2.4). Connection of the tandem LA/LIBS system to the mass spectrometer was achieved using PTFE tubing. Helium at a flow rate of 0.8 L min^{-1} was used as ablation gas; argon at a flow rate of 0.8 L min^{-1} was admixed to the He gas stream directly after the ablation chamber outlet to be used as make-up gas. LIBS and LA-ICP-MS analysis were run from the same sample spots simultaneously.

The instrumental performance of the LIBS system, as well as the LA-ICP-MS device were checked on a daily basis using NIST612 glass standard (trace elements in glass, National Institute of Standards and Technology, Gaithersburg, MD) to ensure constant operating conditions of the used instrumentation. For LIBS, the intensity of multiple wavelengths distributed over a wide wavelength range (Mg(I) 285.213 nm, Ca(II) 315.887 nm, Ba(II) 455.403 nm, Li(I) 670.776 nm, Rb(I) 780.027 nm) was investigated. The ICP-MS settings were optimized for maximum sensitivity for the ^{115}In signal. The oxide rate (measured by the $^{140}Ce^{16}O/^{140}Ce$ ratio) was kept below 1.9%; doubly charged ions (determined by Ba^{++}/Ba^{+}) were below 3%. Typical instrumental parameters of the measurements are summarized in Table 1.

Visual images of the samples were taken using an optical microscope in reflective-light mode (Leica DM2500M, Leica Microsystems, Wetzlar, Germany).

Preparation of printed patterns

For optimization of the measurement parameters, printed patterns on paper were used. They were prepared as described earlier by Bonta *et al.*[19] Blue printer ink from a conventional office color laser printer was deposited in defined structures onto conventional white paper. Single patterns were cut out and attached to microscopic glass slides using double sided tape. Copper (contained in pigment of blue ink) was the analyte of interest for the optimization experiments of the LA-ICP-MS parameters.

Preparation of tissue cryo-cuts and sample pretreatment

Silicon wafers (Infineon Technologies Austria AG, Villach, Austria) were found to provide optimal properties as carrier material for elemental analysis of tissue cryo-cuts. Especially the low background signal for all elements of interest, compared to glass slides, was a favorable aspect. However, preliminary experiments showed that tissue thin-cuts would not tightly attach to the silicon wafer. Therefore, surface modification of the wafers was performed. According to a protocol published by Maddox and Jenkins,[20] the natural SiO_2-surface of the wafers was silylated using (3-aminopropyl)-triethoxysilane (APES). This procedure forms a thin layer of basic moieties on the silicon wafers, providing optimal linkage with the acidic amino acid groups of the proteins in the tissue. 500 μL of APES (stored under inert gas) were mixed with 10 μL high purity water and 25 mL acetone. The clean and dry silicon wafers were immersed in the mixture for one minute. Subsequently, the treated wafers were transferred into a bath of high purity water, where they were kept for 2 minutes. Subsequently, the wafers were removed from the water bath and allowed to dry under ambient conditions.

Snap frozen surgical tissue specimen were attached to a sample holder using Shandon Cryomatrix (Thermo Scientific, Cat. no. 6769006). 20 μm thick sections were cut using a cryotome (Leica CM3050 S) at −20 °C. The produced thin sections of the tissues were deposited onto the surface-modified silicon wafers and air-dried at room temperature. After deposition on the silicon wafers, the tissue thin sections were coated with a thin gold layer used as a pseudo-internal standard for LA-ICP-MS analysis. Coating was performed using an Agar B7340 sputter coater (Agar Scientific Ltd, Essex, UK) equipped with a target

Published on 26 October 2015. Downloaded on 11/02/2016 08:21:58.

Table 1 Optimized measurement parameters used for the presented experiments

Laser ablation system	
Laser output energy [mJ]	21.5
Laser ablation crater [μm]	40
Laser repetition rate [Hz]	2
Stage scan speed [μm s^{-1}]	80
Carrier gas flow (He) [L min^{-1}]	0.8
Make-up gas flow (Ar) [L min^{-1}]	0.8
Spectrometer system (Czerny–Turner)	
Detection channels	6
Detector	CCD
Gate delay [μs]	0.1
Gate width [ms]	1.05
ICP-MS (Thermo iCAP Q)	
Coolant gas flow (Ar) [L min^{-1}]	15.0
Auxiliary gas flow (Ar) [L min^{-1}]	0.8
RF power [W]	1550
Dwell time per isotope [ms]	10
Cones	Ni
Measured isotopes	^{31}P, ^{56}Fe, ^{57}Fe, ^{63}Cu, ^{65}Cu, ^{64}Zn, ^{68}Zn, ^{194}Pt, ^{195}Pt, ^{197}Au

from high purity gold. Sputter conditions were set as reported previously.[21]

Simultaneous LIBS and LA-ICP-MS measurements and image construction

The sample surfaces (*i.e.*, printed patterns and tissue sections) were scanned by the laser beam using a linescan pattern. All lines were scanned in the same direction, with a break of five seconds between the ablation of two lines. The horizontal distance between single lines was chosen to be the size of the ablation crater. In preliminary experiments, the optimal laser settings were evaluated. It was desired that the complete sample material on one location was ablated with one laser shot. Additionally, the stage scanning speed had to be adjusted in order to provide short measurement times without considerable washout effects on the LA-ICP-MS signal. Evaluation of the scan speed was performed using the metric area mismatch percentage (AMP) introduced by Bonta *et al.*[19] Microscopic images of the patterns were compared with the elemental distributions obtained from the LA-ICP-MS measurements. The AMP value was calculated, describing the differences between the two images, and thus, the image quality of the elemental distribution image.

LIBS distribution images were constructed using the knowledge about the exact position of one ablation location. Peaks were chosen manually, background correction was performed for every peak by subtracting the integral of a nearby area, which exhibited only background signal. Time-resolved intensity data obtained from the LA-ICP-MS measurements were converted into distribution images using a data import routine in ImageLab (v.1.00, Epina GmbH., Pressbaum, Austria).[22] The data acquired by both domains were combined in ImageLab, which allows the processing of multisensor imaging data.

Results

Optimization of the measurement parameters for simultaneous LIBS and LA-ICP-MS analysis

In order to optimize the measurement process for both parts of the analysis, several parameters had to be taken into consideration. All measurement parameters were optimized considering the fact that the final distribution image should have a lateral resolution of 40 μm per pixel. This resolution was found to be sufficient for medical interpretation of the results, while keeping the measurement time as low as possible.

Optimization of the LIBS parameters for measurement of biological samples. The LIBS signal for the analyzed bulk components of the tissue (C, H, and O) should be optimized in order to obtain highest signal intensities for these elements. A tissue thin cut was used for optimization if the LIBS parameters. Compared to typical solid samples, in the case of tissue thin-cuts, the whole sample material is ablated. To ensure complete ablation of the sample material across the whole area covered by the laser beam (*i.e.*, to obtain the maximum LIBS signal per sample location), the laser output energy was chosen to fully ablate the sample material in one shot. Furthermore, stage scan speed and repetition rate were set in a way that consecutive laser shots would not overlap. Thus, at a laser beam diameter of 40 μm (equal to the area of material ablation), for example, a laser repetition rate of 1 Hz and a stage scan speed of 40 μm s^{-1} would be feasible. Also other pairs of settings were possible, however, if the ratio of repetition rate and stage scan speed was constant, the LIBS signal should not be influenced. The dependence of stage scan speed and image quality should be investigated in a later step.

If laser spot size and the ratio of repetition rate and stage scan speed were constant, the remaining parameters influencing the detected signal intensity were laser energy and gate delay of the spectrometer. A full factorial design of experiments (DoE) was carried out, to define the optimal settings. Thus, a set of feasible parameters was chosen to be examined. Laser output energies providing complete yet controlled ablation of the sample material using a single shot (23.0, 21.5, 16.6, and 12.3 mJ), as well as spectrometer gate delays of 0.05, 0.1, 0.2, and 0.5 μs were taken into consideration for the optimization. In preliminary measurements of human tissue samples, the carbon emission line at 247.856 nm showed to have the weakest abundance, compared to hydrogen at 656.279 nm and oxygen at 777.421 nm. While the other analytes were still monitored, DoE was carried out for the emission line of carbon. Relative standard deviations of the yielded intensities were always below 10% ($n = 10$).

The background corrected signals of the carbon emission line at 247.856 nm showed the highest intensity at a laser output energy of 21.5 mJ and a spectrometer gate delay of 0.1 μs. Thus, these parameters were selected for the following experiments. The chosen settings also allow satisfactory detection of hydrogen and oxygen. The general trend of the results shows that shorter spectrometer gate delays and higher laser output energies promote the intensity of the carbon signal.

 This journal is © The Royal Society of Chemistry 2016

Published on 26 October 2015. Downloaded on 11/02/2016 08:21:58.

Optimization of the LA-ICP-MS parameters. Compared to LIBS, where the emission spectrum of every laser pulse is collected, for LA-ICP-MS, the washout time of the ablation cell is a crucial parameter. The range of feasible measurement settings is already very limited by the favorable factors for the LIBS part of the experiment. Thus, only four pairs of laser repetition rate and stage scan speed (with a constant ratio of these two values) were evaluated. All other parameters were kept constant, as they had already been optimized for the LIBS measurements. Printed patterns on paper containing copper as the analyte of interest were used for this optimization step. Definition of the most favorable parameters for LA-ICP-MS measurement was performed according to a procedure proposed by Bonta *et al.*[19] Printed patterns on paper were used to determine the laser settings which would depict the actual distribution of the analyte in the best way. A visual image of the printed sample was compared with the measured elemental distribution image at each laser setting. The metric 'area mismatch percentage' (AMP) was employed for this task. While the laser output energy was kept at 21.5 mJ and the ablation crater diameter at 40 μm, stage scan speed and laser repetition rate were altered (1 Hz/0.04 mm s^{-1}, 2 Hz/0.08 mm s^{-1}, 5 Hz/0.20 mm s^{-1}, 10 Hz/0.40 mm s^{-1}). The determination of the AMP value was carried out in three replicate measurements.

A laser repetition rate of 2 Hz at a stage scan speed of 80 μm s^{-1} exhibits the lowest AMP value, *i.e.*, the best conditions for optimal representation of the actual elemental distribution in the LA-ICP-MS image. The appearing trend of the AMP values can be explained easily: slower scan speeds lead to an inconstant signal course, as most of the sample aerosol will already be washed out prior to the next laser pulse. Faster scan speeds will create image blurring owing to incomplete washout of the ablation cell when already ablating the next location.

Analysis of a tissue sample using the optimized conditions

By a combination of the two performed optimization steps, the best measurement settings for a simultaneous LIBS and LA-ICP-MS measurement could be determined. The optimized dependent variables were signal intensity (for LIBS) and image accuracy (for LA-ICP-MS).

To obtain a general overview about the elements to be analyzed by the LIBS-domain of the system, a scan across 1 mm^2 of a representative area of a tumor sample was performed. Measurements were performed as linescans; the optimized parameters were used for the measurements. An area without sample material was ablated using the same instrumental settings, to obtain a blank spectrum of the sample carrier material (silicon wafer). A blank-subtracted LIBS spectrum of the investigated sample area is presented in Fig. 1. 100 spectra acquired from single laser shots were accumulated for this spectrum.

Besides the element of interest, also alkaline (Na, K) and earth alkaline elements (Ca, Mg) can be identified. Typically, abundances of these elements in biomaterials are rather high[23] and LIBS measurements are very sensitive for those elements. Thus, monitoring of these sample constituents using LA-ICP-MS was omitted, as analysis using LIBS showed to be feasible. Abundances of typical trace elements in biological tissues, as well as the administered drug were considered for selection of the isotopes for LA-ICP-MS measurement, yielding count rates ranging between some thousand counts per second (^{195}Pt) to several hundred thousand counts for ^{56}Fe.

Elemental mapping of a human tumor sample

Elemental mapping of tumor sections for their metal content using LA-ICP-MS, is already well established in the life sciences. However, also information about the bulk elements of biological tissues might be of important value to give information about tissue composition, which can be obtained using LIBS. Thus, in this study, simultaneous mapping of trace and bulk elements using a simultaneous LIBS and LA-ICP-MS system was performed. The measurement parameters determined during the optimization procedure described above were used for the elemental mapping experiment. A cryo-cut of a human malignant pleural mesothelioma (MPM) sample with a thickness of

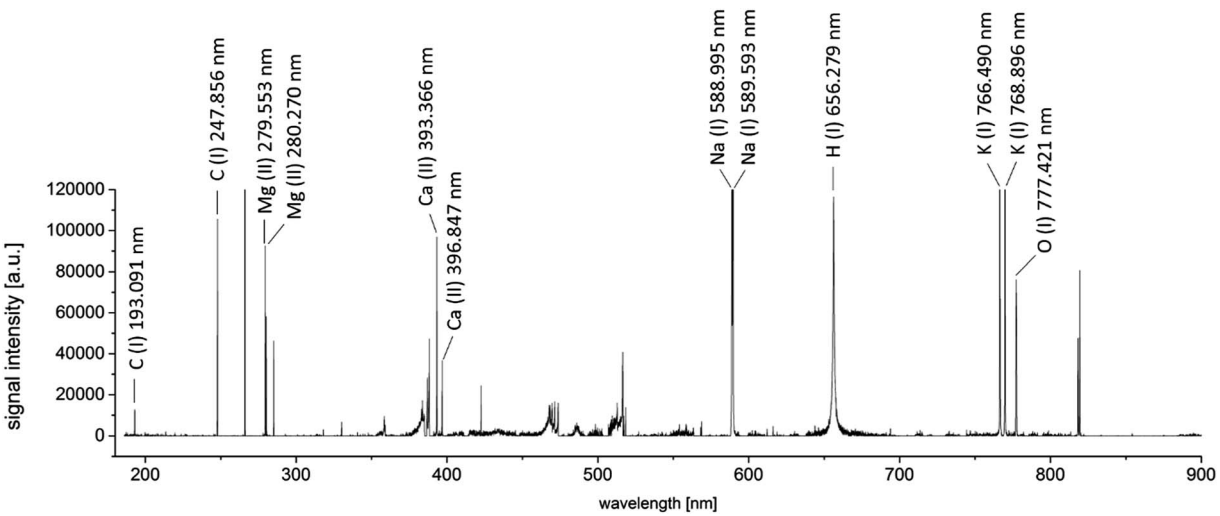

Fig. 1 LIBS spectrum of a tissue sample, accumulated signals from 100 laser shots.

Published on 26 October 2015. Downloaded on 11/02/2016 08:21:58.

20 μm deposited on a surface-modified silicon wafer was fully ablated during one cycle of analysis. To correct instrumental drifts of the ICP-MS device during operation, the ^{197}Au signal, derived from a sputtered gold layer on the sample surface, was used as a pseudo-internal standard. The elemental distribution images for selected elements (lateral resolution 40 μm) are displayed in Fig. 2.

The hematoxylin and eosin staining of a consecutive tissue thin-cut displayed in Fig. 2l reveals areas with tumor tissue (purple) and regions without viable tumor cells (pink). The two consecutive tissue slices are not perfectly matching. Still, areas with viable tumor cells can be identified. Together with this information, the obtained elemental distributions can be interpreted. The bulk elements carbon and hydrogen (Fig. 2g and h) are rather homogeneously distributed over the thin section of the tissue. Still, some areas show altered signal intensities, most probably indicating higher or lower tissue density in the respective regions. Also differing tissue thickness might be contributing to these signal changes. The distributions of carbon and hydrogen show a numerical correlation. Linear regression of the signal intensities of corresponding pixels yielded a correlation coefficient of 0.9599. This finding leads to the conclusion that the C/H-ratio is rather constant throughout the tissue. In comparison, phosphorus (Fig. 2b) and oxygen (Fig. 2i) exhibit heterogeneous distribution throughout the section. Higher intensities of these two elements correlate well with the tumor regions (especially in the right part of the tissue). A good correlation between the distributions of the elements might point towards a high phosphate concentration in those regions. This could be explained by a high number of activated proteins (*i.e.*, phosphorylated species), high DNA content, and a high amount of phospholipids in the tumor

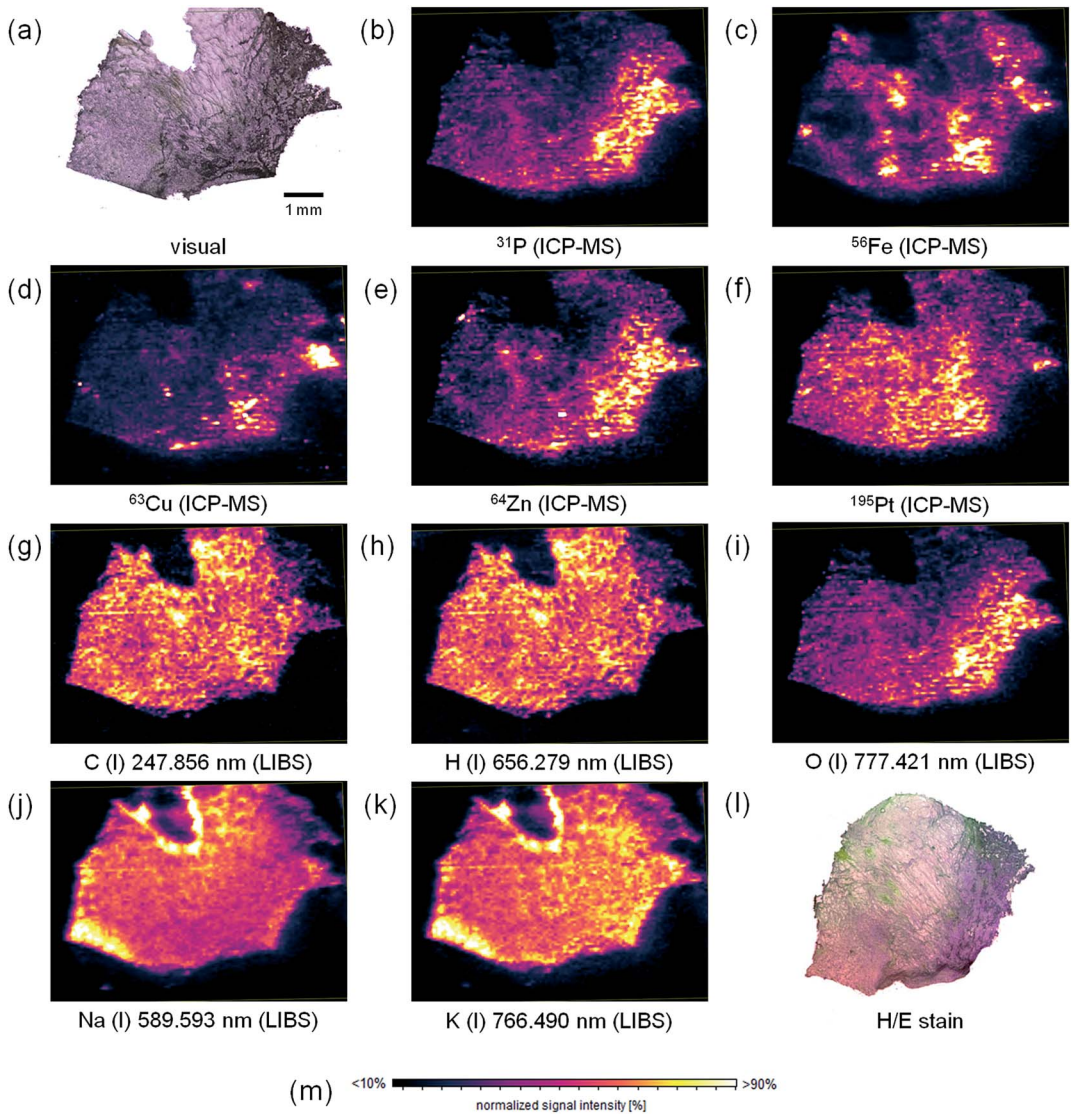

Fig. 2 Microscopic image of the analyzed sample (a), elemental images of ^{31}P (b), ^{56}Fe (c), ^{63}Cu (d), ^{64}Zn (e), and ^{195}Pt (f) determined by LA-ICP-MS, elemental distributions of carbon (g), hydrogen (h), oxygen (i), sodium (j), and potassium (k) measured using LIBS, a consecutive tissue thin-cut after hematoxylin and eosin staining (l), color scale for the displayed images (m).

 This journal is © The Royal Society of Chemistry 2016

Published on 26 October 2015. Downloaded on 11/02/2016 08:21:58.

regions. All these compounds can be found in a higher concentration in tumor tissue, as the growth rate of the cells is increased in such tissue areas. Zinc (Fig. 2e) and copper (Fig. 2d) exhibit similar distributions. These elements are important trace elements and often acting as cofactors of proteins. Notable examples of proteins employing Cu and/or Zn as cofactors are for example superoxide dismutase (SOD),[24] or some ATPases.[25] These proteins are essential for tackling oxidative intracellular stress (SOD), and for protein phosphorylation (ATPases).

Compared to analytes detected with higher signal intensities in the tumor tissue, platinum (Fig. 2f), originating from the treatment of the patient with cisplatin, a commonly used anticancer drug, is rather accumulated in healthy tissue areas. This effect has already been described earlier.[8] Probably, the drug has not yet entered tumor regions, or some resistance mechanisms occur, which hamper drug uptake.

Iron (Fig. 2c) exhibits a very inhomogeneous distribution across the tissue sample. However, no histologically relevant structures can be correlated with the obtained elemental distribution. As with copper and zinc described before, also iron is an important cofactor for many proteins[26] with functions for example in oxygen transport or energy storage. Sodium (Fig. 2j) and potassium (Fig. 2k) are homogeneously distributed. The distributions have a good numerical correlation ($R^2 = 0.8781$), potassium shows slightly higher signal intensities in the tumor area. The v-shaped structure in the upper part of the image can be related to a contamination from the embedding medium. The increased intensities of both signals in the left part of the tissue sample cannot be explained. The biological function of sodium and potassium is closely related: a Na/K-gradient keeps up the membrane pressure of the cells and therefore helps to maintain their state.[27] Magnesium and calcium exhibit similar distributions (not shown). These two elements also have similar functions in organisms. Both play a pivotal role in signal transduction.[28]

Conclusion

In the presented study, the simultaneous use of LIBS and LA-ICP-MS (tandem LA/LIBS) has been used for elemental mapping of trace and bulk elements in biological tissues. After thorough method optimization, a human tumor sample has been investigated to show the applicability of this technique. The benefits of this simultaneous application using LA-ICP-MS and LIBS for the analysis of biological samples were highlighted: while LA-ICP-MS is perfectly suited for the laterally resolved analysis of trace elements in the tissue (*e.g.*, Fe, Zn, Cu), LIBS is optimal for mapping of major (C, H, O) and minor elements (Na, K, Ca, Mg) in biological tissues. LIBS also allows the analysis of elements that are affected by high background signals (*e.g.*, K), or polyatomic interferences (*e.g.*, Mg) when employing ICP-MS detection. Most common mass analyzers used for ICP-MS devices operate on a sequential basis (today, only a small fraction of instruments employs time-of-flight or other simultaneous mass analyzers), reducing the number of isotopes monitored by LA-ICP-MS will also increase the accuracy of measurement for the remaining analytes. Thus, the parallel use of LIBS complements classical LA-ICP-MS in many aspects and its application for elemental mapping of biological samples represents a number of improvements. Biological functions of the trace elements could be well correlated with their respective distributions. The additional information obtained by using LA-ICP-MS and LIBS simultaneously might yield information which is also relevant for medical questions. For example, the well correlated phosphorus and oxygen distributions suggest a high abundance of phosphates. Such information can help to make the results of elemental analysis more valuable for the use in drug development and medication.

Acknowledgements

The research was supported by the Office of Basic Energy Sciences, Chemical Science Division and the Defense Nuclear Nonproliferation Research and Development Office of the U.S. Department of Energy under contract number DE-AC02-05CH11231 at the Lawrence Berkeley National Laboratory. M. B. wants to acknowledge the MEIBio PhD program of the TU Wien for providing a scholarship for the period 2013–2016.

References

1 N. S. Mokgalaka and J. L. Gardea-Torresdey, Laser Ablation Inductively Coupled Plasma Mass Spectrometry: Principles and Applications, *Appl. Spectrosc. Rev.*, 2006, **41**(2), 131–150.
2 D. Günther and B. Hattendorf, Solid sample analysis using laser ablation inductively coupled plasma mass spectrometry, *TrAC, Trends Anal. Chem.*, 2005, **24**(3), 255–265.
3 R. E. Russo, *et al.*, Laser Ablation in Analytical Chemistry, *Anal. Chem.*, 2013, **85**(13), 6162–6177.
4 J. S. Becker, *et al.*, Bioimaging of metals by laser ablation inductively coupled plasma mass spectrometry (LA-ICP-MS), *Mass Spectrom. Rev.*, 2010, **29**(1), 156–175.
5 D. Hare, C. Austin and P. Doble, Quantification strategies for elemental imaging of biological samples using laser ablation-inductively coupled plasma-mass spectrometry, *Analyst*, 2012, **137**(7), 1527–1537.
6 E. Moreno-Gordaliza, *et al.*, Elemental bioimaging in kidney by LA-ICP-MS as a tool to study nephrotoxicity and renal protective strategies in cisplatin therapies, *Anal. Chem.*, 2011, **83**(20), 7933–7940.
7 J. S. Becker, *et al.*, Bioimaging of metals in brain tissue by laser ablation inductively coupled plasma mass spectrometry (LA-ICP-MS) and metallomics, *Metallomics*, 2010, **2**(2), 104–111.
8 M. Bonta, *et al.*, Quantitative LA-ICP-MS imaging of platinum in chemotherapy treated human malignant pleural mesothelioma samples using printed patterns as standard, *J. Anal. At. Spectrom.*, 2014, **29**(11), 2159–2167.
9 D. Hare, *et al.*, Elemental bio-imaging of melanoma in lymph node biopsies, *Analyst*, 2009, **134**(3), 450–453.
10 D. A. Frick and D. Günther, Fundamental studies on the ablation behaviour of carbon in LA-ICP-MS with respect to

Published on 26 October 2015. Downloaded on 11/02/2016 08:21:58.

the suitability as internal standard, *J. Anal. At. Spectrom.*, 2012, **27**(8), 1294–1303.
11 D. W. Hahn and N. Omenetto, Laser-induced breakdown spectroscopy (LIBS), part II: Review of instrumental and methodological approaches to material analysis and applications to different fields, *Appl. Spectrosc.*, 2012, **66**(4), 347–419.
12 A. W. Miziolek, V. Palleschi and I. Schechter, *Laser induced breakdown spectroscopy (LIBS): Fundamentals and applications*, 2006, p. 1–620.
13 J. Kaiser, *et al.*, Trace elemental analysis by laser-induced breakdown spectroscopy – Biological applications, *Surf. Sci. Rep.*, 2012, **67**(11–12), 233–243.
14 D. Santos Jr, *et al.*, Laser-induced breakdown spectroscopy for analysis of plant materials: A review, *Spectrochim. Acta, Part B*, 2012, **71–72**, 3–13.
15 L. Sancey, *et al.*, Laser spectrometry for multi-elemental imaging of biological tissues, *Sci. Rep.*, 2014, **4**, 6065.
16 M. Dong, *et al.*, Elemental analysis of coal by tandem laser induced breakdown spectroscopy and laser ablation inductively coupled plasma time of flight mass spectrometry, *Spectrochim. Acta, Part B*, 2015, **109**, 44–50.
17 K. Subedi, T. Trejos and J. Almirall, Forensic analysis of printing inks using tandem laser induced breakdown spectroscopy and laser ablation inductively coupled plasma mass spectrometry, *Spectrochim. Acta, Part B*, 2015, **103–104**, 76–83.
18 J. R. Chirinos, *et al.*, Simultaneous 3-dimensional elemental imaging with LIBS and LA-ICP-MS, *J. Anal. At. Spectrom.*, 2014, **29**(7), 1292–1298.
19 M. Bonta, *et al.*, A metric for evaluation of the image quality of chemical maps derived from LA-ICP-MS experiments, *J. Anal. At. Spectrom.*, 2015, 1809–1815.
20 P. H. Maddox and D. Jenkins, 3-Aminopropyltriethoxysilane (APES): a new advance in section adhesion, *J. Clin. Pathol.*, 1987, **40**(10), 1256–1257.
21 M. Bonta, *et al.*, Application of gold thin-films for internal standardization in LA-ICP-MS imaging experiments, *Analyst*, 2014, **139**(6), 1521–1531.
22 http://www.imagelab.at/.
23 M. L. Carvalho, *et al.*, Trace elements in human cancerous and healthy tissues: A comparative study by EDXRF, TXRF, synchrotron radiation and PIXE, *Spectrochim. Acta, Part B*, 2007, **62**(9), 1004–1011.
24 B. Sarkar, Metal protein interactions, *Prog. Food Nutr. Sci.*, 1987, **11**(3–4), 363–400.
25 O. Sitsel, *et al.*, Structure and function of Cu(I)- and Zn(II)-ATPases, *Biochemistry*, 2015, 5673–5683.
26 R. Lill, Function and biogenesis of iron–sulphur proteins, *Nature*, 2009, **460**(7257), 831–838.
27 E. J. Conway, Principles underlying the exchanges of K and Na ions across cell membranes, *J. Gen. Physiol.*, 1960, **43**, 17–41.
28 G. G. Somjen and G. Kato, Effects of magnesium and calcium on neurones in the central nervous system, *Brain Res.*, 1968, **9**(1), 161–164.

This journal is © The Royal Society of Chemistry 2016

A metric for evaluation of the image quality of chemical maps derived from LA-ICP-MS experiments

Maximilian Bonta, Andreas Limbeck, C. Derrick Quarles Jr, Dayana Oropeza, Richard E. Russo and Jhanis J. Gonzalez, *Journal of Analytical Atomic Spectroscopy*, 2015

Volume 30 | Number 8 | August 2015 | Pages 1681–1830

JAAS

Journal of Analytical Atomic Spectrometry

www.rsc.org/jaas

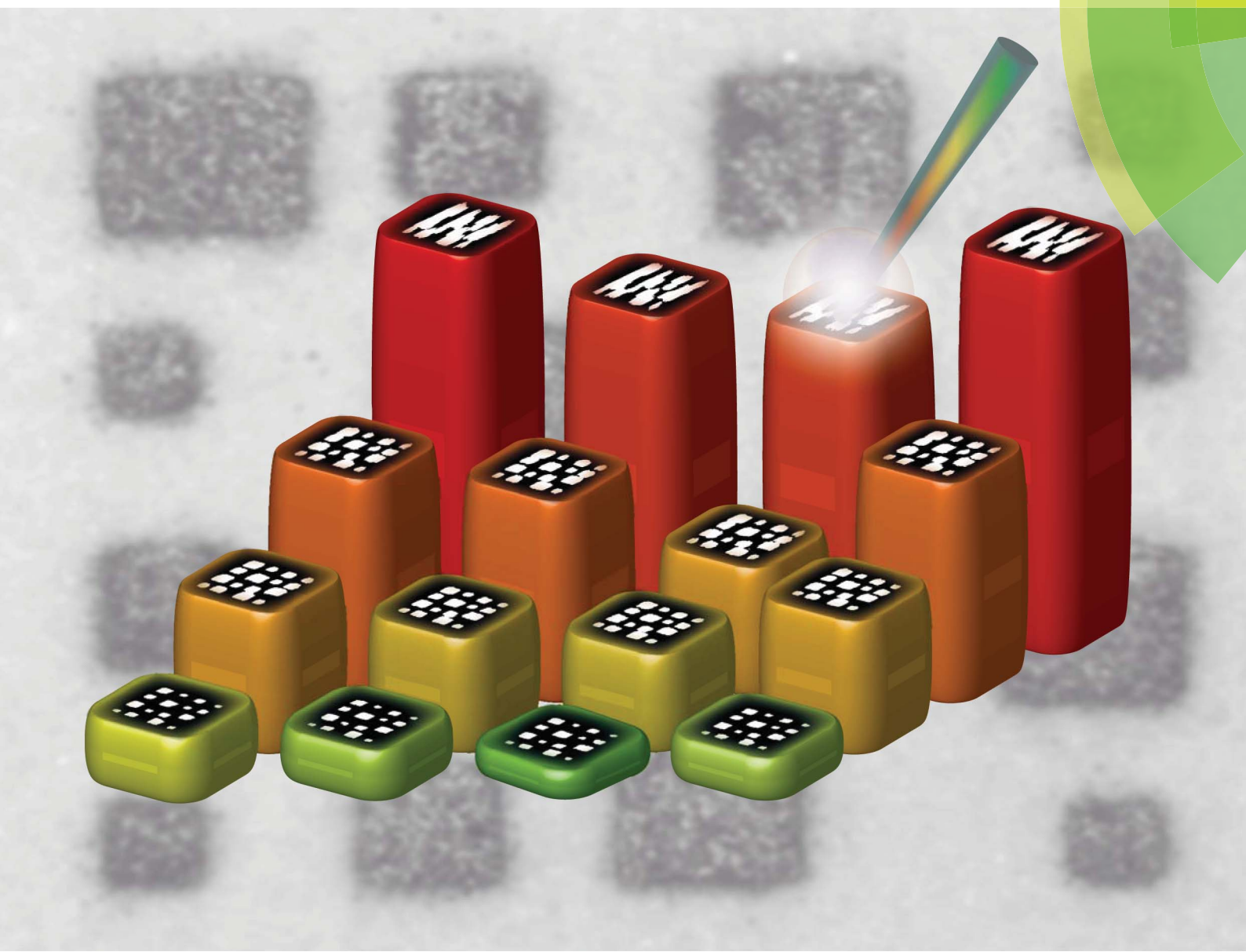

ISSN 0267-9477

ROYAL SOCIETY OF CHEMISTRY

TECHNICAL NOTE

Gonzalez *et al.*

A metric for evaluation of the image quality of chemical maps derived from LA-ICP-MS experiments

JAAS

TECHNICAL NOTE

Cite this: *J. Anal. At. Spectrom.*, 2015, **30**, 1809

A metric for evaluation of the image quality of chemical maps derived from LA-ICP-MS experiments

Maximilian Bonta,[a] Andreas Limbeck,[a] C. Derrick Quarles Jr,[b] Dayana Oropeza,[c] Richard E. Russo[bc] and Jhanis J. Gonzalez*[bc]

For laser ablation-inductively coupled plasma-mass spectrometry (LA-ICP-MS) imaging experiments – as well as other techniques used for elemental or molecular mapping – the accordance of the measured distribution with the actual distribution is of utmost importance to guarantee reliability of the obtained images. In most experiments reported in the past, the experimental conditions have been chosen so that washout effects and signal carry-over are minimized by scanning the sample surface very slowly. Therefore, measurement times become very long and decently resolved images will require acquisition times of several hours up to more than one day. To increase the application range of LA-ICP-MS for imaging it is important to decrease the measurement times, which is best accomplished by increasing the scanning rates. However, depending on the instrumentation, this can lead to blurring and compromised image quality. In this work, we present a metric to compare the measured elemental distribution with their actual distribution based on a sample with visually distinguishable features. This approach allows quantitative determination of the image quality and enables comparison of multiple measurement conditions. This information can be used for method optimization, to get a reasonable tradeoff between image quality and measurement time.

Received 20th February 2015
Accepted 26th February 2015

DOI: 10.1039/c5ja00056d

www.rsc.org/jaas

Introduction

Laser ablation-inductively coupled plasma-mass spectrometry (LA-ICP-MS) has gathered interest in various fields of science during the past decades.[1–6] The opportunity to perform laterally resolved analyses combined with sub-μg g^{-1} detection limits for most elements using modern ICP-MS instrumentation is valuable for addressing a large range of scientific applications. Besides the use of LA-ICP-MS for bulk analysis, circumventing the problem of complex and time consuming sample preparation, this technique is also frequently utilized for elemental mapping (imaging) of samples in two or three dimensions.[7] Typically, imaging experiments are employed for mapping of elements in minerals,[8,9] biological materials,[10–14] and other sample types.[15] Typical lateral resolutions range between 20 and 100 μm. Recent achievements in LA-ICP-MS imaging, especially involving bio-imaging, have lead to improved lateral resolutions down to 1 μm.[16,17]

A challenge for LA-ICP-MS imaging measurements is to reduce the long acquisition time required for these experiments. Depending on the desired lateral resolution and sample area, some measurements may take up to 30 hours or more,[18] making this technique laborious for routine analyses especially if fast sample throughput is required. Typically, two approaches are used for imaging experiments with LA-ICP-MS. The first one is a spotscan over the sample surface. The laser is systematically fired onto discrete spots subsequently covering the whole region of interest on the sample. Typical waiting times between two spots are from microseconds to a few seconds (0.1–10 s, depending on the cell volume) to ensure total particulate washout from the cell. Certainly, this method allows for the most reliable imaging by avoiding image blurring. However, a long measurement time is required for complete aerosol washout from the chamber. The second and more often employed method[18,19] uses linescans covering the area of interest on the sample. Using the desired laser beam diameter, line after line is scanned and the recorded signals are either saved as one file or as single files for every line, depending on the software or algorithm used for data evaluation and image construction. The crucial parameters of linescans are the laser repetition rate and the scan speed, both of which will influence the image quality of the resulting elemental maps. At a constant laser beam diameter, the total measurement time is determined only by the scan speed. In many experiments, laser scan speeds

[a]*Vienna University of Technology, Institute of Chemical Technologies and Analytics, Vienna, Austria*

[b]*Applied Spectra, Inc., Fremont, CA, USA. E-mail: jjgonzalez@lbl.gov; Fax: +1 510-4867303; Tel: +1 510-4952899*

[c]*Lawrence Berkeley National Laboratory, Environmental Energy Technologies Division, Berkeley, CA, USA*

This journal is © The Royal Society of Chemistry 2015

are set based on the laser beam diameter. Often, very slow scan speeds have been reported to be used. Still, compared to a spotscan, this approach drastically reduces the measurement time. Moreover, even higher scan speeds may be applied and still deliver a satisfactory image quality with further reduced measurement time, as stated in previous publications.[20] In both approaches, the material washout of the cell is important, and in this latest approach a slow washout combined with high scan speeds might lead to signal carryover to following sample locations leading to distortion of the image.

Already earlier, Lear *et al.*[20] investigated the effect of changing sampling parameters on image quality. It showed that fast scan speeds are applicable for imaging experiments, making the measurements more time efficient. However, it has been stated that the washout behavior of the used cell plays a significant role for the maximum obtainable scan speed and thus, image quality might suffer from blurring effects.

In this work, we present an approach for evaluation of the image quality in terms of correlation with a visual image of the sample. The correlation is described by a metric, to accurately determine the quality of the elemental distribution image. In contrast to previously presented studies with the goal to optimize imaging parameters, the aim of this study was the quantitative determination of the image quality. Metrics obtained from different images can be easily compared, without being influenced by the instrument where the measurement has been performed or the method of image construction. For method development, printed patterns on paper have been used, which have already been shown to be a valuable tool for evaluation of parameters in imaging experiments.[21,22]

Methods

Instrumentation

Experiments were performed using a femtosecond laser ablation instrument (J200, Applied Spectra Inc., Fremont, CA) coupled to an inductively coupled plasma mass spectrometer (Bruker Aurora elite, Bruker, Billerica, MA). The instrumental conditions were checked on a daily basis to ensure proper function of the instrumentation using the certified reference material NIST610 trace elements in glass (National Institute of Standards and Technology, Gaithersburg, MD). Typical instrumental parameters are shown in Table 1.

Ablation of the sample material was performed under a constant helium gas flow, which was subsequently mixed with argon as make-up gas using a glass T-piece in close proximity of the ablation chamber outlet. Helium gas flow was optimized in preliminary experiments to obtain the shortest possible washout times. Two different cell volumes (33 mL and 16 mL) were evaluated for washout effects. Both cells were of drop-shaped geometry with the in- and outlet positioned along the axis of symmetry. In this work, the cell with an inlet–outlet distance of 65 mm will be referred to as 'large cell' and the cell with a 45 mm inlet–outlet distance as 'small cell'. The described cells are commercially available standard equipment of the used laser ablation system. For measurement each sample was placed along the axis of symmetry one centimeter from the cell outlet.

Preparation of printed patterns

Printed patterns were designed in Microsoft Power Point 2010 (Microsoft Corp., Redmond, WA). Blue color (RGB color code #00FFFF) was used to design the patterns. Squares sized 200 × 200, 300 × 300 and 400 × 400 μm were drawn with distances between 200 and 400 μm between the edges of the squares. The patterns were printed using a conventional office laser printer (Brother, Nagoya, Japan) onto white office paper with a high resolution print setting (2400 dpi). After the printing process, single patterns were cut out and attached to microscopic glass slides using double sided tape. Each slide was equipped with only one pattern to ensure identical position of each sample in the ablation cell, since altered washout due to a changed sample position could affect the results of the measurements.

Processing of the visual images

The pigment from the blue color printed onto the paper samples contains copper; the background signal of copper from the paper was negligible in preliminary experiments. Signals for the copper background yielded around 5000 cps (^{65}Cu), compared to more than 5 000 000 cps on areas with ink application. Therefore, the only considerable source of copper was the ink deposited on the paper. Before the LA-ICP-MS experiments, microscopic images of the samples were taken to enable comparison of the actual copper distribution (represented by the blue color) with the obtained copper distribution maps from

Table 1 Typical instrumental parameters used for the sample measurements

Laser ablation		ICP-MS	
Wavelength	1030 nm	Plasma power	1500 W
Pulse duration	450 fs	Cool gas flow	18.0 L min^{-1}
Laser repetition rate	10, 20, 40 and 80 Hz	Auxiliary flow	1.8 L min^{-1}
Laser beam diameter	40 μm	Cones	Ni
Laser energy	120 μJ	Scanning mode	Peak hopping
Laser scan speed	0.05, 0.1, 0.2, 0.5 mm s^{-1}	Dwell time per isotope	8 ms
Laser beam geometry	Circular	Monitored isotopes	^{13}C, ^{48}Ti, ^{63}Cu, ^{65}Cu
He gas flow	0.7 L min^{-1}	Mass resolution	$300m/\Delta m$
Ar make-up flow	0.7 L min^{-1}		

This journal is © The Royal Society of Chemistry 2015

the LA-ICP-MS analysis. The visual sample images were pre-processed to a size of 680 × 600 pixels, and maximum contrast was set to obtain the best visual differentiation between the blue color and the paper surface. Thereafter, the colored image was processed to a black and white image. Image preprocessing steps were performed using photographic image processing software (Adobe Lightroom 4.1, Adobe Systems, San Jose, CA). The resulting images were imported to Origin Pro 9.0 (OriginLab Corp., Northampton, MA) and processed to binary images consisting of only black and white pixels by setting a proper cutoff value between black and white; areas with ink deposition were white while areas without ink were black.

LA-ICP-MS measurement of the printed pattern samples and image construction

All measurements were performed with a laser beam diameter of 40 μm ablating a total sample area of 2.72 × 2.40 mm. The resulting distribution images were 68 × 60 pixels in size with each pixel covering 40 μm of the sample in both horizontal and vertical direction. In contrast to the other reported optimization study,[20] the quadrupole dwell time was kept constant throughout all experiments, to show only the effects of altered laser sampling conditions on the image quality. Raw data were exported as text files and processed using ImageLab (Epina GmbH, Pressbaum, Austria). Spotscans were performed at a 20 Hz repetition rate firing 10 shots per location (0.5 s ablation time) with a 10 second delay between ablation of each location to let the signal reach background level after each laser shot. The distance between the centers of adjacent laser shots was 40 μm in both the horizontal and vertical directions.

Linescans were performed at varying laser repetition rates and laser scan speeds. All assumptions made here are valid when the whole sample is ablated during the analysis (*i.e.* for thin sections or thin films). The scan direction was kept constant for each line and the delay time between the ablation of two consecutive lines was 10 s. The signals of elements that are constituents of the paper were used for automatic detection of the measured lines using ImageLab.[23] The values for the horizontal pixels were calculated by dividing the signals obtained for the lines into 68 regions, such that every pixel spans 40 μm in horizontal direction. The acquired data points in each one of those regions were averaged to calculate the pixel values for the distribution images. A virtual sample (Fig. 1a) is scanned using two different laser scan speeds. The data treatment for image construction is illustrated in Fig. 1b and c. In this example the laser beam diameter is 40 μm. The regions are set such that the laser beam covers 40 μm in the length of one region; 1.0 s for 0.040 mm s^{-1} and 0.25 s for 0.160 mm s^{-1}, respectively. The intensity averages of the raw signals recorded in each of those regions deliver the pixel values for one horizontal line. When using higher scan speeds the time one region spans gets shorter as the laser covers more distance in the same amount of time. As the washout of the cell is independent from the scan speed more pixels will have wrong values than at slower scan speeds. The illustration in Fig. 1 shows that higher scan speeds promote blurring effects. While in Fig. 1b (0.040 mm s^{-1}) only one region (pixel) is affected by the washout, Fig. 1c shows at least 4 pixels will represent wrong signal intensities before the signal intensity reaches background level again.

For both spot- and linescans, time resolved data were acquired and stored in a single file. The largest squares of the printed pattern (400 × 400 μm) were used to calculate the reference value for the detection threshold. This value was determined using the average intensity of ^{65}Cu at the center of these squares (3 × 25 pixels). Using the 10 percent valley definition commonly used in mass spectrometry to determine peak separation,[24] a signal drop of 90% was regarded as being sufficient evidence that no major blurring effects would occur. Binary distribution images of ^{65}Cu were calculated with white areas representing the presence of a ^{65}Cu signal above the calculated threshold and black areas showing signal intensities below this mark. Matching of the elemental distributions with the visual image was accomplished using the knowledge of the exact position of the ablated area.

Comparison of the binary images

For each analyzed sample, two binary images were created. One shows the presence of copper represented by the blue color in the light microscopic image, and the other shows if a ^{65}Cu signal 10% above the average maximum signal has been detected using LA-ICP-MS. To expose the areas that are similar or different, the two images were treated as matrices and a

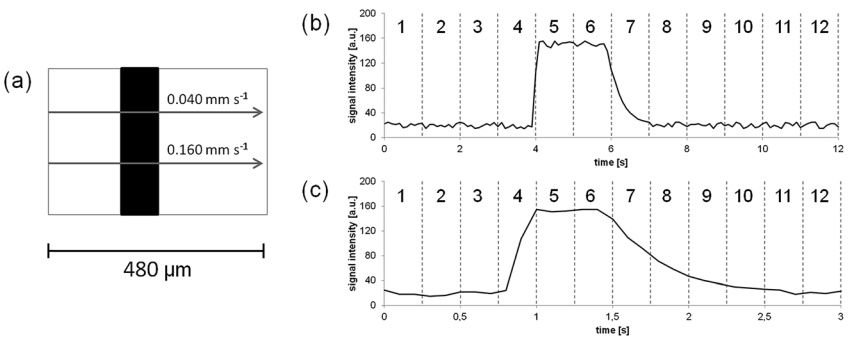

Fig. 1 Illustration of a virtual sample with an 80 μm wide feature containing an arbitrary element (feature in black, (a)), simulated ICP-MS signals for the same element for the scan speeds 0.040 mm s^{-1} (b) and 0.160 mm s^{-1} (c) with the numbered regions for calculation of the pixel intensities.

simple subtraction step was performed. As the two images were initially of different resolution (the resolution of the visual image is typically higher than the one of the elemental image), the image sizes had to be adjusted in order to carry out the subtraction. Therefore, the size of the elemental image was expanded to fit the size of the visual image. If the size of the visual image is an integral multiple of the size of the elemental image this expansion can be performed without interpolation of pixels, *i.e.* pixels of one color divided into more pixels of the same color. When processing the visual image, this aspect has to be considered, and the final visual image has to fulfill this requirement. The process of image resizing is illustrated in Fig. 2.

After the adjustment of the image dimensions, the values of corresponding pixels in the two images can be subtracted. This may result in two different scenarios: both pixels are either white or black, therefore the result of the subtraction will equal zero; or one of the pixels is black and one is white, so the result of the subtraction will be different from zero. If the result of the subtraction is zero, pixels are matching; if the result is unequal to zero pixels are not matching. Therefore, the amount of pixels with a value other than zero can be used as a measure for the area that has been wrongly assigned in the elemental image. A value describing the amount of mismatched areas (area mismatch percentage, AMP) can further be calculated as a percentage of the wrongly assigned area and the total image area. This metric can be used to describe the image quality of each measured elemental distribution image. It has to be pointed out, that after expansion of the initial elemental distribution image the term pixel is no longer referring to the actual lateral resolution of the map but is just used as an area measure.

Results and discussion

Measurement time and optical image comparison

As pointed out earlier, the long measurement time of LA-ICP-MS is a point of concern for the application of this technique for a broader range of imaging applications. Sample throughput can be increased and resources such as gas and electricity can be saved by making imaging analyses using LA-ICP-MS faster. The investigation of the samples presented in this work takes about 12 hours using a spotscan with a 10 s waiting time between the ablation of two adjacent spots. The analysis time can be drastically reduced using linescans (even with slow scan speeds) to 64 minutes for a scan speed of 0.05 mm s^{-1}. Increasing the scan speed can further reduce the measurement time to 38 minutes for 0.1 mm s^{-1}, or even less for faster scan speeds. However, image resolution and reliability of the images should not be affected by the aspect of shortening the measurement time required for the experiments. Therefore, it is important to define the actual image quality, to effectively evaluate the result of faster scan speeds on image quality. Optical analysis of the images is often subjective, as it depends on the color scale used, the scaling method, and, of course, the eyes of the user. Therefore, conclusions drawn from this approach might be misleading and the interpretation of the results may not reveal the actual best measurement conditions. Fig. 3a shows a distribution image of ^{65}Cu and Fig. 3b shows the microscopic image of the very same pattern. The structure of the copper distribution on the printed areas appears to be very smooth and the edges are sharp; no blurring effects can easily be seen.

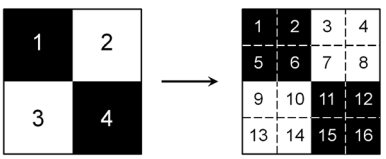

Fig. 2 Illustration of the image expansion from a 2 × 2 pixel image matrix to a 4 × 4 image matrix.

However, the comparison of two or more images is very difficult and it is almost impossible to determine which one of a series of images represents the actual copper distribution better, and which measurement conditions should be preferentially used. The images are converted to binary images (Fig. 3c and d). After subtraction of the two images, differences can be highlighted.

Subtraction of the visual image and the elemental distribution map

Visualization of the differences between the optical and the elemental image provides insight into the occurrence of mismatched areas. After image processing and construction of binary images the individual pixel values of aligned images were subtracted. The results of selected samples are shown as difference images in Fig. 4.

The spotscan (Fig. 4a) clearly shows the best accordance between the visual and elemental images, as only a minimal area is divergent between the visual and the chemical image of copper. Areas where copper is not present, but is detected above the threshold (red), and areas that contain copper, but none is detected (green) are relatively equal in amount and size. These areas mainly occur on the edges of the printed squares leading to the conclusion that shots might not hit areas with only ink or only paper and therefore lead to too low or too high signal intensities. This issue could be minimized using a higher lateral resolution (*e.g.* smaller laser beam diameters). In comparison, the linescan with low scan speed (Fig. 4b) shows similar results. However, the edges are broader and most of the wrongly assigned areas represent overestimated copper signals. Especially in the scan direction (from left to right) the edges are wider, indicating slight blurring effects due to the material washout from the ablation cell. Still, the edges are sharp and the actual copper distribution is well represented in most of the image areas. The image with the high scan speed (Fig. 4c) shows strong image blurring in scan direction and squares with less distance in between each other even become connected. This first step of the image analysis already reveals the differences between different sampling modes and measurement conditions. If the size of the wrongly assigned areas is set in relation to the overall image area, the area mismatch percentage (AMP) can be calculated.

This journal is © The Royal Society of Chemistry 2015

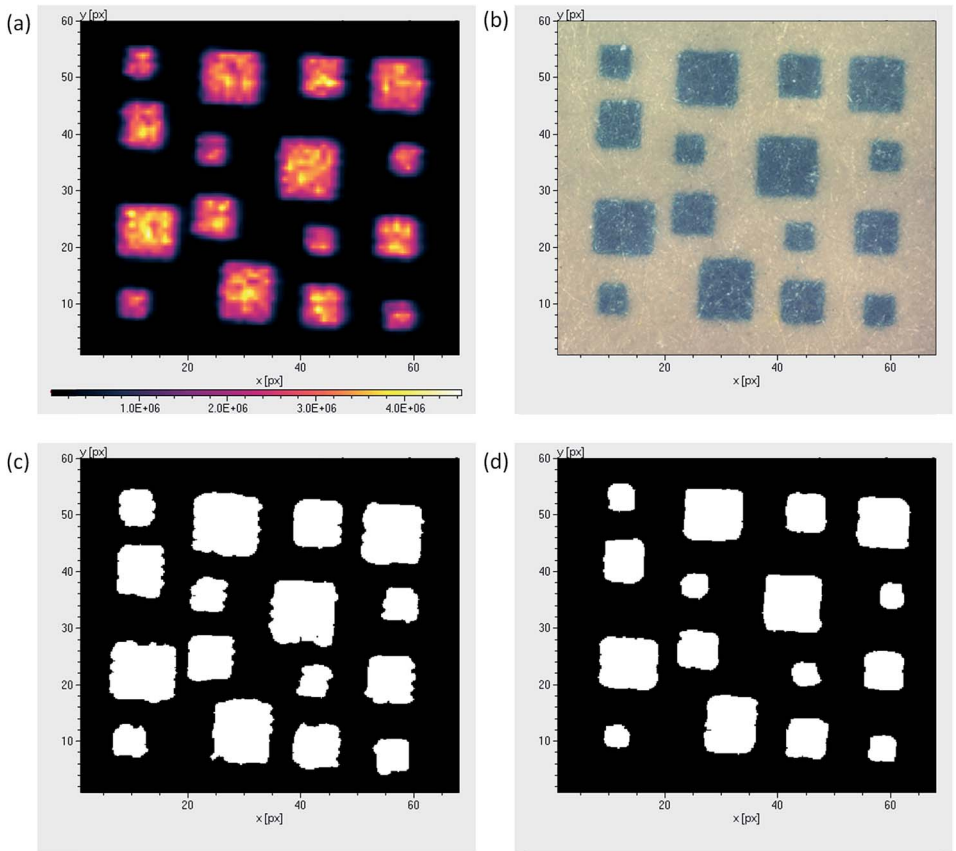

Fig. 3 Elemental distribution of ^{65}Cu (a) and the microscopic image of the same pattern taken before sample analysis (b). LA-ICP-MS analysis was performed using a scan speed of 0.05 mm s^{-1} and a laser repetition rate of 40 Hz with the small washout cell. Elemental distribution (c) and visual image (d) after conversion to binary images.

Comparison of measurement conditions and washout cells

Using the proposed method for calculation of the wrongly assigned image area, measurement conditions and instrumental features can be compared. In the presented study, the method has been used to compare the following measurement conditions on the quality of the resulting elemental images of copper: laser repetition rate, scan speed, and two different cell volumes. An imaging experiment using a spotscan was considered as a reference value for the best obtainable image quality at a constant laser beam diameter; no image blurring will appear here. Sixteen measurement conditions were evaluated and applied to each of the two washout cells. This results in a total of 32 images measured using linescans. Furthermore, three images were measured with the same washout cell and the same

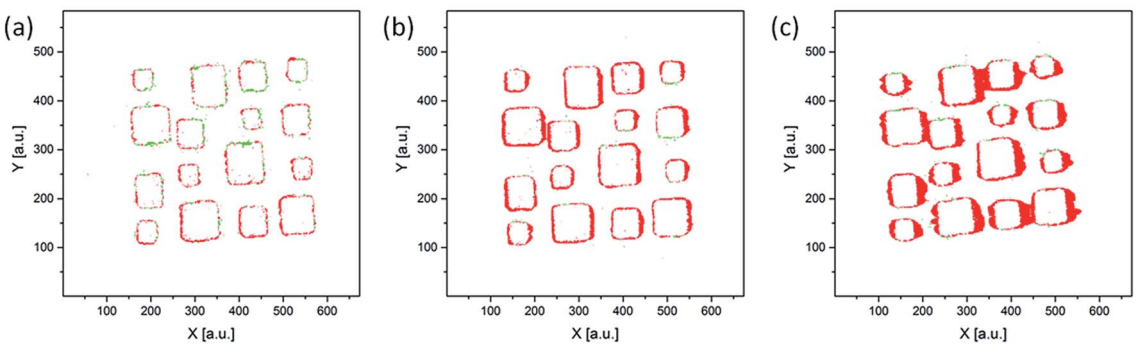

Fig. 4 Difference plots of visual image and elemental distribution (^{65}Cu) for a spotscan (a) and linescans with 0.05 mm s^{-1} (b) and 0.2 mm s^{-1} scan speed (c) acquired at 40 Hz repetition rate using the large washout cell; red areas show ^{65}Cu signal above the threshold and do not have blue color (positive bias), green areas have blue color but the ^{65}Cu signal does not exceed the threshold (negative bias). The laser scan direction of all displayed images is from left to right.

experimental conditions, to evaluate the typical variation of the AMP value. This experiment was carried out using the large ablation cell and 0.1 mm s^{-1} scan speed at 20 Hz repetition rate. The average AMP value of this series of experiments was 3.54 ± 0.13% indicating that the calculated percentages are very accurate. Even small variations may indicate significant changes in the quality of the resulting maps. A plot of the experimental conditions and the resulting AMP values is presented in Fig. 5.

As demonstrated in Fig. 4, higher scan speeds result in larger mismatched areas. This is reflected by the AMP values. Especially at scan speeds of 0.2 and 0.5 mm s^{-1}, the correlation of the visual image and the elemental map gets significantly worse compared to low scan speeds. The spotscan (measurement time: 12 h) has a lower AMP value (1.96%) than all linescans, showing that this approach results in the best image quality. The best AMP values with the linescan approach were achieved using the slowest scan speed and the small washout chamber, ranging between 2.5 and 3.0%. Comparing the two washout cells, the cell with the smaller volume shows overall lower AMP values. This gives the opportunity to use the same scan speed while improving image quality, or increasing the scan speed (shorter measurement time) while maintaining the same AMP value. For example, using a laser repetition rate of 80 Hz at a laser scan speed of 0.2 mm s^{-1} with the small washout cell will result in almost the same AMP value (5.70%) as using the large cell at the same repetition rate and 0.1 mm s^{-1} (5.57%). However, this change reduces the measurement time from 38 min to 24 min. In contrast to changes of the scan speed, variation of the laser repetition rate only shows minor effects on the AMP value. Especially at higher scan speeds, results get slightly better with increased repetition rate. This might be attributed to the fact that the high repetition rate leads to faster complete material ablation, and ablated area overlap is reduced.

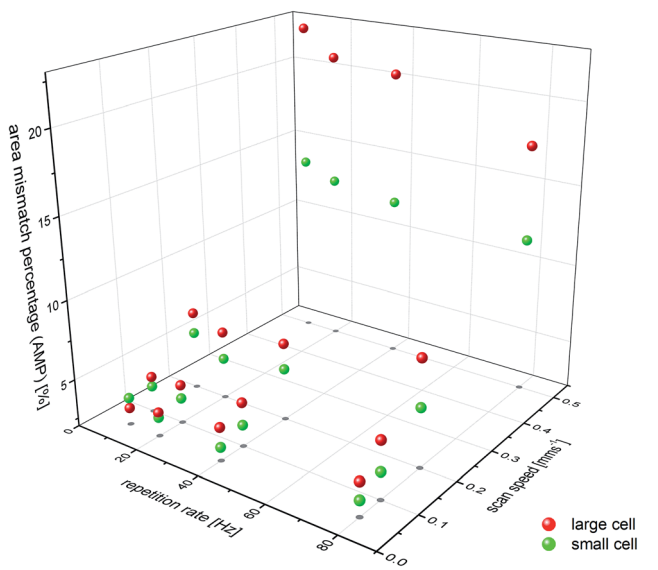

Fig. 5 Area mismatch percentage (AMP) plotted against the experimental conditions using the large (red) and the small (green) aerosol washout cell.

However, if the whole sample material cannot be ablated, the repetition rate optimum might be found at a different value.

Conclusion

The proposed method for evaluation of image quality was shown to be a valuable approach to investigate sampling conditions in LA-ICP-MS imaging experiments. Printed patterns which can be reproducibly manufactured without major workload were used as model samples. As shown, the range of investigated analytes is not limited to elements that are typically constituents of ink.[25] The ink may be spiked with elements of interest in a concentration range that is expected to appear in the samples of interest. However, the washout behavior should not change dramatically between copper and other common metallic analytes. As the threshold values are calculated on a relative basis to the maximum of each measured image, variations in analyte concentration are not considered to be a major factor. Using this new approach, the image quality of the elemental distributions acquired using different experimental conditions and/or instrumentation can be compared on an objective basis. In future research, the effects of different image construction methods will be evaluated, which is also a current topic in the growing range of applications for LA-ICP-MS imaging.

Acknowledgements

The authors want to thank Applied Spectra, Inc. for providing access to instrumentation at their facility that was crucial for performing the experiments. M.B. wants to thank the MEIBio PhD program at the Vienna University of Technology for providing a scholarship over the period of 2013–2016. The research at LBNL was supported by the Chemical Science Division, Office of Basic Energy Sciences, U.S. Department of Energy under Contract no. DE-AC02-05CH11231.

References

1 R. E. Russo, X. Mao, J. J. Gonzalez, V. Zorba and J. Yoo, *Anal. Chem.*, 2013, **85**, 6162–6177, DOI: 10.1021/ac4005327.
2 D. Günther and B. Hattendorf, *TrAC, Trends Anal. Chem.*, 2005, **24**, 255–265, DOI: 10.1016/j.trac.2004.11.017.
3 J. Koch and D. Günther, *Appl. Spectrosc.*, 2011, **65**, 155–162, DOI: 10.1366/11-06255.
4 M. Thompson, J. E. Goulter and F. Sieper, *Analyst*, 1981, **106**, 32–39, DOI: 10.1039/an9810600032.
5 J. J. Gonzalez, A. Fernandez, D. Oropeza, X. Mao and R. E. Russo, *Spectrochim. Acta, Part B*, 2008, **63**, 277–286.
6 J. J. González, D. D. Oropeza, H. Longerich, X. Mao and R. E. Russo, *J. Anal. At. Spectrom.*, 2012, **27**, 1405–1412.
7 J. R. Chirinos, D. D. Oropeza, J. J. Gonzalez, H. Hou, M. Morey, V. Zorba and R. E. Russo, *J. Anal. At. Spectrom.*, 2014, **29**, 1292–1298.
8 B. Paul, J. D. Woodhead, C. Paton, J. M. Hergt, J. Hellstrom and C. A. Norris, *Geostand. Geoanal. Res.*, 2014, **38**, 253–263.

This journal is © The Royal Society of Chemistry 2015

9 P. Liu, F. Liu, C. Liu, J. Liu, F. Wang, L. Xiao, J. Cai and J. Shi, *Precambrian Res.*, 2014, **246**, 334–357.

10 J. S. Becker, M. Zoriy, A. Matusch, B. Wu, D. Salber and C. Palm, *Mass Spectrum. Rev.*, 2010, **29**, 156–175, DOI: 10.1002/mas.20239.

11 C. Austin, D. Hare, A. L. Rozelle, W. H. Robinson, R. Grimm and P. Doble, *Metallomics*, 2009, **1**, 142–147, DOI: 10.1039/b901310p.

12 E. Moreno-Gordaliza, C. Giesen, A. Lazaro, D. Esteban-Fernandez, B. Humanes, B. Canas, U. Panne, A. Tejedor, N. Jakubowski and M. M. Gomez-Gomez, *Anal. Chem.*, 2011, **83**, 7933–7940, DOI: 10.1021/ac201933x.

13 O. Reifschneider, C. A. Wehe, I. Raj, J. Ehmcke, G. Ciarimboli, M. Sperling and U. Karst, *Metallomics*, 2013, **5**, 1440–1447, DOI: 10.1039/c3mt00147d.

14 M. A. da Silva and M. A. Arruda, *Metallomics*, 2013, **5**, 62–67, DOI: 10.1039/c2mt20154b.

15 K. M. Stika, C. S. Westphal, J. Kapur, R. G. Raty, J. Li, J. G. Kopchick, W. J. Gambogi, B. Hamzavytehrany, A. Z. Bradley, J. R. Marsh and B. W. Foltz, *2014 IEEE 40th Photovoltaic Specialist Conference*, PVSC, 2014.

16 C. Giesen, H. A. O. Wang, D. Schapiro, N. Zivanovic, A. Jacobs, B. Hattendorf, P. J. Schuffler, D. Grolimund, J. M. Buhmann, S. Brandt, Z. Varga, P. J. Wild, D. Gunther and B. Bodenmiller, *Nat. Methods*, 2014, **11**, 417–422, DOI: 10.1038/nmeth.2869.

17 H. A. O. Wang, D. Grolimund, C. Giesen, C. N. Borca, J. R. H. Shaw-Stewart, B. Bodenmiller and D. Günther, *Anal. Chem.*, 2013, **85**, 10107–10116.

18 D. Hare, B. Reedy, R. Grimm, S. Wilkins, I. Volitakis, J. L. George, R. A. Cherny, A. I. Bush, D. I. Finkelstein and P. Doble, *Metallomics*, 2009, **1**, 53–58, DOI: 10.1039/b816188g.

19 J. Lear, D. J. Hare, F. Fryer, P. A. Adlard, D. I. Finkelstein and P. A. Doble, *Anal. Chem.*, 2012, **84**, 6707–6714, DOI: 10.1021/ac301156f.

20 J. Lear, D. Hare, P. Adlard, D. Finkelstein and P. Doble, *J. Anal. At. Spectrom.*, 2012, **27**, 159–164, DOI: 10.1039/c1ja10301f.

21 D. J. Bellis and R. Santamaria-Fernandez, *J. Anal. At. Spectrom.*, 2010, **25**, 957–963, DOI: 10.1039/b926430b.

22 M. Bonta, H. Lohninger, M. Marchetti-Deschmann and A. Limbeck, *Analyst*, 2014, **139**, 1521–1531, DOI: 10.1039/c3an01511d.

23 http://www.imagelab.at.

24 A. D. McNaught and A. Wilkinson, *IUPAC. Compendium of Chemical Terminology*, The "Gold Book", WileyBlackwell, 2nd edn, 1997.

25 M. Bonta, H. Lohninger, V. Laszlo, B. Hegedus and A. Limbeck, *J. Anal. At. Spectrom.*, 2014, **29**, 2159–2167, DOI: 10.1039/c4ja00245h.

This journal is © The Royal Society of Chemistry 2015

Recent advances in quantitative LA-ICP-MS analysis: challenges and solutions in the life sciences and environmental chemistry

Andreas Limbeck, Patrick Galler, Maximilian Bonta, Gerald Bauer, Winfried Nischkauer and Frank Vanhaecke, *Analytical and Bioanalytical Chemistry*, 2015

Anal Bioanal Chem
DOI 10.1007/s00216-015-8858-0

REVIEW

Recent advances in quantitative LA-ICP-MS analysis: challenges and solutions in the life sciences and environmental chemistry

Andreas Limbeck[1] · **Patrick Galler**[2] · **Maximilian Bonta**[1] · **Gerald Bauer**[1] · **Winfried Nischkauer**[1,3] · **Frank Vanhaecke**[3]

Received: 26 March 2015 / Revised: 9 June 2015 / Accepted: 15 June 2015
© The Author(s) 2015. This article is published with open access at Springerlink.com

Abstract Laser ablation–inductively coupled plasma–mass spectrometry (LA-ICP-MS) is a widely accepted method for direct sampling of solid materials for trace elemental analysis. The number of reported applications is high and the application range is broad; besides geochemistry, LA-ICP-MS is mostly used in environmental chemistry and the life sciences. This review focuses on the application of LA-ICP-MS for quantification of trace elements in environmental, biological, and medical samples. The fundamental problems of LA-ICP-MS, such as sample-dependent ablation behavior and elemental fractionation, can be even more pronounced in environmental and life science applications as a result of the large variety of sample types and conditions. Besides variations in composition, the range of available sample states is highly diverse, including powders (e.g., soil samples, fly ash), hard tissues (e.g., bones, teeth), soft tissues (e.g., plants, tissue thin-cuts), or liquid samples (e.g., whole blood). Within this article, quantification approaches that have been proposed in the past are critically discussed and compared regarding the results obtained in the applications described. Although a large variety of sample types is discussed within this article, the quantification approaches used are similar for many analytical questions and have only been adapted to the specific questions. Nevertheless, none of them has proven to be a universally applicable method.

Keywords LA-ICP-MS · Quantitative analysis · Certified reference material · Matrix-matched standards · Internal standard correction · Liquid standards

ABC Highlights: authored by *Rising Stars and Top Experts.*

✉ Andreas Limbeck
a.limbeck@tuwien.ac.at

[1] Institute of Chemical Technologies and Analytics, Division of Instrumental Analytical Chemistry, TU Wien, Getreidemarkt 9/164, 1060 Vienna, Austria

[2] Elkem AS, Technology, Central Analytical Laboratory, Fiskaaveien 100, P.O. Box 8040, Vaagsbygd 4675, Kristiansand, Norway

[3] Department of Analytical Chemistry, Ghent University, Krijgslaan 281 - S12, 9000 Ghent, Belgium

Introduction

Laser ablation (LA) in combination with inductively coupled plasma–mass spectrometry (ICP-MS) is a powerful technique for the direct elemental analysis of solid samples. This technique provides major, minor, and trace element information with a wide elemental coverage, excellent limits of detection, and a linear dynamic range of up to 10 orders of magnitude, while also enabling microanalysis, depth profiling analysis, and 2-dimensional elemental mapping. Further advantages of LA-ICP-MS are minimal sample preparation, high sample throughput, access to isotopic information, and the possibility of analyzing both conductive and non-conductive and opaque and transparent materials [1–4].

However, two fundamental aspects of processes involved constrain the ability of LA-ICP-MS to act as a universal method for direct analysis of solid samples. The first major drawback of LA-ICP-MS is that the abundances of the ions detected after m/z separation are often not entirely representative of the composition of the original sample. In the literature, this problem is often referred to as "elemental fractionation" [5, 6], although this term is also used to describe time-dependent changes in the composition of the ion beam in the mass spectrometer. Besides the ablation process itself (e.g., non-stoichiometric effects due to the preferred ablation of more volatile compounds), the transport of the aerosol particles

Published online: 14 July 2015

from the ablation chamber into the ICP (e.g., differences in gravitational settling between smaller and larger particles) and vaporization, atomization, and ionization in the ICP (less efficient for larger particles) are also important contributors to fractionation effects. A detailed discussion of the individual contributions to elemental fractionation and the strategies developed for minimizing the influence exerted can be found in the literature [7–14].

The second major problem connected with the use of LA-ICP-MS for direct analysis of solid samples is the difference in the interaction between the laser beam and the sample surface observed for various matrices, causing changes in the mass of analyte ablated per pulse due to differences in the properties of the matrices investigated (e.g., absorptivity, reflectivity, and thermal conductivity). The aerosol particles produced during ablation of different matrices may vary in size and geometry, thus having an effect on the sample transport efficiency from the ablation cell to the plasma [15]. Both effects contribute to differences in the mass load of the plasma and give rise to matrix effects, since the vaporization, atomization, and ionization efficiencies of the analytes introduced into the plasma depend on the mass load [16]. Sample-related "matrix effects" therefore jeopardize the accuracy of LA-ICP-MS analysis and complicate quantification [2–4, 17–20].

As a result, elemental fractionation and matrix effects occur simultaneously, leading to LA-ICP-MS signals that are not representative of the elemental composition of the sample investigated. The sensitivity or absolute signal intensity can vary significantly for samples with the same analyte concentrations, but different matrix compositions and/or physical properties. At this point, it has to be mentioned that mass spectrometric separation and detection of the ions generated can also contribute to the bias in LA-ICP-MS results. However, an explanation of the corresponding sources of bias is beyond the scope of this work; details on these issues can be found in a recently published review article [21]. Figure 1 schematically summarizes the individual steps of LA-ICP-MS analysis prone to elemental fractionation and matrix effects.

As a consequence of the increasing interest in the use of LA-ICP-MS in various scientific fields, research has been devoted to overcoming the aforementioned drawbacks. In the few last years, attempts were made to address the limitations of LA-ICP-MS by improving the instrumental parameters relevant to aerosol formation. Most of this work focused on the influence of the wavelength of the laser radiation (especially important for transparent materials) and the pulse duration (especially important for metallic samples). With the use of shorter ultraviolet wavelengths and pulse durations in the femtosecond (fs) range, instead of the nanosecond range, a significant reduction of elemental fractionation and matrix effects is enabled. Furthermore, the laser beam profiles were changed from Gaussian to (pseudo) flat-top profiles, leading to optimized ablation performance. However, complete elimination of these effects is still not possible. Ongoing research is therefore dedicated to methodological developments that permit correct quantification with the currently available instrumentation for LA-ICP-MS analysis.

The purpose of this review is to summarize state of the art procedures and recent developments in quantitative LA-ICP-MS analysis of samples originating from the fields of life sciences and environmental chemistry. In addition to traditional approaches, novel concepts for the preparation of matrix-matched standards, such as the deposition of elemental coatings or thin polymeric films containing an internal standard on the sample surface, as well as quasi-simultaneous measurement of standard and sample using a spinning platform will be presented. Capabilities and limitations of the different approaches will be compared, critically examined, and evaluated on the basis of their suitability for general use.

Common concepts for quantification in LA-ICP-MS

Even though the application range of LA-ICP-MS is wide and the sample types analyzed are various, some approaches for quantification are applied to a large variety of sample types. The basic principles of the methods described below are the same, while modifications thereof will be presented in the sections dedicated to specific sample types.

External calibration utilizing certified reference materials (CRMs) which match the composition of the sample to be investigated to the largest possible extent—preferably exactly—is the most reliable method for accurate quantification in LA-ICP-MS [20, 22–24]. If this prerequisite is met, ablation, transport, atomization, and ionization of sample and standard can be considered to be (nearly) identical, enabling reliable quantification. For each CRM, a detailed certificate is available containing information regarding component concentrations. Additionally, in the literature, preferred concentration values are available for non-certified sample constituents [25]. However, the lack of appropriate CRMs for the majority of sample types (in particular for samples from environmental, biological, or medical origin) limits the applicability of this approach. Thus, alternative quantification strategies are mandatory.

A promising approach for quantification is the preparation of matrix-matched calibration standards, prepared from material with the same matrix as the sample [26–29]. Procedures for sample preparation preceding LA-ICP-MS analysis reported in the literature include fusion with borate, embedding in a polymer resin, or preparation of a pressed disk in the presence of a binder. Benefits of these sample preparation approaches are that they facilitate the addition of one or more internal standards, known amounts of the analyte(s) of interest (for standard addition purposes) or isotopically enriched spikes (for isotope dilution purposes), as well as the possibility to

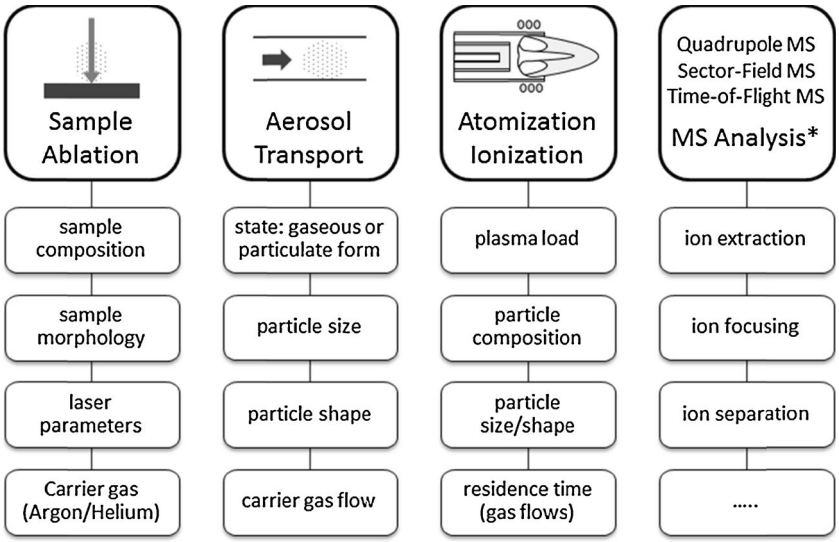

Fig. 1 Sources of error in LA-ICP-MS analysis, * not discussed within this review

adjust the analyte concentrations as required (dilution). A major drawback is the applicability to powdered samples only; samples that are compact in their native form require additional sample pretreatment (i.e., milling, grinding). Furthermore, it has to be considered that this type of adjustment of the sample matrix is automatically accompanied by analyte dilution, which decreases the detection power of the analysis approach.

A frequently applied method in combination with external calibration (i.e., CRMs and in-house standards) is signal normalization to an internal reference or internal standard [30–33]. This approach can be used to further improve the accuracy of the quantification results, since the influence of remaining differences between sample and standard can be minimized. Variations in sample ablation and transport as well as ICP-related alterations in signal intensity (e.g., changing plasma conditions) can be corrected for using an internal standard. A precondition for the successful application of this method is that the internal standard element and the analyte element are homogeneously distributed within the sample, and that their behavior during ablation, transport, and ionization is similar. In this course, crucial parameters are, e.g., the form in which the element is transported from the ablation cell into the ICP (gaseous or particulate) and its mass and ionization potential. The element being used as internal standard can either occur naturally in the sample or is added during the sample preparation process. Optimally, the concentration of the element used as internal standard in the sample is known. However, for successful application it is sufficient that the concentrations in the standard and sample are equal.

"Solid–liquid" calibration in which a dual flow system allows simultaneous introduction of a nebulized aqueous standard solution and laser ablated material is an attractive alternative to the use of matrix-matched solid standards [3, 34, 35]. In this procedure, the carrier gas flow coming from the ablation cell is mixed with an aerosol generated by nebulization of an aqueous standard solution. Besides the addition of aerosol to the gas lines leading to the ICP [36], the use of micronebulizers has also been proposed to add the aerosol to the gas flow directly at the site of material ablation [36, 37]. Not only standards with natural isotopic composition [36] but also isotopically enriched standards [37] have been used for such experiments. Standard and blank solution are alternately added to the sample stream, such that the accompanying difference in signal intensity can be used to quantify the analyte concentrations in the sample. A correction for the differences in ablation efficiency is required and when aiming to maintain the advantages of "dry plasma" conditions, such as a reduced level of oxide interferences, the wet aerosol must be desolvated prior to its mixing with the sample aerosol. However, for special applications, wet plasma conditions may also offer improved measurement conditions, e.g., in terms of signal stability [38]. This method enables quantification based on aqueous standards, and can compensate for matrix-related ionization differences. However, possible variations in ablation efficiency or altered transport efficiencies cannot be accounted for.

Although the quantification approaches mentioned above have been successfully applied in several research fields, including material sciences, geo- and cosmochemistry, environmental chemistry, biology, and medicine [3, 4, 14, 19, 22, 23, 39], their successful application to any kind of sample is not guaranteed. Thus, further improvements are required, which could be achieved either by reducing the extent of matrix effects by using optimized instrumental parameters (e.g., laser radiation wavelength, pulse duration, robustness of ICP) or by developing alternative strategies for quantification.

Analysis of hard tissues and compact samples

Naturally occurring compact materials, such as rocks and minerals, bones, teeth, claws, feathers, or nails, require no

pretreatment like milling or pressing prior to LA-ICP-MS analysis. However, often it might be necessary to flatten the exposed sample surface using a grinding and/or polishing step. Within this review, only samples of biological origin will be discussed. Samples of geological origin will not be described in detail here; for this kind of samples, detailed information can be found in journals devoted to geology and geochemistry.

While quantitative determination of major, minor, and trace elements in the samples mentioned above is the main field of application of LA-ICP-MS, the technique also offers the possibility of performing spatially resolved analysis, which is of interest for studying element distributions (mapping or imaging and depth profiling analysis) or inhomogeneities (solid or fluid inclusions) in many materials. Applications solely dedicated to visualizing elemental distributions are also beyond the scope of this paper, which focuses on those applications in which estimation of bulk or local concentrations forms at least part of the investigation and, possibly, some effort is made for cross-validation using an alternative analytical approach. Yet, calibration approaches discussed here can self-evidently also be deployed in mapping or imaging applications.

Biogenic carbonates: calibration

Although LA-ICP-MS lends itself specifically well to spatially resolved analysis, its application for bulk analysis is justified in cases where a dedicated area across a given set of samples has to be reproducibly analyzed in situ in order to enable comparison. This has been specifically exploited for the investigation of fish otoliths at their cores and edges for the purpose of origin determination of fish populations [31, 40–47], or for the investigation of changes in the prevailing conditions, reflected in the microchemistry of very narrow otolith bands [32, 48–50]. The daily accretion of calcium carbonate layers in otoliths and their permanent retention of chemical fingerprints in the form of various elemental impurities make them an ideal target for this type of investigation [51]. Similar incremental growth behavior and chemical matrix are found in mussel shells and corals. Combined with their immobility, it makes these objects valuable environmental monitors [26, 27, 52–54]. Also larvae tracking applications have been reported for mussels [55, 56]. This type of investigation can be summarized under the term *sclerochronology*.

The different NIST SRM glasses 610, 612, and 614 (National Institute of Standards and Technology, Gaithersburg, USA), with certified trace element concentrations over approximately three orders of magnitude, from the low microgram per gram level to hundreds of micrograms per gram, are by far the most frequently used materials for calibrating biogenic calcium carbonate measurements by LA-ICP-MS [31, 32, 40–43, 46, 48–50, 52–56]. Trying to improve the analytical results, Arkhipkin et al. compensated for the difference in matrix composition between the NIST SRM glass and biogenic calcium carbonate via the introduction of in-house correction factors [46]. However, according to Jochum et al., calibration using NIST SRM glasses as such already results in accurate values for the refractory elements, whereas a closer matrix-matching using calcium carbonate pellets has to be applied for low boiling point elements, such as Pb [53]. Another decisive parameter for measurement accuracy when using the NIST SRM glasses for calibration is the set of reference concentrations used for these materials [53, 57, 58]. Custom-made fused glasses are an alternative to the NIST SRM glasses for calibration purposes. Such glasses were prepared by Sinclair et al. by blending biogenic carbonate (coral powder) with silica in a ratio of 1:1, followed by fusion at 1650 °C and by Perkins et al. by blending $Li_2B_4O_7$ in excess with synthetic $CaCO_3$, MgO, and gravimetric additions of the analytes of interest, followed by fusion over a burner flame [26, 27]. Sinclair et al. obtained reference concentrations for their glasses using solution-based isotope dilution either by ICP-MS or thermal ionization mass spectrometry for all elements other than B, which was calibrated via LA-ICP-MS against NIST SRM 612 using B concentrations from the literature [26].

Besides NIST SRM glasses, carbonate pellets represent the second largest group of calibration materials in the field of biogenic carbonate analysis by LA-ICP-MS [27, 44, 45, 47, 52, 53, 59]. Different carbonate materials pressed into pellets have been used, including the commercially available synthetic calcium carbonates USGS MACS-1 and MACS-3 (United States Geological Survey, Reston, VA, USA) [44, 52, 53], fish otolith powder NRC FEBS-1 (National Research Council Canada, Ottawa, Canada) [47], synthetic in-house carbonates prepared by co-precipitation [45], or in-house standards prepared from gravimetric blends of the analytes of interest and either commercially available calcium carbonate or crushed biogenic carbonate [27]. In one case, the authors blended NIST SRM glasses and carbonate pellets to obtain calibration standards, without revealing whether all materials were used in the same calibration function [52]. However, despite the multitude of calibration materials obviously at hand, the fact that otoliths also contain a significant amount of organic matter is commonly not accounted for [27, 51].

Without exception, all authors use Ca as internal standard element for normalization, albeit with little agreement regarding their choice of the Ca nuclide used for this purpose. This is mainly a question of user experience, instrumental sensitivity, and the means available to overcome spectral interference. All Ca isotopes, apart from the most abundant (^{40}Ca) and the least abundant (^{46}Ca), have been reported in papers related to LA-ICP-MS analysis of biogenic calcium carbonates and referenced in this review. There is also a fair amount of disagreement with respect to the Ca concentration assumed or

measured for otoliths, which is critical for obtaining accurate data. Whereas some authors calculate a theoretical Ca concentration based on $CaCO_3$ stoichiometry [32, 40, 41, 45, 48, 50], others measure it in advance using conventional solution nebulization ICP-MS or ICP-OES [31, 47]. As a result, reported Ca concentrations range from 35 to 40 %. Even when estimates are based on $CaCO_3$ stoichiometry only, some disagreement is possible.

Biogenic hard tissues: claws, feathers, fish scales, and hair: calibration

LA-ICP-MS also becomes an asset when minimally invasive sampling and analysis are required. LA-ICP-MS has been used for the quantitative analysis of animal claws, feathers, fish scales, snake tail clippings, animal hair, human hair, and human finger nails [60–71].

Ethier et al. and Kaimal et al. used the NIST SRM 612 glass as a standard in the context of multi-element analysis of badger claws and bird feathers, respectively [60–62]. Both teams used concentration data obtained via LA-ICP-MS for statistical classification of their results. Whereas Ethier et al. used S as an internal standard as a consequence of the high cysteine content of the sample matrix keratin [60, 61], Kaimal et al., used ^{42}Ca, assuming a homogeneous Ca distribution [62]. For Ethier et al., the use of S as internal standard, quantified in advance using conventional solution nebulization ICP-MS, required the introduction of inter-element sensitivity factors, established from the ICP-MS mass response curve obtained upon ablation of NIST SRM glass. The authors indicated that this approach only yields semiquantitative data. Human and animal hair, as well as human finger nails or clippings thereof, all predominantly comprised of keratin, have been the subject of many studies owing to their capability as a biomonitor of past (trace) element exposure [66–70]. The application of in-house hair or nail material for calibration is quite commonplace in this context [66–70]. Rodushkin and Axelsson used in-house finger nail material, powdered and pressed into a pellet, for calibration of finger nail measurements [70]. Reference concentrations were obtained from conventional solution nebulization ICP-MS after sample digestion. For hair analysis, the certified GBW07601 hair reference material (Institute of Geophysical and Geochemical Exploration, Lanfang, China) was used for calibration [70]. Similarly, Stadlbauer et al. used BCR CRM 397 hair reference material (Institute for Reference Materials and Measurements, Geel, Belgium), pressed into a pellet with polyethylene as a binder [71]. Bartkus et al. and Arriaza et al. both used whole in-house hair standards, quantified for Pb and As by conventional solution nebulization and hydride generation ICP-MS, for calibration of LA-ICP-MS measurements [68, 69]. Dressler et al. pursued calibration of LA-ICP-MS measurements of mouse and human hair by simultaneous aspiration of multi-element solutions (at several concentration levels) via a conventional nebulizer [66]. The wet aerosol was mixed on-line with the dry aerosol coming from the ablation chamber in the injector tube of the ICP torch. Differences in aerosol generation and transport efficiencies between solution nebulization and LA were assessed by ablating in-house hair material with known analyte element concentrations. The in-house hair standard material was prepared by immersion of hair strands in a multi-solution, subsequent drying, and digestion of the material thus obtained for the determination of reference concentrations via conventional solution nebulization ICP-MS. Sela et al. used a similar approach, but one based on standard addition using an ultrasonic nebulizer equipped with a desolvation unit [67]. The dry aerosol intended for calibration was directed through the ablation cell for mixing with the LA aerosol before introduction into the ICP. Concentrations were determined for single hair strands and hair powder, both fixed on carbon tabs. As for the internal standard, both ^{32}S and ^{34}S have been used for hair and finger nail samples [66, 67, 70]. Rodushkin and Axelsson report S concentrations of 4.77± 0.41 % and 3.30±0.56 % for hair and finger nails, respectively [70]. S concentrations were obtained on the basis of hair and finger nail samples of approximately 100 Swedish individuals. Stadlbauer et al. used a quadrupole-based ICP-MS instrument equipped with a reaction cell and adopted sulfur in the form of $(^{32}S^{16}O)^+$ as internal standard to avoid spectral overlap of the $^{32}S^+$ peak with that from the oxygen dimer ion $^{16}O_2^+$ at m/z=32 [71]. Also ^{13}C has been reported as an internal standard for LA-ICP-MS analysis [68, 69]. However, the use of ^{13}C as internal standard is associated with some major drawbacks. Those will be described in the chapter ‘measurement of soft tissues and protein samples’ in the section ‘internal standards’ in more detail.

Holá et al. and Flem et al. both developed LA-ICP-MS methods for trace element quantification in fish scales as an alternative to otolith sampling [63, 64]. Since fish scales contain (Ca-deficient) hydroxyapatite, Holá et al. used NIST SRM 1486 bone meal for external calibration [63]. In contrast, Flem et al. used not less than six different glass reference materials for calibration, namely NIST SRMs 610, 612, 614, 616, NIST SRM 1830 soda limestone float glass, and USGS TB-1 basaltic glass [64]. TB-1 was only introduced for calibration of Sr. Flem et al. commented that for the purpose of their study, normalized data only would have sufficed, yet calibration against the different glasses was included in order to be able to at least provide concentration estimates for later use. Both groups used Ca as an internal standard, determined by electron microprobe analysis in both cases [63, 64]. Flem et al. quote an average Ca concentration of 37.4±0.4 % for a set of fish scales [64], whereas Holá indicate Ca concentrations for three line scans on one fish scale ranging from 23.5 to 26.5 % [63]. Holá et al. also gave some indication of the homogeneity of Ca in fish scales through a spatial distribution

map obtained by electron microprobe analysis [63]. Alternatively, calibration using spiked hydroxyapatite prepared as in-house calibration materials has been reported for LA-ICP-MS investigations of (human) bone and teeth [71].

The last example given describes the direct analysis of water snake tail clippings by LA-ICP-MS as an ecotoxicology tool [65]. Given the complexity of the sample material containing inorganic bone, calcium carbonate, muscle blood, and skin, Jackson et al. resorted to in-house preparation of matrix calibration standards from water snake tail sample material [42]. Reference concentrations were obtained from conventional solution nebulization ICP-MS and ^{13}C was used as internal standard for LA-ICP-MS.

Validation

It is not uncommon to omit validation from the analytical procedure entirely, which may be justified in cases where consistency of results is more important than accuracy, such as in statistical classification of the samples analyzed among different groups [40, 42, 43, 46, 62, 64]. In cases where analyte concentrations are obtained via LA-ICP-MS using non-matrix-matched standards, one should refrain from comparing results to other sets of data obtained for the same sample type by a different analytical approach without validating the quantitative results. Several approaches for this purpose were reported in the literature. Validation by re-measuring the calibration standard, in this case NIST SRM 610 glass, as a sample has also been described, but this is clearly a far from ideal assessment of measurement accuracy [32]. This is appreciated by some authors through the introduction of a reference material as an unknown in the analytical protocol. Different reference materials including USGS MACS-1 and MACS-3 synthetic calcium carbonate, NIES-022 fish otolith powder (National Institute for Environmental Studies, Tsukuba, Japan), and NRC FEBS-1 fish otolith powder have been used for this purpose, as have the limestone reference materials GSJ JLS-1 (Geological Survey of Japan, Tsukuba, Japan), GSR-6 (Ministry of Land and Resources, Beijing, China), and BAS CRM-393 (Bureau of Analysed Samples Ltd, Middlesbrough, UK) [27, 41, 44, 47, 53].

Some authors also validated their LA-ICP-MS results by conventional solution nebulization ICP-MS. Phung et al. performed LA-ICP-MS analysis in holes left by micro-drill sampling for solution nebulization ICP-MS analysis and subsequently compared results from both procedures involving two different LA-ICP-MS facilities [52]. Results agree generally within the quoted analytical errors, with a few exceptions depending on the hole analyzed. Sinclair et al. converted LA-ICP-MS line scans on corals into average concentrations for five elements and compared these to results from solution nebulization ICP-MS of a digest of the same sample [26]. Deviations ranged from approximately −3 to 30 % between the two methods. Dressler et al., Sela et al., and Rodushkin and Axelsson all compare their LA-ICP-MS results for human hair and nail samples to results from conventional solution nebulization ICP-MS [66, 67, 70]. Dressler et al. achieve agreement within analytical error [66], and the results of Rodushkin and Axelsson also showed a good correlation of LA-ICP-MS and solution nebulization ICP-MS results; generally, LA-ICP-MS results are within 30 % of solution nebulization ICP-MS results. Average LA-ICP-MS results obtained by Holá et al. for fish scales are generally higher than the corresponding solution nebulization ICP-MS data, which is also explained by the complexity of the sample matrix, i.e., analyte enrichment in the uppermost layer ablated from fish scales [63].

There is a general agreement between the authors regarding the use of gas blanks for baseline correction. Typically, limits of detection are calculated from three or ten times the standard deviation of the gas blank, divided by the slope of the calibration line or the instrumental sensitivity [31, 42, 44–46, 48]. However, as discussed by Rodushkin and Axelsson, detection limits in LA-ICP-MS depend on the volume of ablated material, the analyte mass, the ionization energy of the analyte, its isotopic abundance, and the ion transmission efficiency [70]. Aerosol size distribution and transport efficiency to the ICP-MS presumably play a role too. For the analysis of hair and nail, detection limits in LA-ICP-MS range from picograms per gram to nanograms per gram and are quoted as only marginally nferior to conventional solution nebulization ICP-MS as a result of sample dilution after digestion for the latter approach.

Measurement of soft tissues and protein samples

In recent years, LA-ICP-MS has also become a technique of growing interest in the life sciences. The effect of variations in trace elemental concentrations, and especially metal–protein interactions are increasingly studied in biological and biomedical investigations [72]. The sample types reported on vary from native samples, such as plant material [73–76], and thin sections of animal/human body tissues (e.g., liver [77], brain [78–80], eye tissue [81], kidney [82], and others), to electrophoretically separated metalloproteins [83, 84]. Typically, natural element distributions within the biological samples were investigated. In special cases, the use of isotopic analysis has been reported (e.g., as tracers for metal uptake in organisms). For example, Florez et al. exposed *Daphnia magna* to isotopically enriched Zn tracers and produced isotope ratio images with 30-μm spatial resolution [85]. A more detailed description of possibilities and limitations of isotopic analysis can be found elsewhere [86].

Like in every other field of LA-ICP-MS applications, quantification is a crucial aspect. Problems aggravating reliable quantification are the large variety of sample types and

properties, as well as a lack of suitable standard materials. However, especially when thin sections of sample material are used (preparation of thin sections is common practice in the medical sciences), some aspects of quantification are facilitated, and some new issues may arise. Those thin-cuts typically have thicknesses of 5–20 μm, thus providing the opportunity to ablate the sample material (the entire depth) completely with a few laser shots, i.e., during one cycle of analysis. The analysis of thin layers renders the analysis of tissue sample much easier, since differences in penetration depth of the laser beam into the sample material do not need to be considered. This gives the opportunity of applying thin layers containing a standard for signal normalization above or below the sample. Those also have to be completely ablated along with the sample. Independently from the quantification strategy used, reliable quantitative analysis is only possible when the thin sections of the samples have equal thicknesses. Some quantification approaches that will be described in later sections rely on this assumption as they cannot compensate for varying layer thickness. If the tissue thicknesses are varying within one sample or the whole tissue sample can not be ablated in a single run, i.e., for thicker samples or bulk material, internal standardization has to be used as for many other types of samples described in this article.

Quantitative imaging approaches

A large number of LA-ICP-MS applications involving soft tissue samples aim to unravel the 2-dimensional trace element distributions (bioimaging or mapping) [87–89]. To preserve information on the spatial analyte distribution, tissue samples are analyzed as thin slices without any prior homogenization step. Three major problems have to be addressed to ensure reliable analysis results: material ablation and aerosol transport are highly matrix-dependent, the efficiency and location of the ionization process in the ICP are a function of the particle size distribution of the aerosol produced via LA [24], which, similarly, is matrix-dependent, and during the measurement time, instrument instability and signal drift may occur because of changing experimental conditions (e.g., cone conditions, vacuum pressure). As a result of those factors, even the measurement of reliable qualitative distribution maps is not self-evident; ensuring reliable quantitative results is even more challenging. Not all approaches that have been presented in the past are capable of adequately addressing the complete range of limitations mentioned.

Solid standard materials

Another method for quantification is the use of solid standard materials. Thereby, a suitable standard material can be manufactured for almost every sample type. CRMs for tissues are only scarcely available, and are in most cases not compatible with the specific experimental conditions (e.g., tissue types, trace elements selected, and/or concentration range).

While quantitative elemental analysis of homogenous materials using LA-ICP-MS can often rely on matrix-matched standards, biological samples may significantly differ in their composition even within several sections of a single sample, and therefore different methods are needed to ensure accurate quantification. Various approaches have been proposed and used to facilitate and improve the quantification of trace elemental distributions in biological tissues and to overcome the problem of often pronounced sample inhomogeneity. Even though many alternative methods for quantification have been proposed, the classical and still most often used method is the use of matrix-matched standards [90]. Those have to be prepared in-house and tuned to the specific application. The preparation of matrix-matched tissue standards has been described by Hare et al. [90] in detail. In short, the selected tissue is homogenized and spiked with an aqueous standard containing the elements of interest; the spiking process is performed at different concentrations enabling the determination of calibration functions. An aliquot of the homogenized and spiked tissues is acid digested for determining the actual analyte element concentrations in the standards. After freezing of the standard, a cryo-cut of desired thickness is prepared for LA-ICP-MS measurement. Alternative approaches for quantification in LA-ICP-MS analysis of biological tissue using solid standards aim at rendering the process of standard preparation easier. Approaches to facilitate the manufacturing process of standard materials use gelatin [91], agarose gel [92], or sol-gel [93] standards, spiked with appropriate amounts of the elements of interest. The preparation of those materials is similar to that of matrix-matched tissue standards, but less tedious. The goal is to minimize the handling of biological materials and still end up with standards with a similar matrix composition (mostly in terms of carbon content and density). One approach uses a polymeric film, spiked with the elements of interest, applied to a glass slide before attaching a thin section of the sample [94]. Assuming simultaneous ablation of standard and sample material, this approach will lead to correction for matrix effects during the measurement—similar to a single standard addition approach. Another way to facilitate standard preparation for analysis of biological tissues is printing of standards onto paper using a commercially available office inkjet printer [95, 96]. Conventional paper can be used for standard preparation, and the inks may be spiked with elements of interest. This method has been successfully used to quantify trace elements in different biomaterials. Reifschneider et al. proposed a method to reduce matrix effects by embedding biological tissues into epoxy resins [97]. In the embedding method used, complete penetration of the resin into the tissue material was ensured. The standards are prepared from epoxy resins without embedded tissue; as the

main matrix material is the epoxy resin, no major difference in matrix composition exists between standards and samples. All methods discussed so far try to simulate the 'average' matrix conditions in the tissues presented. But, a biological sample can be very inhomogeneous and matrix compositions may vary significantly, even within a single sample. Local variations in the matrix composition can lead to inaccurate quantitative results because of alterations in material ablation, aerosol transport, and analyte ionization efficiencies. The approaches for quantification described can reduce such matrix-related effects on the ablation and analyte ionization. Still, those approaches offer no possibility for the correction of instrument instability and/or signal drift or for the reduction of signal variations originating from inhomogeneities in the sample matrix.

Internal standards

Similar to conventional solution ICP-MS measurements, an internal standard can help to correct for changes in the signal intensity originating from instrument instability and/or signal drift. During the long measurement times of imaging experiments (usually 4–30 h), gas flow rates, cone and vacuum conditions, and other experimental conditions may vary. Furthermore, the pronounced inhomogeneity of the samples investigated with profoundly changing matrix compositions require the use of (an) internal standard(s) for reliable quantification [98]. In most publications, carbon has been proposed as the internal standard, as it is abundant in every biological sample and is often uniformly distributed across the sample. However, it has been shown that carbon is not an optimal internal standard [99], as its ionization potential is significantly higher than those of commonly investigated elements, such as most transition metals, and an altered carbon load in the plasma may change the ionization efficiency of some of the analytes monitored substantially. Furthermore, the transport of carbon into the ICP can partly occur in the form of carbon dioxide, which will lead to transport properties and efficiencies that can markedly differ from those elements that are transported as particulate matter only [99]. Therefore, normalization to carbon as internal standard may lead to distortions of the actual analyte distribution, causing inaccurate quantification results. Sulfur has also been proposed as a sample-inherent internal standard [77]; however, it is not evenly distributed in most tissues and, because of its high first ionization energy, similar problems as mentioned for carbon may be expected. Therefore, alternative approaches for signal normalization have been developed to improve the existing quantification methods. Both online addition of wet aerosol [36, 37] and the method with the spiked polymer layers [94] or the epoxy resin [97] have used signal normalization as part of the quantification approach. However, in the first two approaches mentioned, no internal standard in the traditional meaning was used, as ablation of sample and internal standard take place subsequently, and not simultaneously. Another way to normalize the analyte signal which was proposed by Konz et al. [100] and shown to be feasible for quantification [81, 95] is the sputtering of the samples with a thin gold layer; however, this approach only provides a pseudo-internal standard for the same reason. Only the epoxy embedding method provides a true internal standard. The tissue samples are immersed in the epoxy resin containing the internal standard; the resin completely penetrates the tissue material. Therefore, the internal standard is ablated simultaneously with the sample material. Combining the preparation of external standards with matrices similar to the sample material with the use of an internal or pseudo-internal standard can counteract the matrix-related effects on the material ablation, aerosol transport, and analyte ionization, as well as that of instrument instability and/or signal drift.

The necessity of instrumental drift correction was described by Hare et al. [20] and shown by Bonta et al. [95] in later experiments. As mentioned earlier, the long measurement times of LA-ICP-MS imaging experiments may cause significant changes in the instrument sensitivity. This was illustrated in an imaging experiment of a printed pattern with blue ink [95]. Blue ink contains copper, which was investigated as the analyte of interest. The pattern has been coated with a thin gold layer for use as a pseudo-internal standard. Features with equal amounts of ink deposition (i.e., copper concentration) measured at different time points were compared regarding the signal intensity. Figure 2 shows the signal of ^{65}Cu with and without correction to the gold signal. During the 4.5-h measurement time, the absolute signal intensity for ^{65}Cu decreased by 25 %, indicating a strong sensitivity drift. Normalization to gold as pseudo-internal standard corrects for this drift and keeps the sensitivity constant throughout the measurement time. Thus, the necessity and feasibility of signal normalization is underlined as the results show that an

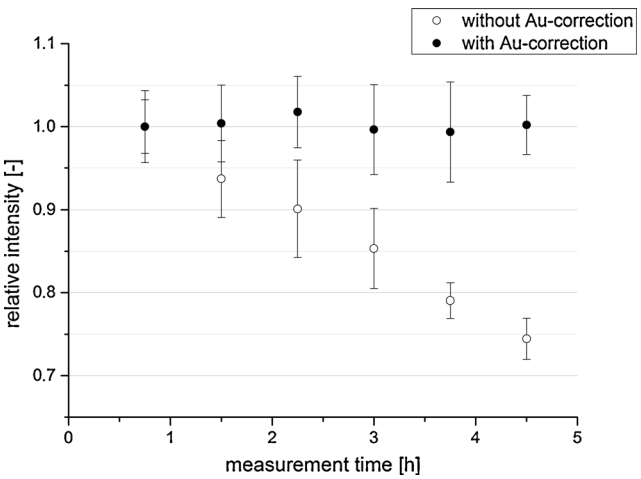

Fig. 2 Signal intensities at different time points with and without gold normalization; averages of 25 data points are displayed (n=25)

internal standard is necessary for reliable LA-ICP-MS imaging experiments.

In summary, quantitative determination of trace elements in biological tissues using LA-ICP-MS is still a challenging task, requiring extensive knowledge of sample composition and properties. Until now, no universal method has been established. Even though the preparation of matrix-matched standards seems to be the most straightforward method, some problems still remain. None of the other alternative methods are recognized as a reliable alternative to matrix-matched tissue standards because, as with every method, some limitations have to be considered.

Electrophoretically separated metalloproteins

Besides the analysis of native soft tissues, also other soft sample materials can be analyzed using LA-ICP-MS. A major group of samples are electrophoretic gels. Separation of proteins or peptides in porous gel matrices is a commonly used bioanalytical method [101, 102]. The biomolecules can be separated on the basis of their mobility in a gel matrix, and visualized using staining methods. Subsequent identification (e.g., using mass spectrometry) can be performed. With the increasing knowledge on metalloproteins, metal detection within the separated proteins has also gained importance. Sensitive elemental analytical techniques that allow for direct analysis of the metals from the gels, like LA-ICP-MS, are a powerful tool to obtain quantitative information on the metal content after electrophoretic separation of the proteins. Quantification of metal contents in electrophoretically separated gels is significantly different from trace element quantification in biological tissues, as a result of the homogeneous composition of the separation gel. However, some crucial aspects also have to be considered to ensure reliable results. Micronebulization of an aqueous standard at the ablation site using either standards with natural isotopic composition [36], or isotopically enriched solutions [37], has been proposed for quantification. In those approaches, changes in ablation and/or ionization behavior of the analytes are not taken into account and therefore an approach with species-specific isotope dilution was proposed by Konz et al. [103]. While in all other methods, the standard is added after material ablation, this method relies on direct addition of the standard to the sample and provides the possibility to compensate for all changes that affect the protein of interest. However, the disadvantage of the method is the fact that the protein of interest has to be available in pure form with an isotopically enriched metal cofactor.

Because the thickness of the gels is typically in the order of 1 mm, the entire thickness is not ablated during a few laser shots. Therefore, the use of carbon as internal standard has been proposed [104]. Still, transferring the proteins to a membrane after separation (blotting) is used far more often, as this allows one to avoid direct analysis of the gel. The investigation of so-called Western blot membranes using LA-ICP-MS has been described in detail elsewhere [105, 106]. In contrast to tissue analysis, the variety of proposed methods in the field of protein analysis is smaller. As with tissue samples, thus far, no optimal quantification method has been found.

Analysis of powdered samples

Sample preparation

Most LA-ICP-MS applications in the fields of environmental research and life sciences focus either on obtaining bulk information (with high precision and accuracy) or on obtaining spatially resolved information, sometimes only semiquantitatively. In contrast to the compact samples discussed in the previous sections, powdered samples require some kind of pretreatment prior to LA-ICP-MS measurement. The approaches most frequently applied for the preparation of compact samples from powders include milling/grinding/sieving for sample homogenization, combined with pelletization [107–112], fusion to sample disks [29, 107, 113–115], or mounting/embedding [110, 116–119] of the sample in a polymeric resin. In some cases, alternative approaches such as ablating standard and sample in quick succession by placing them on a rotary platform or electroplating have been reported [28, 33, 120–125].

During pelletization, the sample powder is compacted using a hydraulic press. Usually, the sample is mixed with a binder to improve powder grain adhesion and to produce stable pellets. Also additives (in liquid or solid form) can be introduced for internal standardization, quantification (e.g., for standard addition or isotope dilution purposes), or to affect laser–sample interaction (i.e., increased energy absorption at the applied laser wavelength). To achieve a better homogeneity, the components are often milled or ground prior to mixing. The pressing step is usually optimized in terms of press power and pressing time. Depending on the ratio of binder to sample, target analytes may be diluted by up to a factor of 10. Thereby, matrix differences between samples will be reduced, but the detection power is decreased. Pelletization is a very easy approach without the need of high-tech equipment. The homogeneity achieved in pressed pellets is sufficient for most applications. However, in some cases the reproducibility achievable is constrained by the sample homogeneity.

For fusion, the sample powder is usually combined with lithium tetraborate or lithium metaborate or a mixture of both. At high temperatures (over 1000 °C), the sample is dissolved in the molten flux and, after cooling, very homogeneous fusion disks are obtained. Like with pelletization, additives can be introduced for internal standardization or quantification. Also by diluting with flux, the matrix similarity increases, while the sensitivity decreases. Fully automated fusion generators are

available, reproducibly delivering homogenous samples and requiring only little analyst effort. Compared to pelletization, borate fusion offers a better homogeneity. However, fusion may be problematic for analytes with low boiling points (below 1000 °C), like As, Cd, or Zn. Analyte losses cannot be eliminated and therefore might give rise to systematic errors. Of course, with this type of sample preparation, information on Li and B as analyte elements is also lost.

The third approach that is frequently used is mounting/embedding. By mounting, the powdered samples are attached on an adhesive surface, like sticky tape or not completely dried epoxy resin. The surface can be coated before or after sample exposition to vary adhesive effects, or to introduce standards. Mounting is mostly used for qualitative and semiquantitative analysis. Adhesiveness is a limiting factor since the surface must be sticky enough to retain powder particles even after the nearby surface has been subjected to laser irradiation; total damage of the investigated particles or removal of particles next to the ablation site has to be prevented. The sample particulates can also be embedded completely in epoxy resin. After embedding, the resins usually need to be cut and polished prior to LA analysis. During preparation of the epoxy resins, standards and other supplements (e.g., surfactants for particle isolation) can also be added to improve the results. With both methods, information on individual particles can be obtained, which is not possible with pelletization or fusion. This aspect extends the possibilities of LA-ICP-MS (e.g., for 2-dimensional mapping), but the sample preparation is very tedious. However, as a result of the possibly widely different composition of the single particles, reliable quantification is practically impossible.

Quantification strategies

Application of CRMs and in-house standards

Signal quantification using solid standards could be accomplished using either CRMs or in-house prepared standards. Usually, sample and standard need to be converted into a compact sample pellet or disk by one of the methods described in the previous section. Regardless of the sample preparation technique used, in all cases an element initially present in the sample and standard or added during sample preparation is used as an internal standard to correct for differences in ablation, transport, and ionization efficiencies. Concentrations of the internal standard in the sample and standard must be determined by complementary techniques (e.g., SEM-EDX, energy dispersive x-ray analysis) or must be sufficiently well known on the basis of stoichiometry.

Hondrogiannis et al. [108] used LA-ICP-TOF-MS to successfully classify 25 vanilla samples according to their origin. Three grams of vanilla powder was directly pressed into a sample pellet. External calibration was achieved versus NIST SRM 1549 (non-fat milk powder), NIST SRM 1575a (trace elements in pine needles), NIST SRM 1515 (apple leaves), NIST SRM 1547 (peach leaves), and NIST SRM 1570a (trace elements in spinach leaves). The method was validated using NIST SRM 1573a (tomato leaves). Eze et al. used LA-ICP-MS to investigate the composition of coal fly ash [33]. Fusion disks of each sample were prepared according to an automatic gas fusion procedure (Claisse M4 gas fusion instrument) with Claisse Flux as binder material. Quantification of 18 elements was achieved via external calibration versus NIST SRM 612 and using ^{29}Si as an internal standard. USGS BCR-2 or BHVO 2G CRMs were used for method validation. Scarciglia et al. investigated soil and paleosoil samples [123]. Thin sections were prepared for LA-ICP-MS analysis and for calibration NIST SRM 612 was relied on because of the lack of soil CRMs. SiO_2, quantified with SEM-EDX, was used as an internal standard. Relative standard deviations (RSDs) were less than 8 % for all elements and less than 5 % for most of them. Further applications include the analysis of Sahara dust samples [118], desert varnish [121], soil samples [116], biomass ashes [29], fly ash samples [113], ash related deposits [120], coral skeletons [125], and forensic investigations [110]. Detailed information can be found in Table 1.

If no suitable CRMs are available, or the range of analytes cannot be covered, the preparation of in-house standards is another possibility for quantification. Coedo et al. determined six elements in electric arc furnace flue dust [111]. Samples were pressed into pellets using paraffin and cellulose/*N*-butylmethacrylate. Standards were prepared by spiking synthetic ZnO/Fe_2O_3 matrix (1:1) with multi-element solution standards and Rh as an internal standard. The approach was validated with four reference materials. Su et al. [112] determined the distribution of metals in single wood fibers. The fibers were fixed by pressing them onto pellets with graphite powder. For quantification, matrix-matched pellets were prepared with cellulose powder and softwood pulp, doped with multi-element standards. The difference in the amount of ablated material was compensated for by introducing a mass coefficient. Fitzpatrick et al. investigated sol-gel processes to establish in-house calibration standards [28]. They showed that S and Se can be added up to 3 % of the total xerogel concentration, while for transition metals the corresponding maximum level is 0.01 %. The xerogels thus obtained were used for calibration in the LA-ICP-MS analysis of NIST SRMs 610 and 612 (trace elements in glass), achieving satisfactory results with RSDs comparable to those achieved using glass CRMs. According to their work, xerogels seem to be a feasible alternative for glass CRMs. However, no accurate results could be produced for samples with high sulfide contents.

Improved standard approaches

Compared to the reported approaches using CRMs and in-house prepared matrix-matched standards, the quantification

Table 1 Pretreatment and quantification approaches for powdered samples

	Sample type	Sample preparation	Quantification	IS	Validation	Recovery	RSD	Ref.
Standard procedures	Vanilla samples	Pressed pellets	NIST SRM 1549, NIST SRM 1575a, NIST SRM 1515, NIST SRM 1547 and NIST SRM 1570a		NIST SRM 1573a	83–106 %	6.2–14.3 %	108
	Coal fly ash	Borate fusion	NIST SRM 612	Si	USGS BCR-2 or BHVO 2G			29
	Soil samples	Thin sections	NIST SRM 612	Si			<5–8 %	123
	Sahara dust samples	Adhesive tape	NIST SRMs 612 and GSD-1G	Si	USGS W-1 and BCR-2, MPI-DING T1-G and GSJ JG-1a	75–125 %	<15 %	118
	Desert varnish	Direct analysis	NIST 61X series		NIST SRM 612	80–120 %	<20 %	121
	Biomass ash	Borate fusion	NIST SRMs 610 and 612					33
	Fly ash samples	Borate fusion	NIST SRM 2691					113
	Ash related deposits	Embedded in epoxy resin	NIST SRM 2691					120
	Soil samples	Ashing, mounting in epoxy resin	NIST SRM 2691 and NIST SRM 1633b				15–40 %	116
	Coral skeletons	Glass-fused/cut into thin sections	NIST SRMs 610 and 612 and MPI-DING KL2-G	Ca	USGS MACS-1/NIST SRM 614	80–120 %	<4–15 %	125
	Forensic applications	Tape mounting and pelletization	USGS PACS-2, NIST SRM 2704, NIST SRM 2710 and NIST SRM 2710a	Sc, Lu			<15 %	110
	Furnace flue dust	Pressed pellets	Synthetic ZnO/Fe_2O_3 matrix	Rh	CRM 876-1, AG-6203, AG-6201, and AG-SX3705	85–115 %	<7 %	111
	Wood fibers	Pressed pellets	Pellets prepared with cellulose powder, softwood pulp					112
	Glass, silicate	Xerogel disks	NIST SRMs 610 and 612					32
	Aerosol samples	Direct analysis	Standard addition				<10–18 %	124
	Sunflower leaves	Direct analysis	Standard addition					73
	Compost samples	Pressed pellets	BCR-144R and CRM029-050 and standard addition				<10 %	109
Improved procedures	Various CRMs	Borate fusion	Isotope dilution		NIST SRM 1944, 2586, 2702, 2710a, 2711a, and 2780	95–120 %	<3 %	114
	Various CRMs	Pressed pellets, borate fusion	On-line isotope dilution		NIST SRM 610, 612, and 614, MESS-2 and PACS-2 and NIST SRM 2710a, 2711a, 1944, 2702, and 2780	85–110 %	3–21 %	107
	Oxide grains	Mounted on epoxy resin	On-line isotope dilution, ratio analysis		SRM U950a and U010 as well as natural uraninite grains		0.4–2.7 %	117
Specific approaches	Environmental samples	Borate fusion	Standard addition		NIST SRM 612	85–115 %	~10 %	115
	Carbonate	Adhesive tape	MPI-DING reference glasses		NIST SRM 610	90–110 %	1.6–24 %	119
	Soil & dust samples	Electroplating	Ratio analysis		NIST SRM 4353			122

strategies can be even further improved by exploiting the concepts of single standard addition, multiple standard additions, or isotope dilution. Thus, remaining differences between sample and standard can be further compensated for, enhancing the quality of LA-ICP-MS analysis. Okuda et al. used LA-ICP-MS to analyze aerosol samples collected on cellulose nitrate filters [124]. The filters were directly ablated and 15 elements were investigated. Calibration was achieved by spiking the filters with standard solutions. Precisions better than 10 % RSD could be achieved, except for Al (11 %) and Cu (18 %).

da Silva and Arruda [73] prepared sample pellets for the measurement of Se and S in sunflower leaves, which were spiked with different amounts of the elements of interest. Different certified materials were used for validation of the method. Jiménez et al. [109] investigated compost samples for the presence of toxic metals. The samples were homogenized, ground, sieved several times, and pressed into pellets (200 mg). Quantification was achieved by external calibration versus matrix-matched standards (BCR-144R and CRM029-050) and standard addition with aqueous standards. The RSDs for quantification were better than 10 % for most elements. Particle size and therefore milling time were identified as factors having a high impact on the method precision.

If applicable for the target analyte(s), the addition of isotope-enriched spikes is also feasible, enabling analyte quantification using isotope dilution. This approach offers best results in terms of precision and accuracy, but is also expensive and limited to elements for which at least two isotopes can be measured interference-free. Malherbe et al. investigated the potential of this approach for the analysis of different CRMs. Prior to LA-ICP-MS measurement, sample disks were prepared by borate fusion [114]. NIST SRM 1944 (New York/New Jersey waterway sediment), NIST SRM 2586 (trace elements in soil containing lead from paint), NIST SRM 2702 (inorganics in marine sediment), NIST SRM 2710a (Montana I soil), NIST SRM 2711a (Montana II soil), and NIST SRM 2780 (hard rock minewaste) and a meteorite sample were analysed. The results obtained were in good agreement with the corresponding certified values and the precision was better than 3 % RSD for all elements investigated. For the analysis of powdered samples, the previously described concept of liquid standard nebulization is also used for quantification of LA-generated aerosols. Fernández et al. [107] proposed a quantification method with on-line double isotope dilution for a wide range of matrices. Samples were either analyzed directly (NIST SRMs 610, 612, and 614), pressed into pellets (USGS MESS-2 and PACS-2), or fused with lithium borate (NIST SRMs 2710a, 2711a, 1944, 2702, and 2780). The ablated aerosol of either standard or sample is mixed with the nebulized isotope-enriched spike solution or blank solution. The RSDs ranged from 6 to 21 % for pressed pellets and from 3 to 21 % for borate fusion. Lloyd et al. analyzed uranium oxide grains, retrieved from soil and dust samples [117]. The grains were mounted on epoxy resin; the latter was then ground and polished to access the interior of the grains. As a result of the lack of a suitable standard reference material containing ^{236}U, quantification was achieved by introducing liquid reference materials NBL U950a (uranium particles) and NBL U010 (uranium isotopic standard) via a desolvating nebulizer. Natural uraninite grains were used as tertiary reference material to correct for mass bias. U isotope ratio analysis was implemented successfully with precisions of 0.4 % and 2.7 % RSD for $^{235}U/^{238}U$ and $^{236}U/^{238}U$, respectively.

Specific approaches

Claverie et al. [115] proposed a new approach for quantification of six elements of environmental concern, e.g., in soil or sediment samples, using pellets fixed on a spinning platform. Samples as well as standards were prepared by lithium borate fusion. By placing standard and sample next to each other on a platform, which is spinning at a high speed during laser ablation, quasi-simultaneous ablation of sample and standard is achieved. The mixed ablation aerosols are analyzed and quantification is based on standard addition or isotope dilution. For five standard reference materials and meteorite rock, an average precision of 10 % RSD could be achieved. The experimental results obtained compared well with the corresponding certified values with maximum deviations of 15 %. Lu et al. [119] tried to overcome the need for an internal standard for LA-ICP-MS analysis of carbonate materials. Using an equation-based approach, the so-called MRM-NoIS calibration strategy, a successful quantification of different carbonate minerals was achieved by using four reference materials (NIST SRM 610, USGS MACS-3, USGS GP-4, MPI-DING). For trace elements RSDs of less than 10 % and for rare earth elements (REEs) and major compounds RSDs of less than 5 % were observed. Cizdziel et al. investigated plutonium in US soil and dust samples [122]. Pu was spiked with a tracer, leached from the sample, and extracted from the leachate by anion exchange chromatography. Afterwards, the recovered analyte was electroplated on a stainless steel planchette disk for LA-ICP-MS analysis. LA-ICP-MS results were compared with liquid ICP-MS results, which were validated using NIST SRM 4350b (river sediment, radioactivity), NIST SRM 4353 (rocky flats soil number 2), and IAEA 385 (radionuclides in Irish Sea sediment). The authors reported a successful fingerprinting of Pu in soil and dust samples with LA-ICP-MS.

Figures of merit

Since detection limits and data for the level of reproducibility achieved have not been published in any of the reviewed contributions, this section aims at providing a comparison between the methods, accounting for all special applications.

Besides the approach used for preparation of compact samples, the quantification strategy also has to be taken into consideration. Furthermore, sample homogeneity is another limiting factor (especially for pressed pellets). Also, the concentration ranges of the target analytes as well as the instrumentation applied influence the quality of the results obtained.

In general, detection limits (LOD) were found to vary between several micrograms per kilogram and some milligrams per kilogram, depending on the instrumentation used and the analyte of interest. With pelletization, LODs around 0.035 mg kg^{-1} were obtained for different elements in vanilla samples [108]; for compost samples [109], values ranging from 0.01 to 0.8 mg kg^{-1} were reported. For fusion, the LODs varied from 0.02 to 4 mg kg^{-1} [114] with SF-ICP-MS and Q-ICP-MS. For tape mounting analysis and subsequent LA-ICP-MS analysis using SF-ICP-MS, detection limits from 0.3 μg kg^{-1} to 10 mg kg^{-1} were observed [118]. LODs varying from 0.001 to 0.5 mg kg^{-1} were reported for direct analysis of the sample without pretreatment [121].

In contrast to sensitivity, the reproducibility of a measurement is less dependent on the MS instrumentation used. Overall, reported RSDs were in the order of less than 3 to 50 %. The pelletization approach resulted in measurement reproducibilities varying between 6 and 21 % for the elements Pb, Rb, and Sr [107], and 6 to 14 % for 11 elements in vanilla [108] and less than 15 % for 12 elements in soil [110]. Fusion approaches showed comparably lower RSDs, a result which could be attributed to the improved sample homogeneity obtained with this approach. Published results vary between less than 3 % [114], 3 and 21 % for Pb, Rb, and Sr [107], and 10 % for six elements in environmental matrices [115], depending on target element and calibration strategy. For applications using the mounting/embedding approach for sample preparation, RSDs ranged from 15 to 50 % for the halogens Cl, Br, and I in ashed soil samples [116], and 15 to 25 % for 60 elements in dust samples using fs-LA-ICP-MS [118]. Poorer RSDs often result from the low analyte signals observed when analyzing single particles, which give rise to very small amounts of ablated material only.

Dried droplet analysis of liquid samples

As demonstrated in the previous sections, LA-ICP-MS is a versatile tool for solid sampling, suited for both bulk analysis and for mapping analyte distributions, as well as for combinations thereof. Consequently, the vast majority of samples being analyzed by LA-ICP-MS today are solids, especially since LA-ICP-MS circumvents the sometimes cumbersome digestion procedures otherwise required. For liquid samples and sample solutions, sample introduction in ICP-MS analysis is traditionally accomplished using a nebulizer. Pneumatic nebulizers are available in numerous modifications to suit practically any kind of liquid matrix [126]. However, heavily matrix-loaded liquid samples, such as urine or blood, present a challenge even for the most matrix-tolerant nebulizers. Such demanding matrices require at least dilution or partial digestion, which results in an increased workload. If high sample throughput is required, alternative sample introduction methods are therefore necessary.

As an alternative to pneumatic nebulization, laser ablation of dried liquids offers the aforementioned matrix-tolerance and sample throughput. In this section, the concept and some practical aspects of dried droplet laser ablation will be discussed. The performance of the method, as well as instrumental limitations will be highlighted, and a comprehensive overview of the related literature, including application examples, will be given.

The concept of dried droplet laser ablation

The basic concept of dried droplet laser ablation consists of depositing a well-defined volume of liquid sample on a solid support, evaporating the solvent, and examining the remaining dried residue by means of LA-ICP-MS. To unmistakably state that only the dried residue of a liquid sample is being analyzed, the term “dried droplet laser ablation” will be used throughout. To the best of our knowledge, Yang et al. introduced this method to ICP-MS in 2005 [127]. The present review will focus exclusively on the ablation of dried liquid samples, although it has been demonstrated that direct liquid ablation is also possible [128, 129].

As simple as the concept of dried droplet laser ablation may seem, its implementation can hold some pitfalls. One risk is to compromise the natural homogeneity inherent to the liquid sample. Method development in dried droplet laser ablation should therefore aim at preserving the sample’s original elemental composition throughout the analytical process, or at providing a sound strategy to compensate for any inhomogeneities introduced artificially during sample preparation. There are some methods reported in the literature that appear to be similar to dried droplet laser ablation in the sense that some part of a liquid sample is dried and analyzed by laser ablation. However, with those methods, the homogeneity of the liquid sample is abandoned by design. Hence, it is difficult or impossible to obtain quantitative information. Such methods are, for example, the combination of thin-layer chromatography with laser ablation [130–134] or the analysis of substrates which are immersed in a sample, removed from the liquid, and subsequently dried [135, 136].

The motivation for using dried droplet laser ablation instead of more established sample introduction techniques is in all cases reported to be (a combination of) the following four features: coverage of (sub-)microliter sample volumes, while offering (sub-)microgram per liter detection limits in case of ICP-MS detection, removal of solvent to allow

coupling ICP-MS as an element-specific detector to chromatographic systems and to obtain less polyatomic interferences arising from the solvent, simplification of sample logistics, as well as direct sampling of challenging liquid matrices. Although some of these features could also be achieved with alternative solid sampling methods, such as solid sampling graphite furnace AAS or electrothermal vaporization (ETV) ICP-MS, dried droplet laser ablation offers two significant advantages over graphite furnace techniques. First, it is a genuine multi-element technique as opposed to conventional AAS, or compared to high-resolution continuum source AAS with limited multi-element capabilities. Secondly, LA allows complete desorption of the sample, whereas in ETV carbide formation may hamper correct quantification (e.g., [137, 138]). Such problems are not observed with LA [139]. In some cases, sample throughput was found to be higher with dried droplet laser ablation than with ETV-ICP-MS [139] but this certainly depends on the measurement protocols deployed and cannot be generalized.

Preparation of dried droplets

As stated above, the key aspect of dried droplet laser ablation is to preserve the inherent homogeneity of the liquid sample throughout sample preparation and measurement. If an artificial inhomogeneity is newly introduced, this should be done in a reproducible way, in order to be able to fully compensate for it. From everyday experience, it is well known that dried residues, e.g., coffee stains in the kitchen, are usually far from being homogeneously shaped. It is the scope of this section to provide some very basic physical insights into the processes involved in droplet-drying, although the literature on this topic is vast and the interested reader is referred to the numerous specialized reviews. Three parameters play a major role in terms of dried droplet shape: (a) choice of the surface used for droplet deposition, (b) drying conditions, and (c) the matrix of the liquid sample:

(a) When drying droplets on hydrophilic surfaces, ring-shaped residues are frequently obtained. This "coffee stain effect" was described by Deegan et al. [140, 141] to be caused by a radial flow, which transports liquid from the core of the droplet to its perimeter, where the solvent evaporates more easily. This radial flow is the consequence of one precondition inherent to this physical model: the contact line (the perimeter of the droplet) does not shrink during the drying process. Several authors provided experimental data to support this model (e.g., [142–144]). Contrarily, in the case of a hydrophobic surface, deposition of concentric rings or small spots in the center of the droplet can be observed [145–147], as the contact line continuously or periodically shrinks while drying.

(b) In addition to the flow patterns that lead to ring deposition, the interaction of dissolved or colloidal matter with the contact area, as well as convective currents can contribute to the dried pattern [144, 148]. Such convective currents are related to the drying rate, which in turn depends on temperature, relative humidity, and heat conductivity of the substrate [144, 149, 150]. Hence, the experimental setup might also influence the shape of the dried residue.

(c) Finally, the matrix of the sample (e.g., salt or protein concentration) also influences the shape of the dried residue [151, 152]. In the first publications that describe dried droplet laser ablation, small sample aliquots of 20 μL were pipetted onto hydrophobic polystyrene plates and dried under ambient conditions [127, 139, 153]. Owing to differences in the matrix (purely inorganic salts in the case of standards, with organic constituents in case of samples), the shape and size of the dried residue depended strongly on the sample matrix [127].

In view of the aforementioned three parameters, a drying droplet is a complex system and it is easy to understand that the morphology of the final dried residue is difficult to predict. Although the references provided show that it is indeed possible to control the morphology of the dried residue, such experiments are most likely beyond the scope of analytical laboratories. However, it is possible to minimize the influence of those factors, which have the most pronounced effect. As the choice of the solid substrate plays a major role in terms of droplet morphology, this factor was considered and optimized in most reported cases of dried droplet laser ablation. The following three types of solid substrates were applied: 1. hydrophobic surfaces, 2. filter paper (paper diameter much greater than droplet diameter), and 3. confined, circular, and hydrophilic areas (diameter of circular area no greater than droplet diameter). For visualization, examples of these approaches are provided in Fig. 3.

Method I Using a hydrophobic surface for droplet deposition results in a small dried residue, as described above. Typical diameters of dried residues are around 100–1600 μm, depending on droplet volume and sample matrix (Table 2). As the droplet shrinks continuously, the coffee stain effect will be observed only at a very late stage of the drying process, or not at all. Hence, it is straightforward to ablate the entire dried residue with only a few laser pulses. Hsieh et al. [154, 155] demonstrated that this approach allows for external calibration when quantifying metals in whole blood. Yet, as other authors have found, the extreme preconcentration on a small spot has the disadvantage of pronounced matrix effects by co-existing sample constituents. For example, Yang et al. [127] showed significant signal suppression by sodium present in the sample. On the other hand, deposition of droplets on a substrate

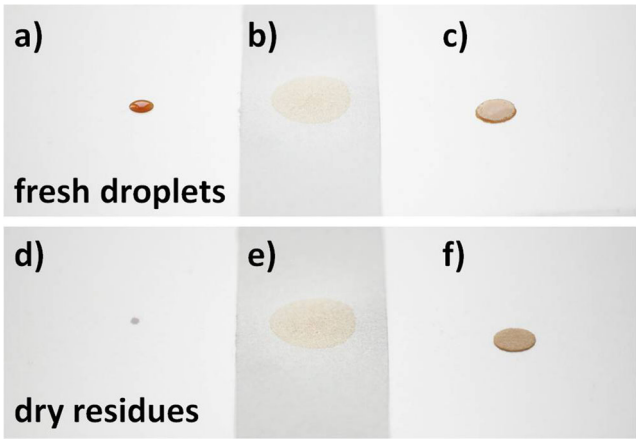

Fig. 3 Strategies for sample application in dried droplet LA analysis. Deposition of a defined sample volume on hydrophobic surfaces (**a**), filter paper with dimensions much greater than droplet diameter (**b**), and confined, circular, hydrophilic areas with diameter of circular area no greater than droplet diameter (**c**). Dried residues after evaporation of the solvent on a hydrophobic surface (**d**), filter paper (**e**), and precut filter disks of filter paper (**f**)

that enhances sample ablation as a result of strong interaction with the laser light has been demonstrated [156, 157], in combination with automated deposition of liquids. Table 2 summarizes the literature that applied the approach of hydrophobic surfaces.

Method II Applying a droplet on a large piece of filter paper makes sample preparation very easy, as the liquid is immediately absorbed by capillary action [158, 159]. Once dried, the residues can be easily transported and stored as the analyte is incorporated in the paper fibers [160]. Consequently, blotting cards are widely used in clinical settings [161], e.g., in collection of blood samples. Yet, even if the dispensed volume of sample is well defined, differences in viscosity can lead to a different migration behavior on the paper, combined with chromatographic effects [162, 163]. Careful design of laser ablation patterns is therefore required. Table 3 gives an overview of papers that report on analysis of "freely migrated" droplets on filter paper, via LA ICP-MS. Also, typical diameters of dried residues and applied sample volumes are given.

Method III By providing a hydrophilic area with a clearly defined border, samples can only migrate within this area. Therefore, samples with low viscosity or challenging matrix are confined on the same area as purely aqueous samples. This approach was used by Choi et al. [164] to analyze photo-resist, deposited on micro-machined polymer pillars. A somewhat different approach was presented by Aramendía et al. [160] who applied precut disks of filter paper on a hydrophobic surface. By doing so, large volumes of sample could be applied on a small area, thus enhancing sensitivity 10-fold [160]. However, the coffee stain effect is very pronounced with this type of sample preparation, since the precut filter disk is the ideal model of a fixed contact line (as described above, a fixed contact line results in a constant droplet area during the drying process. As the evaporation on the rim of the droplet is faster than in the center of the droplet, a liquid flow is created which transports material to the rim of the droplet which is the origin of the coffee stain effect). Crater-shaped analyte distributions were therefore obtained [18, 160, 165]), as also observed in MALDI-MS [166]. Table 4 gives an overview of the related literature and typical sample loadings (microliters per millimeter squared).

Quantification approaches, sensitivity, and reproducibility

The quantification process also needs to be adapted to the approach used for sample preparation. The sensitivity is influenced to a large extent by the analyte loading, i.e., the amount of sample per unit area (e.g., microliters per millimeter squared). In Tables 2–4, this value can be compared for the three application modes (methods I–III), and in general, highest analyte loading is observed with method I. However, as discussed above, matrix effects are most pronounced with this approach; therefore, lower analyte loadings (method II or method III) can be beneficial, depending on the individual analytical setup and sample type.

In the case of sample preparation on a hydrophobic surface (method I), the small residue can be ablated completely using spot, grid, or line patterns. Thus, the entire signal is collected in a short time, giving rise to a sensitivity which is comparable to that achievable with conventional nebulizer systems. Yang et al. [127] even demonstrated a 2–7-fold improved absolute sensitivity (counts per nanogram) compared to pneumatic nebulization when analyzing aqueous standard solutions. This finding is also due to the fact that the transport efficiency of laser ablation systems is superior to that of pneumatic nebulizer systems [127]. The general sensitivity of dried droplet laser ablation in combination with hydrophobic surfaces obtained in practice can therefore be expected to be similar to that with pneumatic nebulization (see Table 2).

Partial ablation of freely deposited droplets (method II) might result in erroneous results, as demonstrated in [160], unless closely matrix-matched standards are used [158]. The reason for this is that sample-to-sample variations in terms of viscosity result in different sample spread across the filter. The complete consumption of the dried residue [159] is a feasible way to avoid this problem, but requires specialized laser equipment. If the deposited volumes are very small [167, 168], quantitative ablation from filter paper becomes easy, especially in the presence of substances that improve the laser ablation yield, such as black ink deposited prior to the droplet [167, 168].

Table 2 Method I: droplet deposition on hydrophobic surface

Sample matrix	Droplet volume	Size of dried residue	Sample loading[a]	Surface material	LOD	Reproducibility	Additional information	Ref.
Drinking water, yeast extract	20 μL	150–500 μm	10^{-4}–10^{-3} μL μm^{-2}	PS	0.08–0.12 ng mL^{-1} (aqueous), 0.06–0.09 ng mL^{-1} (standard addition), 0.05–0.08 ng mL^{-1} (isotope dilution)	4.6–23 % RSD (aqueous with I.S., n=4), 4.7–8.2 % RSD (standard addition with I.S., n=4), 3.5–3.9 % RSD (isotope dilution, n=6); 0.5 % RSD (Se in yeast, isotope dilution, n=5)	NaAc matrix was added to water samples	[127]
HPLC fractions of yeast extract	20 μL	600 μm	7×10^{-5} μL μm^{-2}	PS	36–110 μg g^{-1} (Se)	0.55–0.77 % RSD (species-specific isotope dilution)	No matrix required due to high salt load of samples	[153]
Digested biological tissue, nearshore seawater, and river water	20 μL	100 μm 1.6 mm	10^{-5}–3×10^{-3} μL μm^{-2}	PS	0.033 pg mL^{-1} (Pu), 0.051 pg mL^{-1} (Th), 0.072 pg mL^{-1} (U).	8 % RSD (with I.S., n=10)	Chromogenic matrix investigated	[137]
Cr species via capillary electrophoresis	100 nL	100–500 μm	5×10^{-7}–10^{-5} μL μm^{-2}	PETG	0.2–6.5 μg L^{-1}	Below 3 % RSD	α-Cyano-4-hydroxycinnamic acid	[156]
Blood reference materials	0.5 μL	700–900 μm	8×10^{-7}–10^{-6} μL μm^{-2}	Other	0.1 ng mL^{-1}	Below 10 % RSD for all samples	Methylene blue as indicator and to improve ablation yield	[154]
Cell cultivation medium and cell lysate	<20 nL	<300 μm	3×10^{-7} μL μm^{-2}	PETG	26 fg Cu (100 nL droplet, therefore 26 ng L^{-1})	5 % RSD under optimized conditions for samples	Rhodamine B added for visibility	[157]
Cr species via liquid-liquid micro extraction, synthetic seawater	7 μL	5 mm	4×10^{-7} μL μm^{-2}	PS	0.11 μg L^{-1}	4–8 % RSD	Organic matrix, internal standard	[169]
Various "meat" reference materials (oyster tissue, etc.)	50–100 μL	1 cm	6×10^{-7}–10^{-6} μL μm^{-2}	PTFE, PS	0.05–6 μg kg^{-1} dry mass (corresponds to 1.25–240 ng L^{-1})	5–10 % RSD	No additive, organic digest	[170]
Mineral water, tap water, swimming pool water, and water from two artificial lakes	1 μL	600 μm	4×10^{-6} μL μm^{-2}	PTFE	0.05–0.81 ng mL^{-1}	~5 % RSD (for n=3, recovery experiment)	Methylene blue added for visibility	[171]
Seronorm blood reference material	0.5 μL	–	–	PTFE	0.14–29 ng mL^{-1} (Be–Mg)	6 % RSD within-run precision, 4–8 % RSD between-run precision	Methylene blue added for visibility	[155]
SLRS-4 river water reference material, lake water, and synthetic seawater	1 μL	480–850 μm	2×10^{-6}–6×10^{-6} μL μm^{-2}	PTFE	0.03–0.2 pg mL^{-1} (enrichment factor 32)	2–5 % RSD	Methylene blue added for visibility	[172]
Human urine from Fabry disease patient and control	1 μL	–	–	PTFE[)]	0.003–0.58 μg g^{-1}	<20 % RSD	Spiked samples for calibration	[173]

PS polystyrene, *PETG* poly(ethyleneterephthalate)glycol, *PTFE* polytetrafluoroethylene, *Other* "hydrophobic filter membrane"

[a] Sample volume/area of dried residue (assuming a circular spot)

Table 3 Method II: droplet deposition on large filter paper sheets

Sample matrix	Droplet volume	Size of dried residue	Sample loading[a]	Surface material	LOD	Reproducibility	Additional information	Ref.
Blood spotted on paper, from a lab proficiency test	–	–	–	Whatmann filter paper	0.9 μg dL^{-1} (Pb)	7 % RSD (in-between droplets and also within droplet)	Sample directly spotted without any other treatment	[158]
Co in a drug preparation, Pb in whole blood, and Sn in food samples	500 nL	–	–	Filter paper with additive	1–60 ng L^{-1}	10 % RSD (spot-to-spot)	Different additives to improve laser yield	[168]
Pb and Cd in BCR-634 whole blood reference material	200 pL	–	–	Filter paper with additive	0.5 pg Pb 0.02 pg Cd (equal to 2.5 and 0.1 ng L^{-1} with 200 nL of sample)	25 % for Pb and 8 % for Cd with standard solutions using ^{13}C as internal standard, for samples: 5 % for Pb and 35 % for Cd	Repeated deposition of 65 pL droplets, ablation of several droplets at the same time	[167]
Blood (reference materials and real samples)	5 μL	5–6 mm	3×10^{-7} μL m^{-2}	Filter paper	0.040–0.054 μg L^{-1}	3–9 % RSD (quantitative) 1500 ppm (isotope ratios)	Analysis vial split aerosol-flow (single-collector/multi-collector ICP-MS)	[159]

[a] Sample volume/area of dried residue (assuming a circular spot)

Table 4 Method III: droplet deposition on confined, circular, and hydrophilic areas

Sample Matrix	Droplet volume	Size of dried residue	Sample loading	Surface material	LOD	Reproducibility	Additional information	Ref.
Photo-resistant used in photolithography	64.7 pL	150 μm	4×10^{-6} μL $μm^{-2}$	PDMS-columns (micro-machined)	2.33, 15.4, 5.72 ng mL^{-1} (Al, Cu, Pb)	17.1–46.9 % RSD (due to extremely low sample volume)	No matrix added, photo resist	[164]
Human urine from supposedly healthy patients	300 μL	16 mm	10^{-6} μL $μm^{-2}$	Filter paper (precut saturated filter disks)	0.1–13 μg L^{-1}	2–5 % RSD	No additive	[160]
Cu isotopes in urine of Wilson's disease patients, treated patients and one control patient	300 μL	16 mm	10^{-6} μL $μm^{-2}$	Filter paper (precut saturated filter disks)	–	200–500 ppm RSD intra-spot, and 540 ppm RSD inter-spot	No additive, corona ablation with 10 kHz	[18]
Phosphorus in fermentation media	10 μL	5 mm	5×10^{-7} μL $μm^{-2}$	Filter paper (precut saturated filter disks)	10 μg mL^{-1} (ICP-OES detection)	10 % RSD	Analysis via laser ablation ICP-OES	[165]

[a] Sample volume / area of dried residue (assuming a circular spot)

Table 5 Selection of frequently applied procedures for signal quantification in LA-ICP-MS analysis

Quantification approach	Biogenic carbonates	Hard tissues	Soft tissue	Powdered samples	Liquid samples
CRM/SRM	27, 38–48, 50–54	58–62		108, 118, 121, 123	154
In-house prepared standards					
Non matrix-matched standards					
Use of well-characterized materials	43	64–68			158
Thin films on sample or substrate			94		
Gelatin, agarose gel, sol-gel standards			91, 92, 93	32	
Printed pattern			95, 96		167, 168
Dried droplets (aqueous standards)					127, 138, 154, 157
Matrix-matched standards					
Preparation of pellets	69			71, 109, 111, 112	
Fusion to disks	31, 32			29, 33, 113–115	
Embedding into polymer resin			97	116, 120	
Homogenized tissues			90		
Matrix-adjusted dried droplets					155, 164, 169–173
Specific approaches		63, 66, 67			
Nebulized liquid standards					
Calibration/standard addition	64, 65		88, 89	117	
IDMS			89, 103	107	
Internal standard correction					
Sample-inherent element	27, 28, 38, 39, 43, 46	58–67	75, 104	29, 118, 123, 125	
Homogeneously spiked to the sample			90, 97	110, 114	127, 139, 160, 169
Applied as thin layer on/below sample			79, 94, 95, 100		160
On-line addition of dried aerosol			88, 89		

In the case of uniform sample geometry due to circular hydrophobic areas (method III), the coffee stain effect is very pronounced, as discussed above. Although a quite homogeneous analyte distribution is obtained in the center of the droplet, the extent of ring formation will depend on the sample matrix. Therefore, standard addition or isotope dilution is required if the laser is focused onto the center of the filter disk. In a recent publication, Nischkauer et al. [165] showed that the bias resulting from this centrosymmetric distribution of analytes can be easily compensated for. Instead of performing laser ablation only in the center [160] or only in the rim [18] of the precut filter disk, it was proposed to perform radial line scans that pass across the entire sample, including the center. The resulting U-shaped signal was then integrated and was found to be proportional to the concentration in the initially liquid sample, without the need to ablate the entire filter disk, and without the need for matrix-matching or the use of an internal standard [165].

The reproducibility of dried droplet laser ablation is intrinsically compromised, compared to pneumatic nebulization, as a result of the additional error introduced by repeated droplet deposition and by the transient signal mode. Interdroplet reproducibilities range between 3 % and 23 % RSD for samples measured directly, with typical values ranging between 3 % and 10 % RSD [127, 137, 154, 155, 157, 158, 160, 165, 167–173]. When automated, droplet deposition can be achieved with greater precision [174, 175], but the higher uncertainty inherent to solid sampling techniques will most likely persist. In case of isotope dilution and isotope ratio measurements, better reproducibility was reported (540 ppm RSD interspot [18], 0.55–0.77 % RSD for species-specific isotope dilution [153]) than in the case of pure quantitative measurements.

Conclusions

Although geoscience is still the main field of application of LA-ICP-MS, its use in the fields of environmental research and life sciences increased continuously during the last few years. High sensitivity combined with excellent spatial resolution is the main reason for using LA-ICP-MS in the analysis of hard and soft tissues, as well as of powdered environmental samples. The capabilities for performing imaging studies or isotope ratio measurements are additional advantages of LA-ICP-MS. The applications published so far cover a wide range of sample matrices, target analytes, and concentration ranges. Nevertheless, they have one common problem—reliable

quantification. The strategies used to circumvent the influence of elemental fractionation and matrix effects in LA-ICP-MS analysis, which are considered as the main problems hampering reliable quantification, are rather similar, although the resulting interferences differ between individual applications. Table 5 presents a compilation of the most frequently applied approaches for quantification, indicating that the use of in-house prepared standards in combination with an internal standard is the dominating strategy. Improved concepts for sample preparation as well as for application of matrix-matched standards will further enhance the potential of LA-ICP-MS for the analysis of environmental, biological, and biomedical samples. The choice of an appropriate internal standard is still of major concern in many applications, especially when no sample-inherent element is available. Thus, further methodological developments are required, e.g., in the case of tissue analysis the application of polymeric layers or thin metal coatings has been shown to be promising. Special attention should be paid to the application of fs-laser systems, which offer distinct improvements in terms of matrix effects and elemental fractionation. Another prerequisite for the acceptance of LA-ICP-MS as an alternative to traditional procedures for the quantitative determination of trace elements is the availability of appropriate reference materials. Especially for life science applications, the development and production of a larger range of CRMs is highly desirable. In contrast, for environmental samples (soil, fly ash, dust, etc.) a wide variety of CRMs is available. However, as those materials have been designed for liquid analysis after mineralization, none of them is applicable for direct LA-ICP-MS analysis because of their inhomogeneity on the microscale. Particularly considering the comparability of measurement results, the availability of at least a couple of compact standard materials with sufficient homogeneity should be aspired to.

Acknowledgments The research presented in this contribution was financially supported by the Austrian Science Fund (FWF): P25030-N28. M.B. wants to thank the MEIBio PhD program of the Vienna University of Technology for providing a scholarship for the period 2013–2016. R. Alexandru is acknowledged for providing the photographs in Figure 3.

Open Access This article is distributed under the terms of the Creative Commons Attribution 4.0 International License (http://creativecommons.org/licenses/by/4.0/), which permits unrestricted use, distribution, and reproduction in any medium, provided you give appropriate credit to the original author(s) and the source, provide a link to the Creative Commons license, and indicate if changes were made.

References

1. Russo RE, Mao X, Borisov OV (1998) Laser ablation sampling. TrAC Trends Anal Chem 17(8–9):461–469. doi:10.1016/s0165-9936(98)00047-8
2. Durrant SF (1999) Laser ablation inductively coupled plasma mass spectrometry: achievements, problems, prospects. J Anal At Spectrom 14(9):1385–1403. doi:10.1039/a901765h
3. Becker JS (2002) Applications of inductively coupled plasma mass spectrometry and laser ablation inductively coupled plasma mass spectrometry in materials science. Spectrochim Acta B At Spectrosc 57(12):1805–1820. doi:10.1016/s0584-8547(02)00213-6
4. Günther D, Hattendorf B (2005) Solid sample analysis using laser ablation inductively coupled plasma mass spectrometry. TrAC Trends Anal Chem 24(3):255–265. doi:10.1016/j.trac.2004.11.017
5. Fryer BJ, Jackson SE, Longerich HP (1995) The design, operation and role of the laser-ablation microprobe coupled with an inductively coupled plasma-mass spectrometer (LAM- ICP-MS) in the Earth sciences. Can Mineral 33(2):303–312
6. Longerich HP, Günther D, Jackson SE (1996) Elemental fractionation in laser ablation inductively coupled plasma mass spectrometry. Anal Bioanal Chem 355(5–6):538–542. doi:10.1007/s0021663550538
7. Guillong M, Günther D (2002) Effect of particle size distribution on ICP-induced elemental fractionation in laser ablation-inductively coupled plasma-mass spectrometry. J Anal At Spectrom 17(8):831–837. doi:10.1039/b202988j
8. Hattendorf B, Latkoczy C, Günther D (2003) Peer reviewed: laser ablation-ICPMS. Anal Chem 75(15):341 A–347 A. doi:10.1021/ac031283r
9. Russo RE, Mao XL, Liu C, Gonzalez J (2004) Laser assisted plasma spectrochemistry: laser ablation. J Anal At Spectrom 19(9):1084. doi:10.1039/b403368j
10. Hergenröder R, Samek O, Hommes V (2006) Femtosecond laser ablation elemental mass spectrometry. Mass Spectrom Rev 25(4):551–572. doi:10.1002/mas.20077
11. Koch J, Günther D (2006) Femtosecond laser ablation inductively coupled plasma mass spectrometry: achievements and remaining problems. Anal Bioanal Chem 387(1):149–153. doi:10.1007/s00216-006-0918-z
12. Fernández B, Claverie F, Pécheyran C, Donard OFX (2007) Direct analysis of solid samples by fs-LA-ICP-MS. TrAC Trends Anal Chem 26(10):951–966. doi:10.1016/j.trac.2007.08.008
13. Pisonero J, Günther D (2008) Femtosecond laser ablation inductively coupled plasma mass spectrometry: fundamentals and capabilities for depth profiling analysis. Mass Spectrom Rev 27(6):609–623. doi:10.1002/mas.20180
14. Resano M, Garcia-Ruiz E, Vanhaecke F (2010) Laser ablation-inductively coupled plasma mass spectrometry in archaeometric research. Mass Spectrom Rev 29(1):55–78. doi:10.1002/mas.20220
15. Günther D, Heinrich CA (1999) Comparison of the ablation behaviour of 266 nm Nd:YAG and 193 nm ArF excimer lasers for LA-ICP-MS analysis. J Anal At Spectrom 14(9):1369–1374. doi:10.1039/a901649j
16. Kroslakova I, Günther D (2006) Elemental fractionation in laser ablation-inductively coupled plasma-mass spectrometry: evidence for mass load induced matrix effects in the ICP during ablation of a silicate glass. J Anal At Spectrom 22(1):51. doi:10.1039/b606522h
17. Russo R (2002) Laser ablation in analytical chemistry—a review. Talanta 57(3):425–451. doi:10.1016/s0039-9140(02)00053-x
18. Resano M, Aramendía M, Rello L, Calvo ML, Bérail S, Pécheyran C (2012) Direct determination of Cu isotope ratios in dried urine spots by means of fs-LA-MC-ICPMS. Potential to diagnose Wilson's disease. J Anal At Spectrom 28(1):98. doi:10.1039/c2ja30262d
19. Shaheen ME, Gagnon JE, Fryer BJ (2012) Femtosecond (fs) lasers coupled with modern ICP-MS instruments provide new and

improved potential for in situ elemental and isotopic analyses in the geosciences. Chem Geol 330–331:260–273. doi:10.1016/j.chemgeo.2012.09.016
20. Hare D, Austin C, Doble P (2012) Quantification strategies for elemental imaging of biological samples using laser ablation-inductively coupled plasma-mass spectrometry. Analyst 137(7):1527. doi:10.1039/c2an15792f
21. Agatemor C, Beauchemin D (2011) Matrix effects in inductively coupled plasma mass spectrometry: a review. Anal Chim Acta 706(1):66–83. doi:10.1016/j.aca.2011.08.027
22. Orellana FA, Gálvez CG, Roldán MT, García-Ruiz C (2013) Applications of laser-ablation-inductively-coupled plasma-mass spectrometry in chemical analysis of forensic evidence. TrAC Trends Anal Chem 42:1–34. doi:10.1016/j.trac.2012.09.015
23. Konz I, Fernández B, Fernández ML, Pereiro R, Sanz-Medel A (2012) Laser ablation ICP-MS for quantitative biomedical applications. Anal Bioanal Chem 403(8):2113–2125. doi:10.1007/s00216-012-6023-6
24. Koch J, Günther D (2011) Review of the state-of-the-art of laser ablation inductively coupled plasma mass spectrometry. Appl Spectrosc 65(5):155–162. doi:10.1366/11-06255
25. Jochum KP, Nohl U, Herwig K, Lammel E, Stoll B, Hofmann AW (2005) GeoReM: a new geochemical database for reference materials and isotopic standards. Geostand Geoanal Res 29(3):333–338. doi:10.1111/j.1751-908X.2005.tb00904.x
26. Sinclair DJ, Kinsley LPJ, McCulloch MT (1998) High resolution analysis of trace elements in corals by laser ablation ICP-MS. Geochim Cosmochim Acta 62(11):1889–1901. doi:10.1016/s0016-7037(98)00112-4
27. Perkins WT, Fuge R, Pearce NJG (1991) Quantitative analysis of trace elements in carbonates using laser ablation inductively coupled plasma mass spectrometry. J Anal At Spectrom 6(6):445. doi:10.1039/ja9910600445
28. Fitzpatrick AJ, Kurtis Kyser T, Chipley D, Beauchemin D (2008) Fabrication of solid calibration standards by a sol–gel process and use in laser ablation ICPMS. J Anal At Spectrom 23(2):244. doi:10.1039/b712366c
29. Vassilev SV, Vassileva CG, Baxter D (2014) Trace element concentrations and associations in some biomass ashes. Fuel 129:292–313. doi:10.1016/j.fuel.2014.04.001
30. Longerich HP, Jackson SE, Günther D (1996) Inter-laboratory note. Laser ablation inductively coupled plasma mass spectrometric transient signal data acquisition and analyte concentration calculation. J Anal At Spectrom 11(9):899. doi:10.1039/ja9961100899
31. Davies CA, Brophy D, Jeffries T, Gosling E (2011) Trace elements in the otoliths and dorsal spines of albacore tuna (Thunnus alalunga, Bonnaterre, 1788): an assessment of the effectiveness of cleaning procedures at removing postmortem contamination. J Exp Mar Biol Ecol 396(2):162–170. doi:10.1016/j.jembe.2010.10.016
32. Ranaldi MM, Gagnon MM (2008) Zinc incorporation in the otoliths of juvenile pink snapper (Pagrus auratus Forster): the influence of dietary versus waterborne sources. J Exp Mar Biol Ecol 360(1):56–62. doi:10.1016/j.jembe.2008.03.013
33. Eze CP, Fatoba O, Madzivire G, Ostrovnaya TM, Petrik LF, Frontasyeva MV, Nechaev AN (2013) Elemental composition of fly ash: a comparative study using nuclear and related analytical techniques / SkŁad Pierwiastkowy PopioŁÓw Lotnych: Studium Przypadku Z Wykorzystaniem Metod Nuklearnych I Analitycznych. Chem Didact Ecol Metrol 18(1–2):19–29. doi:10.2478/cdem-2013-0014
34. Gunther D, Cousin H, Magyar B, Leopold I (1997) Calibration studies on dried aerosols for laser ablation-inductively coupled plasma mass spectrometry. J Anal At Spectrom 12(2):165–170. doi:10.1039/A604531F
35. Leach JJ, Allen LA, Aeschliman DB, Houk RS (1998) Calibration of laser ablation inductively coupled plasma mass spectrometry using standard additions with dried solution aerosols. Anal Chem 71(2):440–445. doi:10.1021/ac980855i
36. O' Connor C, Sharp BL, Evans P (2006) On-line additions of aqueous standards for calibration of laser ablation inductively coupled plasma mass spectrometry: theory and comparison of wet and dry plasma conditions. J Anal At Spectrom 21(6):556–565. doi:10.1039/b600916f
37. Pickhardt C, Izmer AV, Zoriy MV, Schaumloffel D, Becker JS (2006) On-line isotope dilution in laser ablation inductively coupled plasma mass spectrometry using a microflow nebulizer inserted in the laser ablation chamber. Int J Mass Spectrom 248(3):136–141. doi:10.1016/j.ijms.2005.11.001
38. Aramendia M, Resano M, Vanhaecke F (2010) Isotope ratio determination by laser ablation-single collector-inductively coupled plasma-mass spectrometry. General capabilities and possibilities for improvement. J Anal At Spectrom 25(3):390–404. doi:10.1039/B922856J
39. Liu Y, Hu Z, Li M, Gao S (2013) Applications of LA-ICP-MS in the elemental analyses of geological samples. Chin Sci Bull 58(32):3863–3878. doi:10.1007/s11434-013-5901-4
40. Wang CH (2014) Otolith elemental ratios of flathead mullet Mugil cephalus in Taiwanese waters reveal variable patterns of habitat use. Estuar Coast Shelf Sci 151:124–130. doi:10.1016/j.ecss.2014.08.024
41. D'Avignon G, Rose GA (2013) Otolith elemental fingerprints distinguish Atlantic cod spawning areas in Newfoundland and Labrador. Fish Res 147:1–9. doi:10.1016/j.fishres.2013.04.006
42. Fairclough DV, Edmonds JS, Lenanton RCJ, Jackson G, Keay IS, Crisafulli BM, Newman SJ (2011) Rapid and cost-effective assessment of connectivity among assemblages of Choerodon rubescens (Labridae), using laser ablation ICP-MS of sagittal otoliths. J Exp Mar Biol Ecol 403(1–2):46–53. doi:10.1016/j.jembe.2011.04.005
43. Kemp J, Swearer SE, Jenkins GP, Robertson S (2011) Otolith chemistry is more accurate than otolith shape in identifying cod species (genus Pseudophycis) in the diet of Australian fur seals (Arctocephalus pusillus doriferus). Can J Fish Aquat Sci 68(10):1732–1743. doi:10.1139/f2011-088
44. Schuchert PC, Arkhipkin AI, Koenig AE (2010) Traveling around Cape Horn: otolith chemistry reveals a mixed stock of Patagonian hoki with separate Atlantic and Pacific spawning grounds. Fish Res 102(1–2):80–86. doi:10.1016/j.fishres.2009.10.012
45. Tabouret H, Bareille G, Claverie F, Pécheyran C, Prouzet P, Donard OFX (2010) Simultaneous use of strontium:calcium and barium:calcium ratios in otoliths as markers of habitat: application to the European eel (Anguilla anguilla) in the Adour basin, South West France. Mar Environ Res 70(1):35–45. doi:10.1016/j.marenvres.2010.02.006
46. Arkhipkin AI, Schuchert PC, Danyushevsky L (2009) Otolith chemistry reveals fine population structure and close affinity to the Pacific and Atlantic oceanic spawning grounds in the migratory southern blue whiting (Micromesistius australis australis). Fish Res 96(2–3):188–194. doi:10.1016/j.fishres.2008.11.002
47. Vasconcelos RP, Reis-Santos P, Tanner S, Maia A, Latkoczy C, Günther D, Costa MJ, Cabral H (2008) Evidence of estuarine nursery origin of five coastal fish species along the Portuguese coast through otolith elemental fingerprints. Estuar Coast Shelf Sci 79(2):317–327. doi:10.1016/j.ecss.2008.04.006
48. Ranaldi MM, Gagnon MM (2010) Trace metal incorporation in otoliths of pink snapper (Pagrus auratus) as an environmental monitor. Compar Biochem Physiol C Toxicol Pharmacol 152(3):248–255. doi:10.1016/j.cbpc.2010.04.012
49. Collingsworth PD, Van Tassell JJ, Olesik JW, Marschall EA (2010) Effects of temperature and elemental concentration on

the chemical composition of juvenile yellow perch (Perca flavescens) otoliths. Can J Fish Aquat Sci 67(7):1187–1196. doi:10.1139/F10-050

50. Ranaldi MM, Gagnon MM (2009) Accumulation of cadmium in the otoliths and tissues of juvenile pink snapper (Pagrus auratus Forster) following dietary and waterborne exposure. Compar Biochem Physiol C Toxicol Pharmacol 150(4):421–427. doi:10.1016/j.cbpc.2009.06.007
51. Sturrock AM, Trueman CN, Darnaude AM, Hunter E (2012) Can otolith elemental chemistry retrospectively track migrations in fully marine fishes? J Fish Biol 81(2):766–795. doi:10.1111/j.1095-8649.2012.03372.x
52. Phung AT, Baeyens W, Leermakers M, Goderis S, Vanhaecke F, Gao Y (2013) Reproducibility of laser ablation–inductively coupled plasma–mass spectrometry (LA–ICP–MS) measurements in mussel shells and comparison with micro-drill sampling and solution ICP–MS. Talanta 115:6–14. doi:10.1016/j.talanta.2013.04.019
53. Jochum KP, Scholz D, Stoll B, Weis U, Wilson SA, Yang Q, Schwalb A, Börner N, Jacob DE, Andreae MO (2012) Accurate trace element analysis of speleothems and biogenic calcium carbonates by LA-ICP-MS. Chem Geol 318–319:31–44. doi:10.1016/j.chemgeo.2012.05.009
54. Edinger EN, Azmy K, Diegor W, Siregar PR (2008) Heavy metal contamination from gold mining recorded in Porites lobata skeletons, Buyat-Ratototok district, North Sulawesi, Indonesia. Mar Pollut Bull 56(9):1553–1569. doi:10.1016/j.marpolbul.2008.05.028
55. Dunphy BJ, Millet M-A, Jeffs AG (2011) Elemental signatures in the shells of early juvenile green-lipped mussels (Perna canaliculus) and their potential use for larval tracking. Aquaculture 311(1–4):187–192. doi:10.1016/j.aquaculture.2010.12.016
56. Fodrie FJ, Becker BJ, Levin LA, Gruenthal K, McMillan PA (2011) Connectivity clues from short-term variability in settlement and geochemical tags of mytilid mussels. J Sea Res 65(1):141–150. doi:10.1016/j.seares.2010.09.001
57. Pearce NJG, Perkins WT, Westgate JA, Gorton MP, Jackson SE, Neal CR, Chenery SP (1997) A compilation of new and published major and trace element data for NIST SRM 610 and NIST SRM 612 glass reference materials. Geostand Geoanal Res 21(1):115–144. doi:10.1111/j.1751-908X.1997.tb00538.x
58. Jochum KP, Weis U, Stoll B, Kuzmin D, Yang Q, Raczek I, Jacob DE, Stracke A, Birbaum K, Frick DA, Günther D, Enzweiler J (2011) Determination of reference values for NIST SRM 610–617 glasses following ISO guidelines. Geostand Geoanal Res 35(4):397–429. doi:10.1111/j.1751-908X.2011.00120.x
59. Barats A, Pécheyran C, Amouroux D, Dubascoux S, Chauvaud L, Donard OFX (2007) Matrix-matched quantitative analysis of trace-elements in calcium carbonate shells by laser-ablation ICP–MS: application to the determination of daily scale profiles in scallop shell (Pecten maximus). Anal Bioanal Chem 387(3):1131–1140. doi:10.1007/s00216-006-0954-8
60. Ethier DM, Kyle CJ, Nocera JJ (2014) Tracking animal movement by comparing trace element signatures in claws to spatial variability of elements in soils. Sci Total Environ 468–469:699–705. doi:10.1016/j.scitotenv.2013.08.091
61. Ethier DM, Kyle CJ, Kyser TK, Nocera JJ (2013) Trace elements in claw keratin as temporally explicit indicators of geographic origin in terrestrial mammals. Ann Zool Fenn 50(1–2):89–99. doi:10.5735/086.050.0108
62. Kaimal B, Johnson R, Hannigan R (2009) Distinguishing breeding populations of mallards (Anas platyrhynchos) using trace elements. J Geochem Explor 102(1):44–48. doi:10.1016/j.gexplo.2009.02.001
63. Holá M, Kalvoda J, Nováková H, Škoda R, Kanický V (2011) Possibilities of LA-ICP-MS technique for the spatial elemental analysis of the recent fish scales: line scan vs. depth profiling. Appl Surf Sci 257(6):1932–1940. doi:10.1016/j.apsusc.2010.09.029
64. Flem B, Moen V, Grimstvedt A (2005) Trace element analysis of scales from four populations of Norwegian Atlantic salmon (*Salmo salar* L.) for stock identification using laser ablation inductively coupled plasma mass spectrometry. Appl Spectrosc 59(2):245–251. doi:10.1366/0003702053085188
65. Jackson BP, Hopkins WA, Baionno J (2003) Laser ablation-ICP-MS analysis of dissected tissue: a conservation-minded approach to assessing contaminant exposure. Environ Sci Technol 37(11):2511–2515. doi:10.1021/es026416p
66. Dressler VL, Pozebon D, Mesko MF, Matusch A, Kumtabtim U, Wu B, Sabine Becker J (2010) Biomonitoring of essential and toxic metals in single hair using on-line solution-based calibration in laser ablation inductively coupled plasma mass spectrometry. Talanta 82(5):1770–1777. doi:10.1016/j.talanta.2010.07.065
67. Sela H, Karpas Z, Zoriy M, Pickhardt C, Becker JS (2007) Biomonitoring of hair samples by laser ablation inductively coupled plasma mass spectrometry (LA-ICP-MS). Int J Mass Spectrom 261(2–3):199–207. doi:10.1016/j.ijms.2006.09.018
68. Bartkus L, Amarasiriwardena D, Arriaza B, Bellis D, Yañez J (2011) Exploring lead exposure in ancient Chilean mummies using a single strand of hair by laser ablation-inductively coupled plasma-mass spectrometry (LA-ICP-MS). Microchem J 98(2):267–274. doi:10.1016/j.microc.2011.02.008
69. Arriaza B, Amarasiriwardena D, Cornejo L, Standen V, Byrne S, Bartkus L, Bandak B (2010) Exploring chronic arsenic poisoning in pre-Columbian Chilean mummies. J Archaeol Sci 37(6):1274–1278. doi:10.1016/j.jas.2009.12.030
70. Rodushkin I, Axelsson MD (2003) Application of double focusing sector field ICP-MS for multielemental characterization of human hair and nails. Part III. Direct analysis by laser ablation. Sci Total Environ 305(1–3):23–39. doi:10.1016/s0048-9697(02)00463-1
71. Stadlbauer C, Reiter C, Patzak B, Stingeder G, Prohaska T (2007) History of individuals of the 18th/19th centuries stored in bones, teeth, and hair analyzed by LA–ICP–MS—a step in attempts to confirm the authenticity of Mozart's skull. Anal Bioanal Chem 388(3):593–602. doi:10.1007/s00216-007-1266-3
72. Fu D, Finney L (2014) Metalloproteomics: challenges and prospective for clinical research applications. Expert Rev Proteomics 11(1):13–19. doi:10.1586/14789450.2014.876365
73. da Silva MA, Arruda MA (2013) Laser ablation (imaging) for mapping and determining Se and S in sunflower leaves. Metallomics 5(1):62–67. doi:10.1039/c2mt20154b
74. Wu B, Becker JS (2012) Imaging techniques for elements and element species in plant science. Metallomics 4(5):403–416. doi:10.1039/c2mt00002d
75. Koelmel J, Amarasiriwardena D (2012) Imaging of metal bioaccumulation in hay-scented fern (Dennstaedtia punctilobula) rhizomes growing on contaminated soils by laser ablation ICP-MS. Environ Pollut 168:62–70. doi:10.1016/j.envpol.2012.03.035
76. Lefevre I, Vogel-Mikus K, Jeromel L, Vavpetic P, Planchon S, Arcon I, Van Elteren JT, Lepoint G, Gobert S, Renaut J, Pelicon P, Lutts S (2014) Differential cadmium and zinc distribution in relation to their physiological impact in the leaves of the accumulating Zygophyllum fabago L. Plant Cell Environ 37(6):1299–1320. doi:10.1111/pce.12234
77. M-M P, Weiskirchen R, Gassler N, Bosserhoff AK, Becker JS (2013) Novel bioimaging techniques of metals by laser ablation inductively coupled plasma mass spectrometry for diagnosis of fibrotic and cirrhotic liver disorders. PLoS ONE 8(3):e58702. doi:10.1371/journal.pone.0058702
78. Hare DJ, Lee JK, Beavis AD, van Gramberg A, George J, Adlard PA, Finkelstein DI, Doble PA (2012) Three-dimensional atlas of

iron, copper, and zinc in the mouse cerebrum and brainstem. Anal Chem 84(9):3990–3997. doi:10.1021/ac300374x
79. Becker JS, Matusch A, Palm C, Salber D, Morton KA (2010) Bioimaging of metals in brain tissue by laser ablation inductively coupled plasma mass spectrometry (LA-ICP-MS) and metallomics. Metallomics 2(2):104–111. doi:10.1039/b916722f
80. Wang LM, Becker JS, Wu Q, Oliveira MF, Bozza FA, Schwager AL, Hoffman JM, Morton KA (2010) Bioimaging of copper alterations in the aging mouse brain by autoradiography, laser ablation inductively coupled plasma mass spectrometry and immunohistochemistry. Metallomics 2(5):348–353. doi:10.1039/c003875j
81. Konz I, Fernandez B, Fernandez ML, Pereiro R, Gonzalez-Iglesias H, Coca-Prados M, Sanz-Medel A (2014) Quantitative bioimaging of trace elements in the human lens by LA-ICP-MS. Anal Bioanal Chem. doi:10.1007/s00216-014-7617-y
82. Moreno-Gordaliza E, Giesen C, Lazaro A, Esteban-Fernandez D, Humanes B, Canas B, Panne U, Tejedor A, Jakubowski N, Gomez-Gomez MM (2011) Elemental bioimaging in kidney by LA-ICP-MS as a tool to study nephrotoxicity and renal protective strategies in cisplatin therapies. Anal Chem 83(20):7933–7940. doi:10.1021/ac201933x
83. Becker JS, Mounicou S, Zoriy MV, Lobinski R (2008) Analysis of metal-binding proteins separated by non-denaturating gel electrophoresis using matrix-assisted laser desorption/ionization mass spectrometry (MALDI-MS) and laser ablation inductively coupled plasma mass spectrometry (LA-ICP-MS). Talanta 76(5): 1183–1188. doi:10.1016/j.talanta.2008.05.023
84. Sanz-Medel A, Montes-Bayon M, del Rosario Fernandez de la Campa M, Encinar JR, Bettmer J (2008) Elemental mass spectrometry for quantitative proteomics. Anal Bioanal Chem 390(1): 3–16. doi:10.1007/s00216-007-1615-2
85. Florez MR, Aramendia M, Resano M, Lapena AC, Balcaen L, Vanhaecke F (2013) Isotope ratio mapping by means of laser ablation-single collector-ICP-mass spectrometry: Zn tracer studies in thin sections of Daphnia magna. J Anal At Spectrom 28(7): 1005–1015. doi:10.1039/C3JA50087J
86. Urgast DS, Feldmann J (2013) Isotope ratio measurements in biological tissues using LA-ICP-MS - possibilities, limitations, and perspectives. J Anal At Spectrom 28(9):1367–1371. doi:10.1039/C3JA50058F
87. Becker JS (2010) Imaging of metals, metalloids, and non-metals by laser ablation inductively coupled plasma mass spectrometry (LA-ICP-MS) in biological tissues. Methods Mol Biol 656:51–82. doi:10.1007/978-1-60761-746[--]4_3
88. Becker JS, Zoriy M, Matusch A, Wu B, Salber D, Palm C (2010) Bioimaging of metals by laser ablation inductively coupled plasma mass spectrometry (LA-ICP-MS). Mass Spectrom Rev 29(1): 156–175. doi:10.1002/mas.20239
89. Konz I, Fernandez B, Fernandez ML, Pereiro R, Sanz-Medel A (2012) Laser ablation ICP-MS for quantitative biomedical applications. Anal Bioanal Chem 403(8):2113–2125. doi:10.1007/s00216-012-6023-6
90. Hare DJ, Lear J, Bishop D, Beavis A, Doble PA (2013) Protocol for production of matrix-matched brain tissue standards for imaging by laser ablation-inductively coupled plasma-mass spectrometry. Anal Methods 5(8):1915–1921. doi:10.1039/C3ay26248k
91. Gholap D, Verhulst J, Ceelen W, Vanhaecke F (2012) Use of pneumatic nebulization and laser ablation-inductively coupled plasma-mass spectrometry to study the distribution and bioavailability of an intraperitoneally administered Pt-containing chemotherapeutic drug. Anal Bioanal Chem 402(6):2121–2129. doi:10.1007/s00216-011-5654-3
92. Stark HJ, Wennrich R (2011) A new approach for calibration of laser ablation inductively coupled plasma mass spectrometry using thin layers of spiked agarose gels as references. Anal Bioanal Chem 399(6):2211–2217. doi:10.1007/s00216-010-4413-1
93. Sela H, Karpas Z, Cohen H, Zakon Y, Zeiri Y (2011) Preparation of stable standards of biological tissues for laser ablation analysis. Int J Mass Spectrom 307(1–3):142–148. doi:10.1016/j.ijms.2011.01.022
94. Austin C, Hare D, Rawling T, McDonagh AM, Doble P (2010) Quantification method for elemental bio-imaging by LA-ICP-MS using metal spiked PMMA films. J Anal At Spectrom 25(5):722–725. doi:10.1039/b911316a
95. Bonta M, Lohninger H, Marchetti-Deschmann M, Limbeck A (2014) Application of gold thin-films for internal standardization in LA-ICP-MS imaging experiments. Analyst 139(6):1521–1531. doi:10.1039/c3an01511d
96. Bellis DJ, Santamaria-Fernandez R (2010) Ink jet patterns as model samples for the development of LA-ICP-SFMS methodology for mapping of elemental distribution with reference to biological samples. J Anal At Spectrom 25(7):957–963. doi:10.1039/b926430b
97. Reifschneider O, Wehe CA, Raj I, Ehmcke J, Ciarimboli G, Sperling M, Karst U (2013) Quantitative bioimaging of platinum in polymer embedded mouse organs using laser ablation ICP-MS. Metallomics 5(10):1440–1447. doi:10.1039/c3mt00147d
98. Vanhaecke F, Vanhoe H, Dams R, Vandecasteele C (1992) The use of internal standards in ICP-MS. Talanta 39(7):737–742
99. Frick DA, Günther D (2012) Fundamental studies on the ablation behaviour of carbon in LA-ICP-MS with respect to the suitability as internal standard. J Anal At Spectrom 27(8):1294–1303. doi:10.1039/c2ja30072a
100. Konz I, Fernandez B, Fernandez ML, Pereiro R, Gonzalez H, Alvarez L, Coca-Prados M, Sanz-Medel A (2013) Gold internal standard correction for elemental imaging of soft tissue sections by LA-ICP-MS: element distribution in eye microstructures. Anal Bioanal Chem 405(10):3091–3096. doi:10.1007/s00216-013-6778-4
101. Rabilloud T, Chevallet M, Luche S, Lelong C (2010) Two-dimensional gel electrophoresis in proteomics: Past, present and future. J Proteomics 73(11):2064–2077. doi:10.1016/j.jprot.2010.05.016
102. Beranova-Giorgianni S (2003) Proteome analysis by two-dimensional gel electrophoresis and mass spectrometry: strengths and limitations. Trac Trend Anal Chem 22(5):273–281. doi:10.1016/S0165-9936(03)00508-9
103. Konz I, Fernandez B, Fernandez ML, Pereiro R, Sanz-Medel A (2011) Absolute quantification of human serum transferrin by species-specific isotope dilution laser ablation ICP-MS. Anal Chem 83(13):5353–5360. doi:10.1021/ac200780b
104. Jiménez M, Gomez M, Rodriguez L, Martinez L, Castillo J (2009) Some pitfalls in PAGE-LA-ICP-MS for quantitative elemental speciation of dissolved organic matter and metalomics. Anal Bioanal Chem 393(2):699–707. doi:10.1007/s00216-008-2384-2
105. Giesen C, Waentig L, Panne U, Jakubowski N (2012) History of inductively coupled plasma mass spectrometry-based immunoassays. Spectrochim Acta B 76:27–39. doi:10.1016/j.sab.2012.06.009
106. Sanz-Medel A, Montes-Bayon M, Bettmer J, Fernandez-Sanchez ML, Encinar JR (2012) ICP-MS for absolute quantification of proteins for heteroatom-tagged, targeted proteomics. Trac Trend Anal Chem 40:52–63. doi:10.1016/j.trac.2012.07.020
107. Fernandez B, Rodriguez-Gonzalez P, Garcia Alonso JI, Malherbe J, Garcia-Fonseca S, Pereiro R, Sanz-Medel A (2014) On-line double isotope dilution laser ablation inductively coupled plasma mass spectrometry for the quantitative analysis of solid materials. Anal Chim Acta 851:64–71. doi:10.1016/j.aca.2014.08.017
108. Hondrogiannis EM, Ehrlinger E, Poplaski A, Lisle M (2013) Use of laser ablation-inductively coupled plasma-time of flight-mass spectrometry to identify the elemental composition of vanilla and determine the geographic origin by discriminant function analysis. J Agric Food Chem 61(47):11332–11337. doi:10.1021/jf4025536

109. Jiménez MS, Gomez MT, Castillo JR (2007) Multi-element analysis of compost by laser ablation-inductively coupled plasma mass spectrometry. Talanta 72(3):1141–1148. doi:10.1016/j.talanta.2007.01.006
110. Jantzi SC, Almirall JR (2014) Elemental analysis of soils using laser ablation inductively coupled plasma mass spectrometry (LA-ICP-MS) and laser-induced breakdown spectroscopy (LIBS) with multivariate discrimination: tape mounting as an alternative to pellets for small forensic transfer specimens. Appl Spectrosc 68(9):963–974. doi:10.1366/13-07351
111. Coedo AG, Padilla I, Dorado MT (2005) Determination of minor elements in steelmaking flue dusts using laser ablation inductively coupled plasma mass spectrometry. Talanta 67(1):136–143. doi:10.1016/j.talanta.2005.02.029
112. Su P, Ek P, Ivaska A (2012) Determination of metal ions in single wood fiber by LA-ICP-MS. Holzforschung 66(7):833–840. doi:10.1515/hf-2011-0182
113. Piispanen MH, Arvilommi SA, Broeck BV, Nuutinen LH, Tiainen MS, Perämäki PJ, Laitinen RS (2009) A comparative study of fly ash characterization by LA-ICP-MS and SEM-EDS. Energy Fuel 23(7):3451–3456. doi:10.1021/ef801037a
114. Malherbe J, Claverie F, Alvarez A, Fernandez B, Pereiro R, Molloy JL (2013) Elemental analyses of soil and sediment fused with lithium borate using isotope dilution laser ablation-inductively coupled plasma-mass spectrometry. Anal Chim Acta 793:72–78. doi:10.1016/j.aca.2013.07.031
115. Claverie F, Malherbe J, Bier N, Molloy JL, Long SE (2013) Standard addition method for laser ablation ICPMS using a spinning platform. Anal Chem 85(7):3584–3591. doi:10.1021/ac303307u
116. Piispanen MH, Niemelä ME, Tiainen MS, Laitinen RS (2012) Prediction of bed agglomeration propensity directly from solid biofuels: a look behind fuel indicators. Energy Fuel 26(4):2427–2433. doi:10.1021/ef300173w
117. Lloyd NS, Parrish RR, Horstwood MSA, Chenery SRN (2009) Precise and accurate isotopic analysis of microscopic uranium-oxide grains using LA-MC-ICP-MS. J Anal At Spectrom 24(6):752. doi:10.1039/b819373h
118. Macholdt DS, Jochum KP, Stoll B, Weis U, Andreae MO (2014) A new technique to determine element amounts down to femtograms in dust using femtosecond laser ablation-inductively coupled plasma-mass spectrometry. Chem Geol 383:123–131. doi:10.1016/j.chemgeo.2014.06.001
119. Lu C, Yongsheng L, Zhaochu H, Shan G, Keqing Z, Haihong C (2011) Accurate determinations of fifty-four major and trace elements in carbonate by LA–ICP-MS using normalization strategy of bulk components as 100 %. Chem Geol 284:283–295
120. Piispanen MH, Tiainen MS, Laitinen RS (2009) Comparative study of deposits with laser ablation inductively coupled plasma mass spectrometry and scanning electron microscopy–energy-dispersive spectrometry. Energy Fuel 23(7):3446–3450. doi:10.1021/ef801039g
121. Nowinski P, Hodge V, Lindley K, Cizdziel J (2010) Elemental analysis of desert varnish samples in the vicinity of coal-fired power plants and the Nevada Test Site using laser ablation ICPMS. Open Chem Biomed Methods J 3(1):153–168. doi:10.2174/1875038901003010153
122. Cizdziel JV, Ketterer ME, Farmer D, Faller SH, Hodge VF (2008) (239, 240, 241)Pu fingerprinting of plutonium in western US soils using ICPMS: solution and laser ablation measurements. Anal Bioanal Chem 390(2):521–530. doi:10.1007/s00216-007-1741-x
123. Scarciglia F, Tuccimei P, Vacca A, Barca D, Pulice I, Salzano R, Soligo M (2011) Soil genesis, morphodynamic processes and chronological implications in two soil transects of SE Sardinia, Italy: traditional pedological study coupled with laser ablation ICP-MS and radionuclide analyses. Geoderma 162(1–2):39–64. doi:10.1016/j.geoderma.2011.01.004
124. Okuda T, Tenmoku M, Kato J, Mori J, Sato T, Yokochi R, Tanaka S (2006) Long-term observation of trace metal concentration in aerosols at a remote island, Rishiri, Japan by using inductively coupled plasma mass spectrometry equipped with laser ablation. Water Air Soil Pollut 174(1–4):3–17. doi:10.1007/s11270-005-9000-2
125. Mertz-Kraus R, Brachert TC, Jochum KP, Reuter M, Stoll B (2009) LA-ICP-MS analyses on coral growth increments reveal heavy winter rain in the Eastern Mediterranean at 9 Ma. Palaeogeogr Palaeoclimatol Palaeoecol 273(1–2):25–40. doi:10.1016/j.palaeo.2008.11.015
126. Mora J, Maestre S, Hernandis V, Todolí JL (2003) Liquid-sample introduction in plasma spectrometry. TrAC Trends Anal Chem 22(3):123–132. doi:10.1016/s0165-9936(03)00301-7
127. Yang L, Sturgeon RE, Mester Z (2005) Quantitation of trace metals in liquid samples by dried-droplet laser ablation inductively coupled plasma mass spectrometry. Anal Chem 77(9):2971–2977. doi:10.1021/ac048275a
128. Günther D, Frischknecht R, Müschenborn H-J, Heinrich CA (1997) Direct liquid ablation: a new calibration strategy for laser ablation-ICP-MS microanalysis of solids and liquids. Fresenius J Anal Chem 359(4–5):390–393. doi:10.1007/s002160050594
129. Boué-Bigne F, Masters BJ, Crighton JS, Sharp BL (1999) A calibration strategy for LA-ICP-MS analysis employing aqueous standards having modified absorption coefficients. J Anal At Spectrom 14(11):1665–1672. doi:10.1039/a905479k
130. Resano M, García Ruiz E, Mihucz VG, Móricz ÁM, Záray G, Vanhaecke F (2007) Rapid screening method for arsenic speciation by combining thin layer chromatography and laser ablation-inductively coupled plasma-dynamic reaction cell-mass spectrometry. J Anal At Spectrom 22(9):1158. doi:10.1039/b704963c
131. Lafleur JP, Salin ED (2008) Speciation of chromium by high-performance thin-layer chromatography with direct determination by laser ablation inductively coupled plasma mass spectrometry. Anal Chem 80(17):6821–6823. doi:10.1021/ac8010582
132. Meermann B, Möller I, Nowak S, Luftmann H, Karst U (2010) Iodine speciation using thin-layer chromatography coupled to inductively coupled plasma-mass spectrometry by means of an extraction device. J Anal At Spectrom 25(10):1654. doi:10.1039/c003512b
133. Vorapalawut N, Martinez Labrador M, Pohl P, Caetano M, Chirinos J, Arnaudguilhem C, Bouyssiere B, Shiowatana J, Lobinski R (2012) Application of TLC and LA ICP SF MS for speciation of S, Ni and V in petroleum samples. Talanta 97:574–578. doi:10.1016/j.talanta.2012.04.040
134. Chirinos J, Oropeza D, González J, Ranaudo M, Russo RE (2013) Determination of vanadium/nickel proportionality in the asphaltene fraction of crude oil using thin-layer chromatography with femtosecond laser ablation–inductively coupled plasma–mass spectrometry. Energy Fuel 27(5):2431–2436. doi:10.1021/ef3020052
135. Vorapalawut N, Pohl P, Bouyssiere B, Shiowatana J, Lobinski R (2011) Multielement analysis of petroleum samples by laser ablation double focusing sector field inductively coupled plasma mass spectrometry (LA-ICP MS). J Anal At Spectrom 26(3):618. doi:10.1039/c0ja00118j
136. Asai S, Limbeck A (2014) LA-ICP-MS of rare earth elements concentrated in cation-exchange resin particles for origin attribution of uranium ore concentrate. Accessed 9 Jan 2015
137. Grinberg P, Willie S, Sturgeon RE (2005) Determination of U, Th and Pu in natural waters, biological materials and clinical samples by ETV-ICP-MS. J Anal At Spectrom 20(8):717. doi:10.1039/b502550h
138. Nischkauer W, Herincs E, Puschenreiter M, Wenzel W, Limbeck A (2013) Determination of Pt, Pd and Rh in Brassica Napus using

solid sampling electrothermal vaporization inductively coupled plasma optical emission spectrometry. Spectrochim Acta B At Spectrosc 89:60–65. doi:10.1016/j.sab.2013.08.013
139. Grinberg P, Yang L, Mester Z, Willie S, Sturgeon RE (2006) Comparison of laser ablation, electrothermal vaporization and solution nebulization for the determination of radionuclides in liquid samples by inductively coupled plasma mass spectrometry. J Anal At Spectrom 21(11): 1202. doi:10.1039/b607911c
140. Deegan RD, Bakajin O, Dupont TF, Huber G, Nagel SR, Witten TA (1997) Capillary flow as the cause of ring stains from dried liquid drops. Nature 389(6653):827–829. doi:10.1038/39827
141. Deegan R, Bakajin O, Dupont T, Huber G, Nagel S, Witten T (2000) Contact line deposits in an evaporating drop. Phys Rev E 62(1):756–765. doi:10.1103/PhysRevE.62.756
142. Berteloot G, Hoang A, Daerr A, Kavehpour HP, Lequeux F, Limat L (2012) Evaporation of a sessile droplet: inside the coffee stain. J Colloid Interface Sci 370(1):155–161. doi:10.1016/j.jcis.2011.10.053
143. Kajiya T, Kaneko D, Doi M (2008) Dynamical visualization of "coffee stain phenomenon" in droplets of polymer solution via fluorescent microscopy. Langmuir 24(21):12369–12374. doi:10.1021/la8017858
144. Bhardwaj R, Fang X, Somasundaran P, Attinger D (2010) Self-assembly of colloidal particles from evaporating droplets: role of DLVO interactions and proposition of a phase diagram. Langmuir 26(11):7833–7842. doi:10.1021/la9047227
145. Adachi E, Dimitrov AS, Nagayama K (1995) Stripe patterns formed on a glass surface during droplet evaporation. Langmuir 11(4):1057–1060. doi:10.1021/la00004a003
146. Uno K, Hayashi K, Hayashi T, Ito K, Kitano H (1998) Particle adsorption in evaporating droplets of polymer latex dispersions on hydrophilic and hydrophobic surfaces. Colloid Polym Sci 276(9): 810–815. doi:10.1007/s003960050314
147. Sefiane K (2014) Patterns from drying drops. Adv Colloid Interf Sci 206:372–381. doi:10.1016/j.cis.2013.05.002
148. Ristenpart W, Kim P, Domingues C, Wan J, Stone H (2007) Influence of substrate conductivity on circulation reversal in evaporating drops. Phys Rev Lett 99(23). doi:10.1103/PhysRevLett.99.234502
149. Latterini L, Blossey R, Hofkens J, Vanoppen P, Schryver FC, Rowan AE, Nolte RJM (1999) Ring formation in evaporating porphyrin derivative solutions. Langmuir 15(10):3582–3588. doi:10.1021/la981602n
150. Fang X, Li B, Petersen E, Seo Y-S, Samuilov VA, Chen Y, Sokolov JC, Shew C-Y, Rafailovich MH (2006) Drying of DNA droplets. Langmuir 22(14):6308–6312. doi:10.1021/la060479u
151. Gorr HM, Zueger JM, McAdams DR, Barnard JA (2013) Salt-induced pattern formation in evaporating droplets of lysozyme solutions. Colloids Surf B: Biointerfaces 103:59–66. doi:10.1016/j.colsurfb.2012.09.043
152. Sobac B, Brutin D (2014) Desiccation of a sessile drop of blood: cracks, folds formation and delamination. Colloids Surf A Physicochem Eng Asp 448:34–44. doi:10.1016/j.colsurfa.2014.01.076
153. Yang L, Sturgeon RE, Mester Z (2005) Dried-droplet laser ablation ICP-MS of HPLC fractions for the determination of selenomethionine in yeast. J Anal At Spectrom 20(5):431. doi:10.1039/b500926j
154. Hsieh H-F, Chang W-S, Hsieh Y-K, Wang C-F (2009) Lead determination in whole blood by laser ablation coupled with inductively coupled plasma mass spectrometry. Talanta 79(2):183–188. doi:10.1016/j.talanta.2009.03.027
155. Hsieh H-F, Chang W-S, Hsieh Y-K, Wang C-F (2011) Using dried-droplet laser ablation inductively coupled plasma mass spectrometry to quantify multiple elements in whole blood. Anal Chim Acta 699(1):6–10. doi:10.1016/j.aca.2011.05.002
156. Peš O, Jungová P, Vyhnánek R, Vaculovič T, Kanický V, Preisler J (2008) Off-line coupling of capillary electrophoresis to substrate-assisted laser desorption inductively coupled plasma mass spectrometry. Anal Chem 80(22):8725–8732. doi:10.1021/ac801036x
157. Jungová P, Navrátilová J, Peš O, Vaculovič T, Kanický V, Šmarda J, Preisler J (2010) Substrate-assisted laser desorption inductively-coupled plasma mass spectrometry for determination of copper in myeloid leukemia cells. J Anal At Spectrom 25(5):662. doi:10.1039/b919811c
158. Cizdziel JV (2007) Determination of lead in blood by laser ablation ICP-TOF-MS analysis of blood spotted and dried on filter paper: a feasibility study. Anal Bioanal Chem 388(3):603–611. doi:10.1007/s00216-007-1242-y
159. Aramendía M, Rello L, Bérail S, Donnard A, Pécheyran C, Resano M (2015) Direct analysis of dried blood spots by femtosecond-laser ablation-inductively coupled plasma-mass spectrometry. Feasibility of split-flow laser ablation for simultaneous trace element and isotopic analysis. J Anal At Spectrom 30(1):296–309. doi:10.1039/c4ja00313f
160. Aramendía M, Rello L, Vanhaecke F, Resano M (2012) Direct trace-elemental analysis of urine samples by laser ablation-inductively coupled plasma mass spectrometry after sample deposition on clinical filter papers. Anal Chem 84(20):8682–8690. doi:10.1021/ac3018839
161. Demirev PA (2013) Dried blood spots: analysis and applications. Anal Chem 85(2):779–789. doi:10.1021/ac303205m
162. Cobb Z, Vries R, Spooner N, Williams S, Staelens L, Doig M, Broadhurst R, Barfield M, van de Merbel N, Schmid B, Siethoff C, Ortiz J, Verheij E, van Baar B, White S, Timmerman P (2013) In-depth study of homogeneity in DBS using two different techniques: results from the EBF DBS-microsampling consortium. Bioanalysis 5(17):2161–2169. doi:10.4155/bio.13.171
163. Ren X, Paehler T, Zimmer M, Guo Z, Zane P, Emmons GT (2010) Impact of various factors on radioactivity distribution in different DBS papers. Bioanalysis 2(8):1469–1475. doi:10.4155/bio.10.96
164. Choi H, Ma S, Lee JS, Lim HB (2010) Array-type microchip sampling to determine trace metal in photoresist used in semiconductor manufacturing process. J Anal At Spectrom 25(5):710. doi:10.1039/b916064g
165. Nischkauer W, Vanhaecke F, Bernacchi S, Herwig C, Limbeck A (2014) Radial line-scans as representative sampling strategy in dried-droplet laser ablation of liquid samples deposited on precut filter paper disks. Spectrochim Acta B At Spectrosc 101: 123–129. doi:10.1016/j.sab.2014.07.023
166. Gabriel SJ, Schwarzinger C, Schwarzinger B, Panne U, Weidner SM (2014) Matrix segregation as the major cause for sample inhomogeneity in MALDI dried droplet spots. J Am Soc Mass Spectrom 25(8):1356–1363. doi:10.1007/s13361-014-0913-0
167. Foltynová P, Bednařík A, Kanický V, Preisler J (2014) Diode laser thermal vaporization ICP MS with a simple tubular cell for determination of lead and cadmium in whole blood. J Anal At Spectrom. doi:10.1039/c4ja00113c
168. Foltynová P, Kanický V, Preisler J (2012) Diode laser thermal vaporization inductively coupled plasma mass spectrometry. Anal Chem 84(5):2268–2274. doi:10.1021/ac202884m
169. Razmislevicien I, Padarauskas A, Pranaityt B, Naujalis E (2010) Determination of Cr(VI) by dispersive liquid-liquid microextraction and dried-droplet laser ablation ICP-MS. Curr Anal Chem 6(4):310–315. doi:10.2174/157341101100604031O
170. Narukawa T, Willie S (2010) Dried deposits of biological tissues solubilized using formic acid for LA ICP-TOF-MS. J Anal At Spectrom 25(7):1145. doi:10.1039/b927309c
171. Do T-M, Hsieh H-F, Chang W-C, Chang E-E, Wang C-F (2011) Analysis of liquid samples using dried-droplet laser ablation

inductively coupled plasma mass spectrometry. Spectrochim Acta B At Spectrosc 66(8):610–618. doi:10.1016/j.sab.2011.06.008

172. Hsieh H-F, Chen Y-H, Wang C-F (2011) A magnesium hydroxide preconcentration/matrix reduction method for the analysis of rare earth elements in water samples using laser ablation inductively coupled plasma mass spectrometry. Talanta 85(2):983–990. doi:10.1016/j.talanta.2011.05.011
173. Kumtabtim U, Siripinyanond A, Auray-Blais C, Ntwari A, Becker JS (2011) Analysis of trace metals in single droplet of urine by laser ablation inductively coupled plasma mass spectrometry. Int J Mass Spectrom 307(1–3):174–181. doi:10.1016/j.ijms.2011.01.030
174. Fittschen UEA, Bings NH, Hauschild S, Förster S, Kiera AF, Karavani E, Frömsdorf A, Thiele J, Falkenberg G (2008) Characteristics of picoliter droplet dried residues as standards for direct analysis techniques. Anal Chem 80(6):1967–1977. doi:10.1021/ac702005x
175. Holthoff E, Farrell M, Pellegrino P (2013) Standardized sample preparation using a drop-on-demand printing platform. Sensors 13(5):5814–5825. doi:10.3390/s130505814

Elemental and Molecular Imaging of tumour tissues with ToF-SIMS in combination with LA-ICP-MS

Florian Brenner, Maximilian Bonta, Andreas Limbeck, Herbert Hutter, *Poster at 16th European Conference on Applications of Surface and Interface Analysis*, 2015

Elemental and Molecular Imaging of tumour tissues with ToF-SIMS in combination with LA-ICP-MS

F. Brenner[1*], M. Bonta[1], A. Limbeck[1], H. Hutter[1]

[1]Institute of Chemical Technologies and Analytics; Vienna University of Technology,
Getreidemarkt 9/164, 1060 Wien, Austria
[*]Presenter: florian.brenner@tuwien.ac.at

1. Introduction

Since a few years, Time of Flight Secondary Ion Mass Spectrometry is accepted as a powerful tool for the analysis of biological samples. The technique is suitable for identifying cell structures and for imaging tissues with ppm-ppb sensitivity.[1] ToF-SIMS mass spectra can not only reveal the localisation of an exogenous compound within the tissue, but distinguish also different histological compartments of the sample, due to their molecular composition. Particularly of great importance is the mapping of intracellular distributions of small molecule therapeutics in single cells and tissues, where an essential criterion for successful analysis is a data acquisition mode that provides high spatial and high mass resolutions at the same time.[2, 3]
Besides the localisation of certain anti-cancer drugs, also the efficiency of the treatment is of great interest, thus quantification can provide further essential information.
While ToF-SIMS is not well-known for its strength in quantification, due to its matrix dependency and different ionisation probabilities, a combination with other techniques like LA-ICP-MS can overcome this drawback. The capability of LA-ICP-MS as a multi-element imaging technique combined with quantification of metal distributions in tissue sections of human or animal brain has already been demonstrated.[4, 5]
With a more detailed and better understanding of not only the uptake into the cells, but moreover the effect and impact on the whole human organism, like reactions with the surrounding tissues, could benefit designing future drugs as well as improve the application.

2. Experimental

Tissue samples were provided and treated with Carboplatin. The tissues were cut and prepared with a Cryotome (10µm in thickness) and placed onto a glass target. The experiments were performed on a ToF-SIMS[5], operated in the bunched mode with high mass resolution and low spatial resolution (~2µm), or in the burst alignment mode (imaging mode), with high spatial resolution (~150nm) and low mass resolution.

3. Results and Conclusion

The LA-ICP-MS image shows the distribution of platinum in the cancer tissue (see Fig. 1). The marked area of the very same specimen was previously analysed with ToF-SIMS. The Pt concentration was below the detection limit and could not be compared with the LA-ICP-MS results. Nevertheless, we gathered further information from a characteristic fragment of Carboplatin. The distribution of the fragment does not show the same image as the platinum, probably indication a separation of the platinum core from the organic chelating agent. Furthermore Fig. 2 shows the PO_2 intensity that is refered to remaining tumour

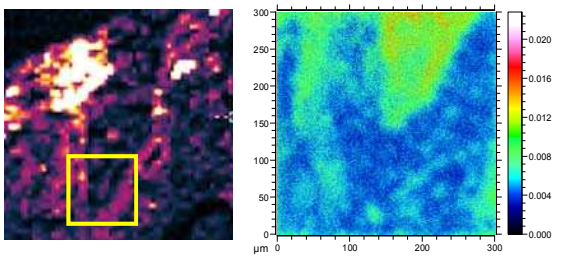

Fig 1: Pt distribution (LA-ICP-MS) image of a cancer tissue (left), organic Carboplatin fragment (ToF-SIMS) in the tissue (right).

compartments (high DNA content), which covers the results from the LA-ICP-MS measurements. Furthermore, some of the essential fatty acids are presented as well in the platinum-poor region.

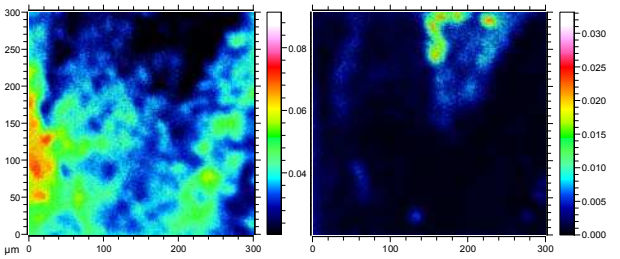

Fig 2: PO_2 distribution in tissue (left), sum of fatty acids (right)

4. References

1. Arlinghaus, H.F., et al., Applied Surface Science, 2006. **252**: p. 6941-6948.
2. Brison, J., et al., Analytical Chemistry, 2013. **85**(22): p. 10869-10877.
3. Judd, A.M., et al., Pharmaceutical Research, 2013. **30**(7): p. 1896-1905.
4. Zoriy, M.V., et al., Spectrochimica Acta Part B-Atomic Spectroscopy, 2008. **63**(3): p. 375-382.
5. Becker, J.S., et al., *(LA-ICP-MS) and metallomics.* Metallomics, 2010. **2**(2): p. 104-111.

Multimodal (FTIR and LA-ICP-MS) imaging of a tumor treated with Sunitinib and Cisplatin

Anna Balbekova, Maximilian Bonta, Johannes Ofner, Andreas Limbeck, Bernhard Lendl,

Poster at SPEC 2016 (Awarded with a poster prize)

MULTIMODAL (FTIR AND LA-ICP-MS) IMAGING OF A TUMOR TREATED WITH SUNITINIB AND CISPLATIN

A. Balbekova[1], M. Bonta[1], A. Limbeck[1], J. Ofner[1], B. Lendl[1]*

[1] *Institute of Chemical Technologies and Analytics, Vienna University of Technology, Getreidemarkt 9, Vienna,Austria.*
**e-mail: bernhard.lendl@tuwien.ac.at*

A combination of different imaging techniques applied to one and the same sample, so called multimodal imaging, offers complementary information for sample characterization that is not accessible by one or the other technique. Here, we present combined analysis of hyperspectral data from FTIR imaging (molecular information) and LA-ICP-MS (elemental information) of a single sample. We studied a tissue thin cut of a tumor that was implanted in mice, treated by antitumor drugs (sunitinib, ciplatin). The discrimination and characterization of the histologically relevant structures induced by the drug treatment is the aim of this study.
The sample was produced cryogenic microtome cuts of a tumor, which was deposited on a one-side polished silicon wafer. Silicon was chosen because it is partly transparent in the mid-IR and only produces a small background in the LA-ICP-MS measurements.

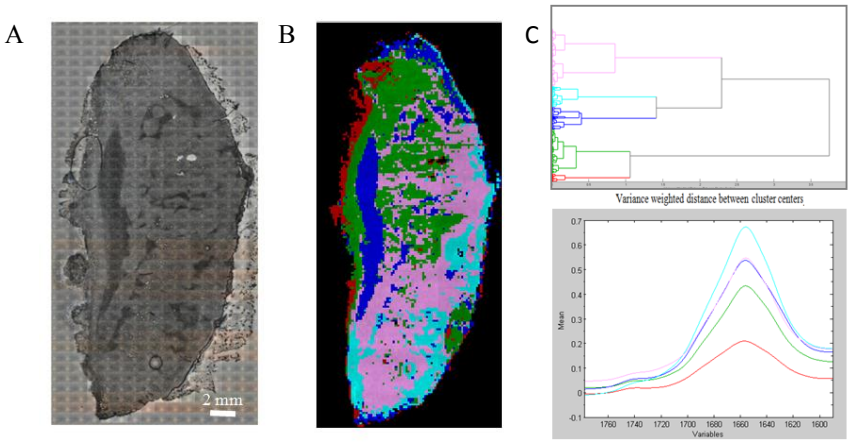

Fig. 1. (A) Microscopic image of the sample. (B) Clustered image produced by multivariate analysis. (C) Dendrogram of hierarchical cluster analysis and mean spectra of the Amide I band in with selected classes.

A hyperspectral FTIR image of the tumor slice acquired with 50-µm resolution, was further analyzed by multivariate analysis. Different structures were discriminated (Fig. 1B) which partially could not be revealed by a conventional histological investigation (staining). Spectra of necrotic tumor reveal an increase of beta sheet structures and a decrease of alpha helices compared to viable tumor.
Accompanying this biochemical analysis, elemental imaging by LA-ICP-MS can provide information of the two different drugs concerning their location and distribution inside the tumor. Application oa simultaneous multimodal data, analogously to [1], will open the possibility to correlate information between two different techniques and thus allow to deepen the understanding on the effects of tumor treatment by these two drugs.

References

[1]Chemometric Analysis of Multisensor Hyperspectral Images of Precipitated Atmospheric Particulate Matter. Ofner, et. al.. *Anal. Chem.*, 2015, **87 (18)**, 9413–9420.

6 List of abbreviations

AMP…Area Mismatch Percentage

DNA…Deoxyribonucleic Acid

(FT)IR Spectroscopy…Fourier Transform Infrared Spectroscopy

LA-ICP-MS…Laser Ablation-Inductively Coupled Plasma-Mass Spectrometry

LIBS…Laser Induced Breakdown Spectroscopy

MALDI-MS…Matrix Assisted Laser Desorption/Ionization-Mass Spectrometry

MPM…Malignant Pleural Mesothelioma

MRI…Magnetic Resonance Imaging

µXRF…Micro X-ray Fluorescence

PIXE…Particle Induced X-ray Emission

ToF-SIMS…Time of Flight-Secondary Ion Mass Spectrometry

7 References

1. Haraguchi, H., *Metallomics as integrated biometal science.* Journal of Analytical Atomic Spectrometry, 2004. **19**(1): p. 5-14.
2. Becker, J.S., et al., *Elemental imaging mass spectrometry of thin sections of tissues and analysis of brain proteins in gels by laser ablation inductively coupled plasma mass spectrometry.* Physica Status Solidi (C) Current Topics in Solid State Physics, 2007. **4**(6): p. 1775-1784.
3. Mokgalaka, N.S. and J.L. Gardea-Torresdey, *Laser Ablation Inductively Coupled Plasma Mass Spectrometry: Principles and Applications.* Applied Spectroscopy Reviews, 2006. **41**(2): p. 131-150.
4. Hare, D., et al., *Quantitative elemental bio-imaging of Mn, Fe, Cu and Zn in 6-hydroxydopamine induced Parkinsonism mouse models.* Metallomics, 2009. **1**(1): p. 53-58.
5. Pozebon, D., et al., *Bioimaging of metals in thin mouse brain section by laser ablation inductively coupled plasma mass spectrometry: Novel online quantification strategy using aqueous standards.* Journal of Analytical Atomic Spectrometry, 2010. **25**(11): p. 1739-1744.
6. Hare, D., et al., *Elemental bio-imaging of melanoma in lymph node biopsies.* Analyst, 2009. **134**(3): p. 450-3.
7. Reyzer, M.L. and R.M. Caprioli, *MALDI-MS-based imaging of small molecules and proteins in tissues.* Current Opinion in Chemical Biology, 2007. **11**(1): p. 29-35.
8. Bhargava, R., *Infrared spectroscopic imaging: the next generation.* Appl Spectrosc, 2012. **66**(10): p. 1091-120.
9. de Roos, A., et al., *Clinical applications of gadolinium-DTPA in MRI.* Magn Reson Annu, 1988: p. 113-45.
10. Bonta, M., et al., *Quantitative LA-ICP-MS imaging of platinum in chemotherapy treated human malignant pleural mesothelioma samples using printed patterns as standard.* Journal of Analytical Atomic Spectrometry, 2014. **29**(11): p. 2159-2167.
11. Hare, D.J., et al., *Protocol for production of matrix-matched brain tissue standards for imaging by laser ablation-inductively coupled plasma-mass spectrometry.* Analytical Methods, 2013. **5**(8): p. 1915-1921.
12. Limbeck, A., et al., *Recent advances in quantitative LA-ICP-MS analysis: Challenges and solutions in the life sciences and environmental chemistry ABC Highlights:*

Authored by Rising Stars and Top Experts. Analytical and Bioanalytical Chemistry, 2015. **407**(22): p. 6593-6617.

13. Wang, H.A.O., et al., *Fast Chemical Imaging at High Spatial Resolution by Laser Ablation Inductively Coupled Plasma Mass Spectrometry.* Anal Chem, 2013.
14. Van Malderen, S.J.M., et al., *Recent developments in the design of rapid response cells for laser ablation-inductively coupled plasma-mass spectrometry and their impact on bioimaging applications.* Journal of Analytical Atomic Spectrometry, 2016. **31**(2): p. 423-439.
15. Hare, D.J., et al., *Three-Dimensional Atlas of Iron, Copper, and Zinc in the Mouse Cerebrum and Brainstem.* Anal Chem, 2012. **84**(9): p. 3990-3997.
16. Paul, B., et al., *Visualising mouse neuroanatomy and function by metal distribution using laser ablation-inductively coupled plasma-mass spectrometry imaging.* Chemical Science, 2015. **6**(10): p. 5383-5393.
17. Van Malderen, S.J., et al., *Quantitative Determination and Subcellular Imaging of Cu in Single Cells via Laser Ablation-ICP-Mass Spectrometry Using High-Density Microarray Gelatin Standards.* Anal Chem, 2016. **88**(11): p. 5783-9.
18. Giesen, C., et al., *Highly multiplexed imaging of tumor tissues with subcellular resolution by mass cytometry.* Nat Meth, 2014. **11**(4): p. 417-422.
19. Al-Ebraheem, A., M.J. Farquharson, and E. Ryan, *The evaluation of biologically important trace metals in liver, kidney and breast tissue.* Appl Radiat Isot, 2009. **67**(3): p. 470-4.
20. Crapo, J.D., et al., *Copper,zinc superoxide dismutase is primarily a cytosolic protein in human cells.* Proc Natl Acad Sci U S A, 1992. **89**(21): p. 10405-9.
21. Cotruvo, J.A., Jr. and J. Stubbe, *Metallation and mismetallation of iron and manganese proteins in vitro and in vivo: the class I ribonucleotide reductases as a case study.* Metallomics, 2012. **4**(10): p. 1020-36.
22. Penner-Hahn, J.E., *Manganese Proteins with Mono- & Dinuclear Sites*, in *Encyclopedia of Inorganic Chemistry*. 2006, John Wiley & Sons, Ltd.
23. Beyer, W.F., Jr. and I. Fridovich, *In vivo competition between iron and manganese for occupancy of the active site region of the manganese-superoxide dismutase of Escherichia coli.* J Biol Chem, 1991. **266**(1): p. 303-8.
24. Carvalho, M.L., et al., *Trace elements in human cancerous and healthy tissues: A comparative study by EDXRF, TXRF, synchrotron radiation and PIXE.* Spectrochimica Acta Part B: Atomic Spectroscopy, 2007. **62**(9): p. 1004-1011.
25. Sychrova, H., *Yeast as a model organism to study transport and homeostasis of alkali metal cations.* Physiol Res, 2004. **53 Suppl 1**: p. S91-8.
26. Boer, J.L., S.B. Mulrooney, and R.P. Hausinger, *Nickel-dependent metalloenzymes.* Arch Biochem Biophys, 2014. **544**: p. 142-52.

27. Ragsdale, S.W., *Nickel and the carbon cycle.* J Inorg Biochem, 2007. **101**(11-12): p. 1657-66.
28. Coleman, J.E., *Zinc proteins: enzymes, storage proteins, transcription factors, and replication proteins.* Annu Rev Biochem, 1992. **61**: p. 897-946.
29. Birka, M., et al., *Diagnosis of Nephrogenic Systemic Fibrosis by means of Elemental Bioimaging and Speciation Analysis.* Analytical Chemistry, 2015. **87**(6): p. 3321-3328.
30. Gale, G.R., et al., *Antitumor action of cis-dichlorobis(methylamine)platinum(II).* J Natl Cancer Inst, 1973. **51**(4): p. 1227-34.
31. Todd, R.C. and S.J. Lippard, *Inhibition of transcription by platinum antitumor compounds.* Metallomics, 2009. **1**(4): p. 280-291.
32. Fichtinger-Schepman, A.M., et al., *Adducts of the antitumor drug cis-diamminedichloroplatinum(II) with DNA: formation, identification, and quantitation.* Biochemistry, 1985. **24**(3): p. 707-13.
33. Fukasawa, H., et al., *Anti-Cancer Agent-Induced Nephrotoxicity.* Anticancer Agents Med Chem, 2014.
34. Dempke, W., et al., *Cisplatin resistance and oncogenes--a review.* Anticancer Drugs, 2000. **11**(4): p. 225-36.
35. Molloy, J.L. and J.R. Sieber, *Classification of microheterogeneity in solid samples using microXRF.* Anal Bioanal Chem, 2008. **392**(5): p. 995-1001.
36. Bourassa, D., et al., *MicroXRF tomographic visualization of zinc and iron in the zebrafish embryo at the onset of the hatching period.* Metallomics, 2016.
37. Shimizu, Y., et al., *In-air microparticle induced X-ray emission analysis of particles in interstitial pneumonia lung tissue obtained by transbronchial biopsy.* J Clin Biochem Nutr, 2011. **49**(2): p. 125-30.
38. Maenhaut, W., *Multielement analysis of biological materials by particle-induced X-ray emission (PIXE).* Scanning Microsc, 1990. **4**(1): p. 43-59; discussion 59-62.
39. Piwowar, A.M., et al., *C60-ToF SIMS imaging of frozen hydrated HeLa cells.* Surf Interface Anal, 2013. **45**(1): p. 302-304.
40. Qin, Z., et al., *Trace metal imaging with high spatial resolution: Applications in biomedicine.* Metallomics, 2011. **3**(1): p. 28-37.
41. Becker, J.S., et al., *Bioimaging of metals by laser ablation inductively coupled plasma mass spectrometry (LA-ICP-MS).* Mass Spectrom Rev, 2010. **29**(1): p. 156-75.
42. Russo, R.E., et al., *Laser Ablation in Analytical Chemistry.* Analytical Chemistry, 2013. **85**(13): p. 6162-6177.
43. Motto-Ros, V., et al., *Mapping nanoparticles injected into a biological tissue using laser-induced breakdown spectroscopy.* Spectrochimica Acta - Part B Atomic Spectroscopy, 2013. **87**: p. 168-174.

44. Bonta, M., et al., *Elemental mapping of biological samples by the combined use of LIBS and LA-ICP-MS.* Journal of Analytical Atomic Spectrometry, 2016. **31**(1): p. 252-258.
45. Vanhaecke, F., et al., *The use of internal standards in ICP-MS.* Talanta, 1992. **39**(7): p. 737-42.
46. Frick, D.A. and D. Günther, *Fundamental studies on the ablation behaviour of carbon in LA-ICP-MS with respect to the suitability as internal standard.* Journal of Analytical Atomic Spectrometry, 2012. **27**(8): p. 1294-1303.
47. Bonta, M., et al., *Application of gold thin-films for internal standardization in LA-ICP-MS imaging experiments.* Analyst, 2014. **139**(6): p. 1521-31.
48. Hare, D., C. Austin, and P. Doble, *Quantification strategies for elemental imaging of biological samples using laser ablation-inductively coupled plasma-mass spectrometry.* Analyst, 2012. **137**(7): p. 1527-1537.
49. Nischkauer, W., et al., *Radial line-scans as representative sampling strategy in dried-droplet laser ablation of liquid samples deposited on pre-cut filter paper disks.* Spectrochimica Acta Part B: Atomic Spectroscopy, 2014. **101**(0): p. 123-129.
50. Shariatgorji, M., et al., *Direct imaging of elemental distributions in tissue sections by laser ablation mass spectrometry.* Methods, 2016. **104**: p. 86-92.
51. Gludovacz, E., et al., *Characterization of recombinant human diamine oxidase (rhDAO) produced in Chinese Hamster Ovary (CHO) cells.* Journal of Biotechnology, 2016. **227**: p. 120-130.
52. Koch, J. and D. Günther, *Review of the state-of-the-art of laser ablation inductively coupled plasma mass spectrometry.* Appl Spectrosc, 2011. **65**(5): p. 155-62.
53. Bonta, M., et al., *Quantification of chloride in concrete samples using LA-ICP-MS.* Cement and Concrete Research, 2016. **86**: p. 78-84.
54. Cakara, A., et al., *Development of a multi-variate calibration approach for quantitative LA-ICP-MS analysis of oxidation resistant Mo-Si-B coatings.* Spectrochimica Acta - Part B Atomic Spectroscopy, 2016. **120**: p. 57-62.

8 Curriculum Vitae – Maximilian Bonta

Personal information

Born on August 15th 1990 in Vienna
Current residence: Vienna; Nationality: Austria
Contact: ✉ maximilian.bonta@tuwien.ac.at ☎ +43 (0)660 4899136

Education

2013–2016 PhD program 'Molecular and Elemental Imaging in Biosciences'

2011–2013 MSc study Biotechnology and Bioanalytics at TU Wien (graduation with excellence). Title of the Master's Thesis: '*Elemental Imaging Using LA-ICP-MS on Biological Samples*'

2008–2011 BSc study Technical Chemistry at TU Wien. Title of the Bachelor's Thesis: '*Molecular Imaging Mass Spectrometry – Method Development for the Identification of Proteins on Tissue Samples*'

2000–2008 Piaristengymnasium Vienna graduation in 2008

1996–2000 Grammar school

Professional experience

11/2013 - PhD student employed at TU Wien: Scientific research, supervision of students during Bachelor's and Master's thesis, teaching assistant in lab courses

09-12/2014 Guest researcher at Lawrence Berkeley National Laboratory, Berkeley, California, USA: Research on LA-ICP-MS and LIBS instrumentation in the group for Laser Material Interaction, supervision by Dr. Richard E. Russo

2011-2013 Tutor in several lab courses at TU Wien: Qualitative Analytical Chemistry, Quantitative Analytical Chemistry, Instrumental Analytical Chemistry, total extent: 16 weekly lecture hours

Work related skills

Languages

Mother tongue German

Fluent in English

Research interests

- Mass Spectrometry Imaging (especially LA-ICP-MS), laterally resolved analysis of metals in biological tissues
- Laser Induced Breakdown Spectroscopy (LIBS) – Analysis of various sample types including data evaluation strategies
- Statistical data analysis. Multi-variate calibration methods and classification approaches

Awards and other academic achievements

- 2 poster awards: SPEC 2016 and 18. Tagung Festkörperanalytik
- Two invited talks at international conferences
- Reviewer for Applied Physics A
- Travelling grant of the TU Wien for the abroad stay in Berkeley, USA
- Participation in the excellence program TUtheTOP of the TU Wien in 2013
- Performance scholarship of the TU Wien in 2010, 2011, and 2012

Signature: Date:

Publications

Peer reviewed articles

M. Bonta, T. Anderl, A. Cognigni, M. Hejazifar, K. Bica, A. Limbeck, *Determination of the residual chloride content in ionic liquids using LA-ICP-MS*, RSC Advances, submitted manuscript

M. Shariatgorji, A. Nilsson, M. Bonta, J. Gan, N. Marklund, F. Clausen, P. Källback, H. Loden, A. Limbeck, P. Andren, *Direct Imaging of Elemental Distributions in Tissue Sections by Laser Ablation Mass Spectrometry*, Methods, accepted manuscript in press, DOI: 10.1016/j.ymeth.2016.05.021

M. Bonta, A. Eitzenberger, S. Burtscher, A. Limbeck, *Quantification of chloride in concrete samples using LA-ICP-MS*, Cem. Concr. Res., 2016, 86, p78-84

E. Gludovacz, D. Maresch, M. Bonta, H. Szöllösi, P.G. Furtmüller, R. Weik, F. Altmann, A. Limbeck, N. Borth, B. Jilma, T. Boehm, *Characterization of recombinant human diamine oxidase (rhDAO) produced in Chinese Hamster Ovary (CHO) cells*, J. Biotech., 2016, 227, p120-130

A. Cakara, M. Bonta, H. Riedl, P.H. Mayrhofer, A. Limbeck, *Development of a multivariate calibration approach for quantitative analysis of oxidation resistant Mo-Si-B coatings using laser ablation inductively coupled plasma mass spectrometry*, Spectrochim. Acta B, 2016, 120, p57-62

M. Brgles, M. Bonta, M. Šantak, M. Jagušić, D. Forčić, B. Halassy, G. Allmaier, M. Marchetti-Deschmann, *Identification of mumps virus protein and lipid composition by mass spectrometry*, Virol. J., 2016, 1, p1-10

M. Bonta, J.J. Gonzalez, C.D Quarles Jr, R.E. Russo, B. Hegedus, A. Limbeck, *Elemental mapping of biological samples by the combined use of LIBS and LA-ICP-MS*, J. Anal. At. Spectrom, 2015, 1, p252-258

M. Bonta, B. Hegedus, A. Limbeck, *Application of dried-droplets deposited on pre-cut filter paper disks for quantitative LA-ICP-MS imaging of biologically relevant minor and trace elements in tissue samples*, Anal. Chim. Acta, 2015, 908, p54-62

A. Limbeck, P. Galler, M. Bonta, G. Bauer, W. Nischkauer, F. Vanhaecke, *Recent advances in quantitative LA-ICP-MS analysis: challenges and solutions in the life sciences and environmental chemistry*, Anal. Bioanal. Chem, 2015, 22, p6593-6617

M. Bonta, A. Limbeck, C.D Quarles Jr, D. Oropeza, R.E. Russo, J.J. Gonzalez, *A metric for evaluation of the image quality of chemical maps derived from LA-ICP-MS experiments*, J. Anal. At. Spectrom., 2015, 8, p1809-1815

M. Bonta, H. Lohninger, M. Marchetti-Deschmann, A. Limbeck, *Application of Gold Thin-Film for Internal Standardization in LA-ICP-MS Imaging Experiments*, Analyst, 2014,139, p1521-1531

M. Bonta, V. Laszlo, H. Lohninger, B. Hegedus, A. Limbeck, *Quantitative LA-ICP-MS imaging of platinum in chemotherapy treated human malignant pleural mesothelioma samples using printed patterns as standard*, J. Anal. At. Spectrom., 2014, 29, p2159-2167

Non-peer reviewed articles

A. Limbeck, A. Eitzenberger, M. Bonta, S. Burtscher, *New Analysis Method for the Accurate Determination of Chloride Content in the Cement Phase of Concrete*, CONCREEP 2015: Mechanics and Physics of Creep, Shrinkage, and Durability of Concrete and Concrete Structures - Proceedings of the 10th International Conference on Mechanics and Physics of Creep, Shrinkage, and Durability of Concrete and Concrete Structures, p800-804

Oral presentations (presenting author underlined)

M. Bonta, R. De Oro Calderon, C. Gierl-Mayr, H. Danninger, A. Limbeck: *Laterally resolved analysis of steels using LIBS: Revealing the distribution of metallic and non-metallic additions,* SciX 2016, Minneapolis, Minnesota, 18/09/2016 – 23/09/2016. *Invited Lecture*

M. Bonta, A. Limbeck: *Tandem LA/LIBS for the comprehensive analysis of trace elements in polymers*, 13th European Workshop on Laser Ablation (EWLA2016), Ljubljana, Slovenia, 12/07/2016 – 15/07/2016

M. Bonta, J.J. Gonzalez, R.E. Russo, B. Hegedus, A. Limbeck: *Elemental Mapping of Biological Samples Using Tandem LA/LIBS*, 2016 Winter Conference on Plasma Spectrochemistry, Tucson, Arizona; 10/01/2016 – 16/01/2016

A. Limbeck, A. Eitzenberger, M. Bonta, S. Burtscher: *New Analysis Method for the Accurate Determination of Chloride Content in the Cement Phase of Concrete*; CONCREEP 10, Vienna, Austria; 21/09/2015 – 23/09/2015

M. Bonta, B. Hegedus, A. Limbeck: *Expanding the possibilities of elemental analysis: Investigations of biological tissues using Tandem LA/LIBS*; 5th International Symposium on Metallomics, Beijing, China; 09/09/2015 – 12/09/2015

M. Bonta, A. Cakara, P.H. Mayrhofer, A. Limbeck: *Quantitative analysis of Mo, Si and B in oxidation resistant coatings*; 18. Tagung Festkörperanalytik, Vienna, Austria; 06/07/2015 – 08/07/2015

M. Bonta, J.J. Gonzalez, D.D. Oropeza, R. Russo, A. Limbeck: *Simultaneous analysis of trace and bulk elements in biological samples using Femtosecond Tandem LA/LIBS*, ANAKON 2015, Graz, Austria; 23/03/2015 – 26/03/2015

M. Bonta, J. Gonzalez, D. Oropeza, B. Hegedus, R. Russo, A. Limbeck: *Femtosecond Laser Ablation ICP-MS - Critical aspects for elemental mapping of biological samples*; 2015 European Winter Conference on Plasma Spectrochemistry, Münster, Germany; 22/02/2015 – 26/02/2015

J. Gonzalez, M. Bonta, A. Limbeck, D. Oropeza, D. Quarles, R. Russo: Simultaneous elemental and isotopic chemical analysis by LIBS and LA-ICP-MS; 2015 European Winter Conference on Plasma Spectrochemistry, Münster, Germany; 22/02/2015 – 26/02/2015

M. Bonta, W. Nischkauer, A. Limbeck: *Analysis of trace and bulk elements in biological samples using a splitstream laser-ablation system with simultaneous ICP-OES and ICP-MS detection*, SciX 2014, Reno, Nevada; 28/09/2014 – 03/10/2014. *Invited Lecture*

M. Bonta, B. Hegedus, J. Lohninger, A. Limbeck: *Quantitative LA-ICP-MS imaging of platinum in tissue samples*; 14. Edelmetallforum, Ulm, Germany; 07/04/2014 – 08/04/2014

M. Bonta, H. Lohninger, B. Hegedus, A. Limbeck: *A novel approach for quantitative LA-ICP-MS imaging experiments on biological samples*; 2014 Winter Conference on Plasma Spectrochemistry, Amelia Island, Florida; 06/01/2014 – 11/01/2014

M. Bonta, H. Lohninger, A. Limbeck: *A comparison of internal standards in LA-ICP-MS imaging experiments on tissue sections*; 4th International Symposium on Metallomics, Oviedo, Spain; 08/07/2013 – 11/07/2013

M. Bonta, H. Lohninger, A. Limbeck*: LA-ICP-MS imaging experiments using gold as internal standard – a feasibility study*; Topical Issues of Rational Use of Natural Resources, St. Petersburg, Russia; 23/04/2013 – 27/04/2013

M. Bonta, S. Fröhlich, M. Hafner, E. Pittenauer, V. Archodoulaki, G. Allmaier, M. Marchetti-Deschmann: *MALDI-RTOF-MS analysis of lipid compounds in synovial fluid*

separated by two dimensional thin layer chromatography; MassSpec Forum Vienna 2012, Vienna, Austria; 21/02/2012 – 22/02/2012

Poster presentations (presenting author underlined)

Anna Balbekova, Maximilian Bonta, Johannes Ofner, Andreas Limbeck, Bernhard Lendl: *Multimodal (FTIR and LA-ICP-MS) imaging of a tumor treated with Sunitinib and Cisplatin*, SPEC 2016, Montreal, Canada; 26/06/2016 – 30/06/2016

M. Bonta, J.J. Gonzalez, R.E. Russo, B. Hegedus, A. Limbeck: *A Comparison Between Different Sample Preparation Techniques of Biological Specimen for Subsequent Use in Elemental Distribution Analysis*, 2016 Winter Conference on Plasma Spectrochemistry, Tucson, Arizona; 10/01/2016 – 16/01/2016

M. Bonta, B. Hegedus, A. Limbeck: *Trace element analysis and quantification in tumor tissues using LA-ICP- MS*; 5th International Symposium on Metallomics, Beijing, China; 09/09/2015 – 12/09/2015

M. Bonta, A. Limbeck: *Elemental Mapping Using LA-ICP-MS – A Versatile Tool for Spatial Trace Element Analysis*; 18. Tagung Festkörperanalytik, Vienna, Austria; 06/07/2015 – 08/07/2015

M. Bonta, J. Gonzalez, D. Oropeza, B. Hegedus, R. Russo, A. Limbeck: *Elemental mapping of biological samples using Femtosecond Tandem LA/LIBS - Simultaneous analysis of trace and bulk elements*; 2015 European Winter Conference on Plasma Spectrochemistry, Münster, Germany; 22/02/2015 – 26/02/2015

W. Nischkauer, M. Bonta, A. Limbeck: *Dried-droplet laser ablation in connection to ICP-MS and ICP-OES for the quantification of major and minor elements in cow milk*; 2015 European Winter Conference on Plasma Spectrochemistry, Münster, Germany; 22/02/2015 – 26/02/2015

A. Cakara, M. Bonta, P.H. Mayrhofer, A. Limbeck: Development of a LA-ICP-MS method for the quantitative analysis of Mo, Si and B in oxidation resistant coatings; 2015 European Winter Conference on Plasma Spectrochemistry, Münster, Germany; 22/02/2015 – 26/02/2015

M. Brgles, M. Bonta, Santak, D. Forcic, G. Allmaier, B. Halassy, M. Marchetti-Deschmann: *Lipidome and proteome of mumps virus*; 8th Central and Eastern European Proteomics Conference, Vienna University of Technology; 30/06/2014 – 04/07/2014

M. Bonta, C. Gierl-Mayr, H. Danninger, A. Limbeck: *Revealing the distribution of non-metallic additions in steel samples using LA-ICP-MS*; 2014 Winter Conference on Plasma Spectrochemistry, Amelia Island, Florida; 06/01/2014 – 11/01/2014

M. Bonta, H. Lohninger, A. Limbeck: *Internal Standards for LA-ICP-MS Imaging Experiments on Biological Samples - Method Development, Evaluation and Application*; 17th Euroanalysis, Warsaw, Poland; 25/08/2013 – 29/08/2013

B. Putz, M. Bonta, C. Gierl-Mayr, H. Danninger, A. Limbeck: *LA-ICP-MS Imaging of Non-Metallic Additives in Powder Metallurgic Iron Alloy Samples*; 17th Euroanalysis, Warsaw, Poland; 25/08/2013 – 29/08/2013

M. Bonta, S. Fröhlich, M. Hafner, E. Pittenauer, V. Archodoulaki, G. Allmaier, M. Marchetti-Deschmann: *MALDI-RTOF mass spectrometric analysis of lipid compounds in synovial fluid separated by 2D thin layer chromatography*; 2nd Graz Lipid Mass Spec Meeting, Graz, Austria; 06/03/2012 – 07/03/2012